CODEN:LUTEDX/(TEIE-5445)/1-98/(2020)

Industrial Electrical Engineering and Automation

# Estimation of Inertia in Power Systems Using Electromechanical Modes



**Vidar Johnsson**

Division of Industrial Electrical Engineering and Automation
Faculty of Engineering, Lund University

# Abstract

The transition to more renewable energy such as wind, leads to a decreased inertia in the power system. As a consequence of this, disturbances lead to larger frequency deviations and the frequency stability of the system is worsened. Therefore, there is a surging interest to estimate the inertia in the power system.

In this thesis, a novel method for inertia estimation is proposed and investigated. It is based on the electromechanical modes of the system. The modes are estimated from measurements, a system model is constructed, and the inertia is found such that the modes of the model correspond to the estimated modes. This divides the method into two parts. One is the estimation of modes, and one is the estimation of inertia from the modes. Furthermore, there is a division between the slow rigid body mode of the entire system and the faster inter-generator modes. Both are possible to use in the method. The former is harder to estimate, while the latter are more difficult to use for inertia estimation.

The mode estimation was investigated by testing estimation methods on simulated systems where the true modes were known. The inertia estimation from the modes was performed by an optimisation routine in PowerFactory, and several systems with a few generators were analysed.

It was concluded that it was possible to estimate the modes in the simulations, at least if they were not too damped. The accuracy was in the range of 10% for the imaginary part of the rigid body mode, and higher for the inter-generator modes.

The rigid body mode was highly valuable for inertia estimation, and the total system inertia could be determined with approximately the same accuracy as the mode could be estimated. Using the imaginary part and the mode shape of inter-generator modes, it was possible to estimate the total inertia with approximately 10% standard deviation. Typically, a few inter-generator modes sufficed for estimation.

Combining the two parts of the method and testing it on the IEEE 14-bus and 39-bus test system with added hydro governors showed that inertia estimation from the electromechanical modes was possible.

The achieved accuracy compares well with what has been achieved with other methods and shows that this method has potential.

# Acknowledgements

I would like to thank my supervisor Olof Samuelsson for introducing me to this subject and making the thesis possible as well as for the help and comments he has provided during the work. Likewise, assistant supervisor Morten Hemmingson also deserves to be thanked for his help and comments. Furthermore, I owe the entire division of IEA gratitude for cordially welcoming and accommodating me during my work on the thesis.

# Contents

**Abstract** i

**Acknowledgements** iii

**Contents** v

**List of abbreviations** vii

**1 Introduction** 1
- 1.1 Inertia . . . 1
- 1.2 Previously used methods for inertia estimation . . . 3
- 1.3 Method in this work . . . 4
- 1.4 A mechanical analogue . . . 5
- 1.5 Objectives and limitations of this thesis . . . 5
- 1.6 Outline of the thesis . . . 6

**2 Models** 9
- 2.1 Generators . . . 9
  - 2.1.1 Several generators modelled as one . . . 9
- 2.2 Governors . . . 10
- 2.3 Hydro power plants . . . 11
- 2.4 Steam power plants . . . 12
- 2.5 Transmission . . . 13
- 2.6 Transformers . . . 14
- 2.7 Excitation system . . . 14
- 2.8 System model . . . 15
  - 2.8.1 Eigenvalues and eigenvectors . . . 16
- 2.9 Variability of load . . . 19
- 2.10 Measurements . . . 21

**3 The dependency of the modes on system parameters** 23
- 3.1 Simple governor and turbine . . . 23
  - 3.1.1 Rigid body mode . . . 23
  - 3.1.2 Inter-generator oscillation . . . 24
- 3.2 Hydro plants for frequency control . . . 25
  - 3.2.1 One-generator system . . . 25
  - 3.2.2 Two-generator system . . . 28
- 3.3 Steam plants for frequency control . . . 29
- 3.4 Conclusions . . . 29

**4 Estimation of electromechanical modes** 31
- 4.1 Simulation . . . 31
- 4.2 AR(MA)(X)-models . . . 32
- 4.3 Estimation from step disturbance . . . 32
  - 4.3.1 Prony's method . . . 33
  - 4.3.2 Eigenvalue realisation algorithm . . . 33
  - 4.3.3 Matrix pencil method . . . 34

4.3.4 Sorting out wrongly identified modes . . . 34
4.4 Estimation from ambient noise . . . 35
4.4.1 AR-model . . . 35
4.5 Estimation of rigid body mode . . . 35
4.5.1 Estimation from ambient noise . . . 35
4.5.2 Estimation from step response . . . 38
4.5.3 Combining several step responses . . . 40
4.5.4 Discussion . . . 41
4.6 Estimation of inter-generator modes . . . 42
4.6.1 Mode shape estimation . . . 42
4.6.2 Estimation from ambient noise . . . 43
4.7 Discussion . . . 44
4.8 Some attempts on mode estimation from real data . . . 45

**5 Inertia estimation from modes** **49**
5.1 System modelling . . . 49
5.2 Mode matching . . . 50
5.3 Optimisation . . . 51
5.4 Inertia estimation using the rigid body mode . . . 53
5.4.1 Five-generator system . . . 54
5.4.2 Ten-generator system . . . 56
5.4.3 Sensitivity to error . . . 57
5.5 Inertia estimation using inter-generator modes . . . 59
5.5.1 Two-generator system . . . 61
5.5.2 Three-generator system . . . 62
5.5.3 Two-area system . . . 63
5.5.4 Five-generator system . . . 64
5.5.5 Ten-generator system . . . 67
5.5.6 Sensitivity to errors . . . 68
5.6 Inertia estimation using both the rigid body mode and the inter-generator modes . . . 70
5.7 Discussion . . . 71

**6 The combined method** **75**
6.1 Discussion . . . 78

**7 Conclusion** **81**

**8 Future work** **83**

**References** **85**

**Appendix A Simplified pseudocode for optimisation algorithm** **89**

# List of abbreviations

AR – Autoregressive
ARMA – Autoregressive-Moving-Average
ARMAX – Autoregressive-Moving-Average with exogenous input
AVR – Automatic Voltage Regulator
ENTSO-E – European Network of Transmission System Operators for Electricity
ERA – Eigenvalue Realisation Algorithm
FFT – Fast Fourier Transform
HVDC – High Voltage Direct Current
IEEE – Institute of Electrical and Electronics Engineers
MPM – Matrix Pencil Method
PEM – Prediction Error Method
PFC – Primary Frequency Control
PMU – Phasor Measurement Unit
PSS – Power System Stabiliser
RoCoF – Rate of Change of Frequency

# 1 Introduction

## 1.1 Inertia

The frequency stability is critical for the functioning of the power system, and the frequency must always be kept close to the nominal. This typically means 50 or 60 Hz. In the Nordic power grid the frequency must stay within an interval of $\pm 0.1$ Hz during normal operation, and within $\pm 1$ Hz at all time [1]. If it falls below this level, automatic load shedding commences. If it falls even further, it may result in a blackout or even system collapse. For larger power grids the restrictions are typically even stricter.

The most acute threat to the frequency stability is sudden step disturbances in the power balance. This happens for example when a generator or High-Voltage DC (HVDC) transmission line is disconnected. An example of a real frequency response is shown in Figure 1. A power system must have $N-1$ security, meaning that the system must at all times be prepared to handle the loss of any single component. Considering frequency the system must withstand loss of the largest generator, which would cause a dramatic step in the power. Even in that case the frequency must remain within the allowed interval [2, p. 5].

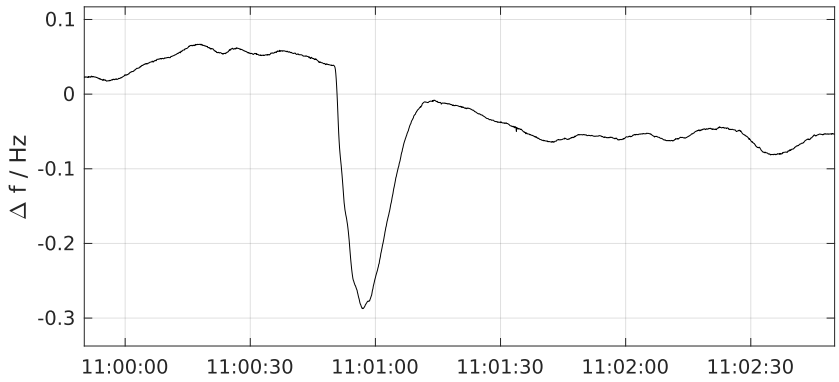


Figure 1: The frequency measured in Lund on June 2, 2005. The dip in frequency was due to unit B2 at the nuclear station Olkiluoto being disconnected, resulting in a loss of 850 MW.

An important factor to contain the frequency within the allowed bound is the constant of inertia $H$. In Figure 2 the effect of $H$ is illustrated. The figure shows the simulated frequency response to a step disturbance in the power balance. This could for example happen when a generator is disconnected. The model is based on hydro power and taken from an ENTSO-E (European Network of Transmission System Operators for Electricity) report. It is presented in more detail in section 2.3.

The influence of $H$ is most clearly seen in the first few seconds of the step response. This is the critical period before any power control has time to respond and when the frequency is in free fall. A lower $H$ means a faster decrease. The initial rate of change of frequency (RoCoF) is calculated as $\frac{-\Delta P}{2H}$ and its asymptotes are plotted as dashed lines. A lower $H$ also means a lower frequency minimum. As generating units may be disconnected both by RoCoF protection and by underfrequency protection, this endangers the stability of the system. On a longer time horizon, however, the inertia does not matter, instead the frequency control determines the final frequency.

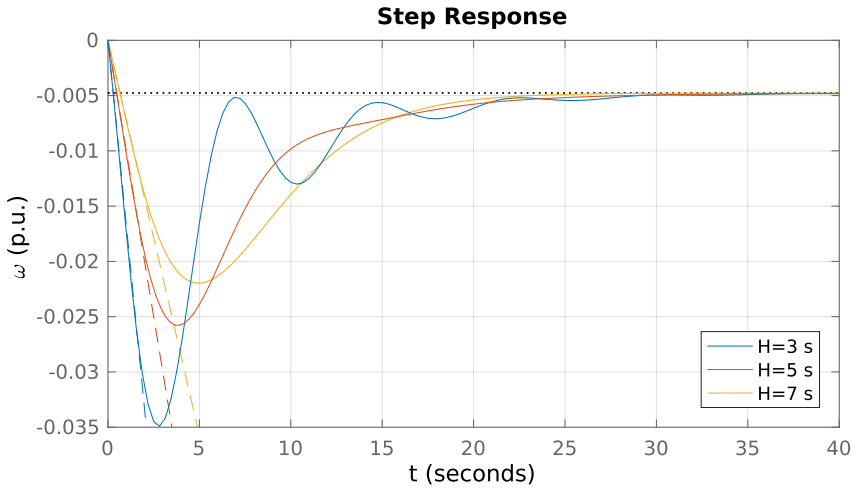


Figure 2: How the frequency response to a step disturbance depends on $H$ in a simple model of a power system.

To understand why the constant of inertia is important, it should be noted that in a power grid there is no significant storage of electric energy. This means that in every instance the generator input power to the grid must correspond to the power output to the loads. Yet both the produced and the consumed power vary with certain unpredictability, most dramatically when a generator is lost, leading to an immediate decrease in production. There are control systems for the production that compensate for this loss, but their response is not immediate. Typically, it takes several seconds for them to respond. The solution to still maintain the energy balance in the system in the meantime is inertia [2, p. 4].

The generators in combination with the turbines, and to a lesser extent the loads, have large rotating masses that store rotational energy. When there is a power imbalance, energy is taken from or stored in these. This means that when the consumed energy is larger than the produced, the rotating masses slow down and the frequency decreases. If the consumed energy is smaller than the produced it is the other way around. The kinetic energy of a rotating mass, $E_r$, is given by $E_r = \frac{J\omega^2}{2}$ where $J$ is the moment of inertia and $\omega$ the angular frequency. The energy is often scaled with the base power of a generator, $S_{base}$, which gives the constant of inertia $H = \frac{J\omega_0^2}{2S_{base}}$, given in seconds, where $\omega_0$ is the nominal angular frequency (typically $50 \cdot 2\pi$ or $60 \cdot 2\pi$ rad/s). The interpretation of $H$ is how many seconds the stored energy would last if the turbine shut down at full electrical load [3, Ch. 3.9]. As can be seen, a larger $H$ means a larger $J$ which means less change in frequency for the same amount of power withdrawn. This means better frequency stability. Therefore, $H$ must be kept sufficiently large at all time.

The major factor that determines $H$ is the energy mix. This also means that the inertia changes with time, as the energy mix varies. In Table 1 values are listed for different types of generating units.

The most notable value is that of wind power; it has no inertia. This stems from the fact the wind turbines are not directly connected to the grid. Instead, they are connected through power electronics. As a result, they have no synchronously rotating mass. The same is true for photo-voltaic solar power.

Table 1: Typical values of $H$ for different forms of generating units. Taken from [4, p. 52].

| **Production type** | $H$ **(s)** |
|---|---|
| Nuclear | 6.3 |
| Other thermal | 4 |
| Conventional hydro | 3 |
| Small-scale hydro | 1 |
| Wind | 0 |

This explains why inertia is important to consider during the ongoing changes in the power system: When more renewable energy is included in the power production it displaces synchronous generator-based units. This reduces $H$ and the stability is threatened. When nuclear is decommissioned, as is the case in Sweden, the problem is further exacerbated. In [4, p. 52] a worst-case inertia scenario in 2025 is presented with 27% of the electricity coming from wind power and 10% from small-scale hydro. (N.B. this scenario describes minimum rotating mass, $J$, not minimum $H$.) According to one scenario, the share of wind in the Nordic electricity generation may increase from 7% in 2013 to 30% in 2050 [5, p. 17]. In [6, p. 83] it is estimated that if the wind power supplies 10% of the energy in a year, the maximum wind power penetration (generation relative to consumption) at one instant will be over 35%. If it supplies 20% or 30% of the energy, the maximum penetration will reach above 70% and 105%, respectively. In scenarios as these, the value of $H$ must be monitored and estimated. To find a method to do this is the goal of this thesis.

## 1.2 Previously used methods for inertia estimation

The most common way to estimate the inertia has been to analyse the frequency response from a step disturbance in the power balance, e.g. in [7, 8, 9]. Based on the initial RoCoF and the magnitude of the disturbance, $H$ can be calculated. An obvious downside of this is that a step disturbance is needed. They are not occurring all the time, and an important aspect of the inertia estimation is to predict how the frequency response to a disturbance will be, meaning that $H$ should be known beforehand. Knowing after a disastrous disturbance that there was too little inertia in the system is not very helpful. Therefore, estimations under normal operating conditions are desired. Furthermore, this assumes that either the magnitude of the disturbance is known or can be accurately estimated.

In literature, estimations under normal conditions are rare. One obvious method is to take the information about which generating units are online, and then use the values from Table 1 to calculate the inertia of the entire system [4, Ch. 4]. This is currently done by the system operators in the Nordic system. There are, however, limitations with this method. The inertia of the generator units is not necessarily exactly known and may differ from the used values, all production might not be included in the calculations, the exact composition must be known, and the inertia in the load is not included. At the time of the report [4] (2015), it was not known how good these estimates were.

In the future power system synthetic inertia may be used to counter the problem of decreasing inertia. This could for example be done by installing control systems at

wind power plants that increase the output (temporarily) when a decrease in frequency is detected [10]. This would then negatively affect the aforementioned method that depend on adding up the inertia from all known sources since the inertia would be spread out among a great amount of more variable wind plants. Therefore, this development would create further need for an alternative method for inertia estimation.

Another method based on ambient noise is used in [11]. The changes in load power is estimated, and based on that an ARMAX-model is constructed with the change in load power as input and the frequency as output. The presented method is applied to the Icelandic power system, with some success. The greatest weakness of this method is probably the need to estimate the change in load power.

## 1.3 Method in this work

A common problem with previous methods, is that they assume knowledge of the load power which is seen as an input signal while the frequency is the output signal. However, the power is often not known or only approximately known. In this work, the inertia is estimated from the electromechanical modes of the power system, for which there is an ample literature on how to estimate. After the modes are estimated, a model of the power system is used. The $H$ of the model is set such that the theoretical modes of the model match the estimated. This $H$ is then the estimate. This method is believed to be new. The procedure is illustrated in Figure 3.

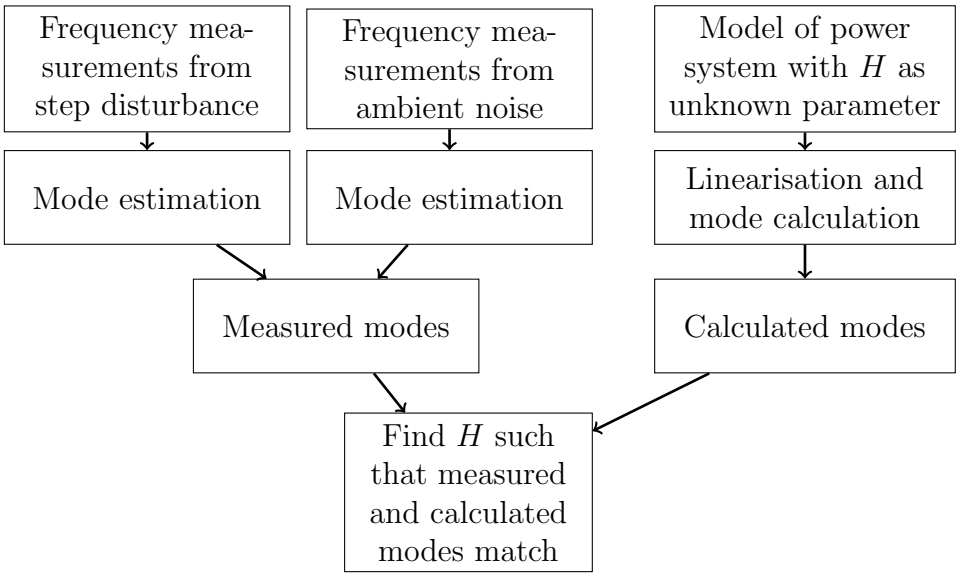


Figure 3: An outline of the method in this thesis.

The task is therefore split into two. The first task is to estimate the modes, based on the frequency measurements. This is treated in section 4. The second task is to estimate $H$ based on the modes. This is done in section 5.

The two tasks are separate and can be solved separately. Any method for mode estimation can be interchangeably used with the estimation of $H$ from the modes. It can therefore be done either from ambient noise, or if that fails, from step disturbances of some kind.

## 1.4 A mechanical analogue

To illustrate the principle of the method, a mechanical analogue to the power system can be constructed with masses and springs. In Figure 4 a system with two masses is shown. Each block represents a generator, and its vertical position represents its frequency. The masses are assumed to be fixed in the horizontal axis and only move vertically. The springs attached to the ground represent the frequency control that applies force (represents power) to the block. The mass of the blocks represents the inertia. If the blocks are moved out of position (a change in load or generation in the power system) the system will start to oscillate vertically. The angular frequency of the oscillation will be $\omega = \sqrt{\frac{k_1+k_2}{m_1+m_2}}$, where $k_1$ and $k_2$ are spring constants. By measuring the frequency and knowing $k_1$ and $k_2$, the mass can be found. This is the method astronauts use to weigh themselves in space, since normal scales do not work in weightlessness. A picture of this is shown in Figure 5. The same idea is intended to be applied to the power system. By measuring the frequency and knowing the frequency control, the inertia can be found. In a power system, however, the frequency control is not simply proportional as the force of a spring is, making the task much more complicated.

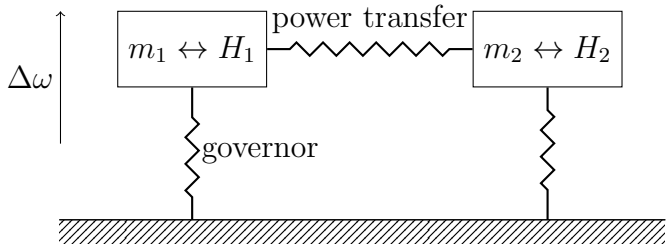


Figure 4: A mechanical analogue of the power system. The masses represent generators, their vertical positions represent their frequency.

There is also a spring between the blocks. If the blocks both have the same vertical position, this spring does nothing. But if they are at different positions one block will pull the other. This represents the fact that in a power system, a difference in frequency gives rise to a difference of angle which gives rise to a power flow. (This analogue is somewhat faulty since the power flow is not proportional to the frequency difference, but the difference in angle which is the integral of the former.) This will also lead to an oscillation between the masses, which represents inter-generator modes in the power system. The frequency of this oscillation also depends on the masses of the blocks, meaning that this oscillation also can be used to calculate the masses.

## 1.5 Objectives and limitations of this thesis

The purpose of this thesis is to perform initial investigations regarding the proposed methods and determine whether it is plausible for inertia estimation. Since the area has not been covered previously, the work is exploratory in its nature, rather than an attempt to create a product that is ready to use.

Research questions that are to be investigated are:

- How can the electromechanical modes be estimated from 1) ambient noise and 2) step disturbances?

Figure 5: A cosmonaut measuring his body mass by holding onto a spring and measuring the frequency with which he oscillates. Photo: NASA

- How should the electromechanical modes be used for inertia estimation?
- What is the accuracy of the method?

The investigation will be conducted by simulations. The most important models that are used in the simulations are the IEEE 14-bus and 39-bus systems that are commonly used in the study of power systems. The use of simulations is due to the fact that real-world power systems are neither accessible nor transparent and the data available from them is limited. Since the method has not been investigated previously, the work starts almost from zero and does not reach beyond relatively small and simple system models. Trying the method on full-fledged models of power systems is outside the scope of the thesis. The work is therefore conceptual, rather than intended to deliver a working product.

The study of mode estimation is an extensive field, making it impossible to cover it completely. Instead, the thesis is limited to consider some of the most common methods. The methods and results found do not aspire to be optimal, rather they are intended to give a general idea of the possibilities and performance. This is in line with the conceptual purpose of the thesis.

## 1.6 Outline of the thesis

- In chapter 1 the background and basic idea of the method are presented.
- In chapter 2 the models that are to be used in the thesis are presented.
- In chapter 3 the relation between the inertia and other parameters and the modes is discussed.
- In chapter 4 it is discussed how the electromechanical modes can be estimated, both from ambient measurements and step responses.

- In chapter 5 it is discussed how the inertia can be estimated from electromechanical modes.
- In chapter 6 a few examples are given on how the two steps can be combined to estimate the inertia.
- In chapter 7 some conclusions from the work are presented.
- In chapter 8 potential future work is discussed.

# 2 Models

## 2.1 Generators

For the purpose of modelling frequency dynamics, a simple model of a synchronous generator is [12, pp. 689-690]:

$$\frac{d\omega(t)}{dt} = \frac{P_m(t) - P_e(t) - D\Delta\omega}{2H\omega(t)}$$

where $\omega$ is the angular frequency of the generator, $P_m$ its mechanical power, $P_e$ its electrical power, $H$ its constant of inertia and $D$ its damping. $\Delta\omega$ is the deviation from the synchronous frequency 1. Everything is given in p.u.

To make the analysis simpler, this expression can be linearised around $\omega = 1$ to remove the dependency on $\omega$ on the right hand side, i.e. setting $\omega \approx 1$, which has negligible effect on the dynamics. This leaves the first order differential equation (1) referred to as the swing equation.

$$\frac{d\omega(t)}{dt} = \frac{P_m(t) - P_e(t) - D\Delta\omega}{2H} \tag{1}$$

with the Laplace transform:

$$\omega(s) = \frac{1}{2Hs + D}\Delta P(s)$$

where $\Delta P$ is the net power input to the generator. What this equation says is simply that the generator accelerates if the net power input $> 0$, and decelerates if it is $< 0$. It is basically a version of Newton's second law.

The damping originates from two sources: one is the frequency dependency of the load, and one is the dynamics of the generator itself. The latter stays the same over time while the former varies as the composition of the load changes. However, the damping in the generator may have a different transient than steady state behaviour, meaning that $D$ might be higher for sudden changes than for slow. This is difficult to take into consideration for an analytical model. One way to improve fast and transient dynamics is to also model the voltage dynamics of the generator. This is further considered in section 2.7. Typical values of $D$ are 0-2.

In reality, the reactive power of a generator must also be taken into consideration. This is controlled by the field current. However, for modelling of frequency dynamics the active power is the main interest. Nevertheless, the reactive power affects the voltage, which affects the power. Preferably, the reactive power should work independently and maintain nominal voltage, and therefore be possible to ignore in the analysis. This is reasonable for slower dynamics because the voltage control is typically much faster than the frequency control. However, it might not be true for faster dynamics in the frequency. This is further discussed in section 2.7.

### 2.1.1 Several generators modelled as one

In a system of several generators, there will be several swing equations. Adding them together, ignoring damping for the moment, gives:

$$\sum_i \left(2H_i \frac{d\omega_i(t)}{dt}\right) = \sum_i \left(P_{m,i}(t) - P_{e,i}(t)\right)$$
$$\Longleftrightarrow$$
$$2\frac{d}{dt}\sum_i H_i\omega_i(t) = P_{m,tot}(t) - P_{e,tot}(t)$$
$$\Longleftrightarrow$$
$$2\left(\sum_i H_i\right)\frac{d}{dt}\frac{\sum_i H_i\omega_i(t)}{\sum_i H_i} = P_{m,tot}(t) - P_{e,tot}(t)$$
$$\Longleftrightarrow$$
$$\frac{d}{dt}\frac{\sum_i H_i\omega_i(t)}{\sum_i H_i} = \frac{P_{m,tot}(t) - P_{e,tot}(t)}{2\sum_i H_i}$$
$$\Longleftrightarrow$$
$$\frac{d\omega_{COI}(t)}{dt} = \frac{P_{m,tot}(t) - P_{e,tot}(t)}{2H_{tot}} \quad \text{where} \quad \omega_{COI} = \frac{\sum_i H_i\omega_i(t)}{\sum_i H_i}$$

This means that the machines can be modelled as one single machine with the frequency $\omega_{COI}$, where COI stands for centre of inertia [13].

Including the damping complicates the matter. To maintain the structure, some assumptions are necessary. If $\Delta\omega_i \approx \Delta\omega_{COI}\ \forall i$, then $D_{tot} = \sum_i D_i$ can be used. This does not mean that all machines must have the same frequency, only that the difference between machines is small in comparison with the deviation from the nominal frequency. Another assumption leading to the same result is $D_i = D_0 H_i\ \forall i$. This is somewhat reasonable, since both the damping and the inertia constant tend to scale with the machine power.

Merging several machines into one has its limitations. The damping has already been mentioned. Power transfers between the machiens might not be taken into adequate account since they depend on the phase angle at a node, and therefore the angular frequency. While the frequency at one specific bus can be measured, this is not true for $\omega_{COI}$. To calculate it, not only the speed of all generators is needed, but also their inertia constant $H$. Therefore $\omega_{COI}$ is not known more than approximately. For this model to work well, the frequencies should be fairly close to one another. This is true when there are strong connections between the generators. Even if this might not be true for the entire power grid, it might be for smaller areas in it. Then each area could be modelled as one machine. This could reduce a large power system into just a handful equivalent machines, making it much easier to handle.

## 2.2 Governors

To maintain frequency stability, the governors control the power output of the power plants, based on the frequency deviations. When the frequency lies below the nominal, the power of the turbine is increased, increasing $P_m$ [3, Ch. 11.1]. In this way the produced power is kept the same as the consumed. A block diagram of this is shown in Figure 6.

The steady state response in power to a frequency change is typically proportional and described by the droop factor $R$. A frequency deviation $\Delta\omega$ makes the turbine increase

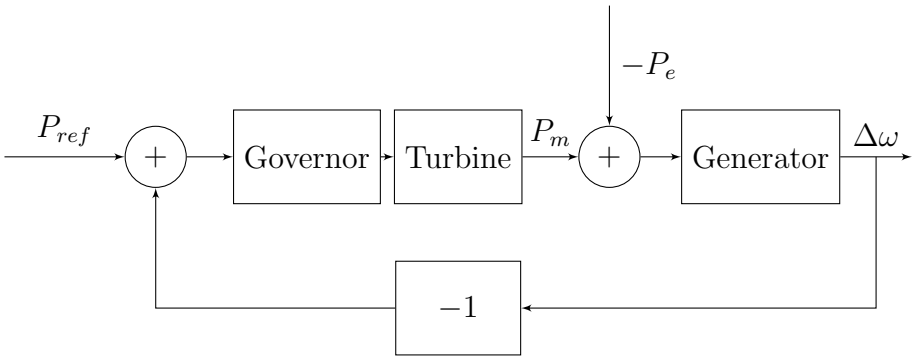


Figure 6: A simple model of the frequency dynamics.

the power input by $\frac{\Delta\omega}{R}$. Everything is given in p.u. This means that the power is increased in proportion to the base power of the generator, given a fixed $R$. A typical value of $R$ is 0.05.

However, this response is not immediate. It may take some time for the governor to respond, and most definitely some time for the turbine to change its power output. There might also be a deadband such that it only reacts when the frequency deviation reaches a certain limit.

The simplest way to model this is as a first order low-pass filter:

$$\Delta P_m = -\frac{1/R}{1 + sT_g}\Delta\omega$$

This model is used for example in [14] for steam turbines. The value of $T_g$ is obviously dependent on the turbine that is modelled, and further models will be discussed. A reasonable range for $T_g$ could be 1-10 s.

The strength of this model is its simplicity. It might however not be very accurate in a realistic situation.

What is discussed here is the primary frequency control (PFC), which acts on the time horizon of seconds. If a disturbance is present for longer time, other control actions are taken. They are slow enough to be neglected in this work, since the inertia is only of interest for the fast dynamics of the power system.

## 2.3 Hydro power plants

Hydro turbines are important in frequency control, and completely dominate in the Nordic system. The other main large-scale type of power production, nuclear, is not used for frequency control here. Therefore, hydro power plants are important to model well. An important characteristic of hydro plants is that they are non-minimum phase due to their physical construction, meaning that when a control action is applied, the initial response is in the opposite direction. The explanation for this is that when the control valve at the bottom of a tall water column is opened to increase the water flow, the pressure initially drops, leading to decreased power output [3, p. 385]. These dynamics puts higher demands on the governor, leading to higher order dynamics.

The so called "Nordic frequency model" is a simplified model of the governor and turbine of a hydro power plant used by Svenska Kraftnät and ENTSO-E [15]. It is presented in Figure 7. The non-linear backlash poses a problem, but can be neglected.

It is also possible to add a D-part to the controller, although it is excluded here. Even without it, the model is fairly complicated with three states.

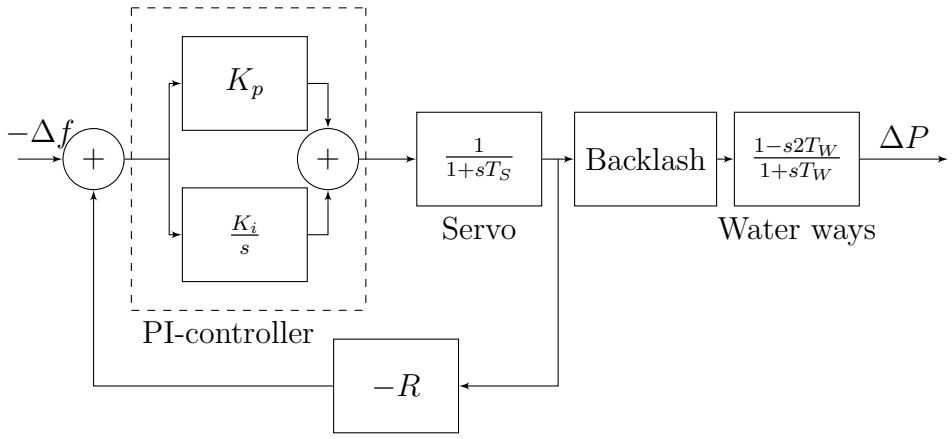


Figure 7: The Nordic frequency model for a hydro governor and turbine. Some typical values are: $K_p = 4$, $K_i = 0.5$, $T_S = 0.2$ s, $T_W = 1$ s and $R = 0.05$.

## 2.4 Steam power plants

The IEEE type G1 steam plant model is recommended by the IEEE Task Force on Turbine-Governor Modeling [16, pp. 2-1−2-3], and is used in the IEEE 39-bus test system model among other [17]. The turbine model is shown in Figure 8 and the governor model in Figure 9. The turbine has four time constants, which represent physical stages in the turbine. A steam turbine typically consists of several blades connected to a shaft, dividing the turbine into segments. The steam flows from one segment to the next, and each time it contributes to the power production.

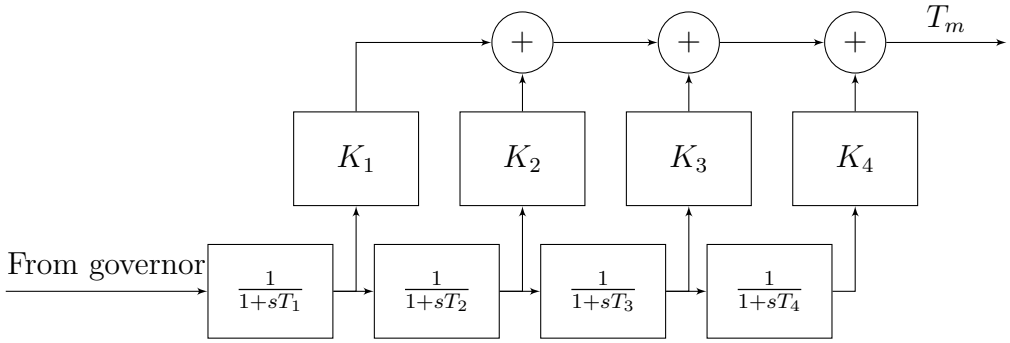


Figure 8: Slightly simplified generic model of a steam turbine. As an example, values used in the IEEE 39-bus test system are: $T_1 = 0.6$ s, $T_2 = 0.5$ s, $T_3 = 0.8$ s, $T_4 = 1$ s, $K_1 = 0.3$, $K_2 = 0.25$, $K_3 = 0.3$ and $K_4 = 0.15$.

A comparison of step responses for different governor and turbine models is given in Figure 10. Notice how the step response for a hydro plant oscillates. This may be useful later for mode detection.

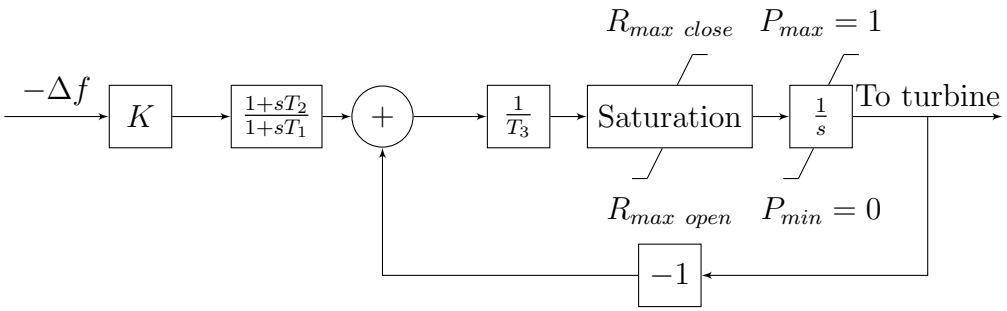


Figure 9: Model for the steam governor in the IEEE type G1 model. As an example, values used in the IEEE 39-bus test system are: $K = 5$, $T_1 = 0.2$ s, $T_2 = 1$ s, $T_3 = 0.6$ s, $R_{max\ open} = 0.3$ p.u./s and $R_{max\ close} = -0.3$ p.u./s.

## 2.5 Transmission

Although a transmission line has series resistance, shunt capacitance and series inductance, the latter is typically dominating. This means that often it suffices to model the line as a pure inductance without any losses.

The active power transmitted on a line is described by the following equation [12, Ch. 6]:

$$P_{12} = \frac{V_1^2}{|Z|}\cos(arg(Z)) - \frac{V_1 V_2}{|Z|}\cos(\theta_1 - \theta_2 + arg(Z)) \tag{2}$$

where $P_{12}$ is the power transmitted from bus 1 to 2, $Z$ is the impedance of the line, $V_1$ and $V_2$ the voltages at bus 1 and 2, and $\theta_i$ their phase angles. The angles are given by $\frac{d\theta}{dt} = \omega$ where $\omega$ is the frequency at the bus.

In the case of a purely inductive line with the reactance $X$, nominal voltages ($V_1 = V_2 = 1$ p.u.), and introducing $\delta_{12} = \theta_1 - \theta_2$, the equation simplifies to (3).

$$P_{12} = \frac{1}{X}\sin(\delta_{12}) \tag{3}$$

Linearised around $\delta_{12,0}$, it simply becomes $\Delta P_{12} = \frac{\cos(\delta_{12,0})}{X}\Delta\delta_{12}$.

A complimentary equation gives the transfer of reactive power:

$$Q_{12} = \frac{V_1^2}{|Z|}\sin(arg(Z)) - \frac{V_1 V_2}{|Z|}\sin(\theta_1 - \theta_2 + arg(Z))$$

Using these two equations for each node in a power system, an equation system can be set up for the power system. Each node has two known and two unknown of the following variables: active power $P$, reactive power $Q$, the angle $\delta$ and the voltage $V$. That is, for each generator there are two unknown variables and two equations (one for active and one for reactive power). The nodes can be of three types:

- swing node (only 1 in each system), where $V$ and $\delta$ are known (reference angle);
- PV node, where $P$ and $V$ is known (typically a generator with voltage control);
- PQ node, where $P$ and $Q$ is known (typically a load).

Solving this equation system is called the load flow problem and is solved numerically. The load flow problem is solved to get the operating point of the system.

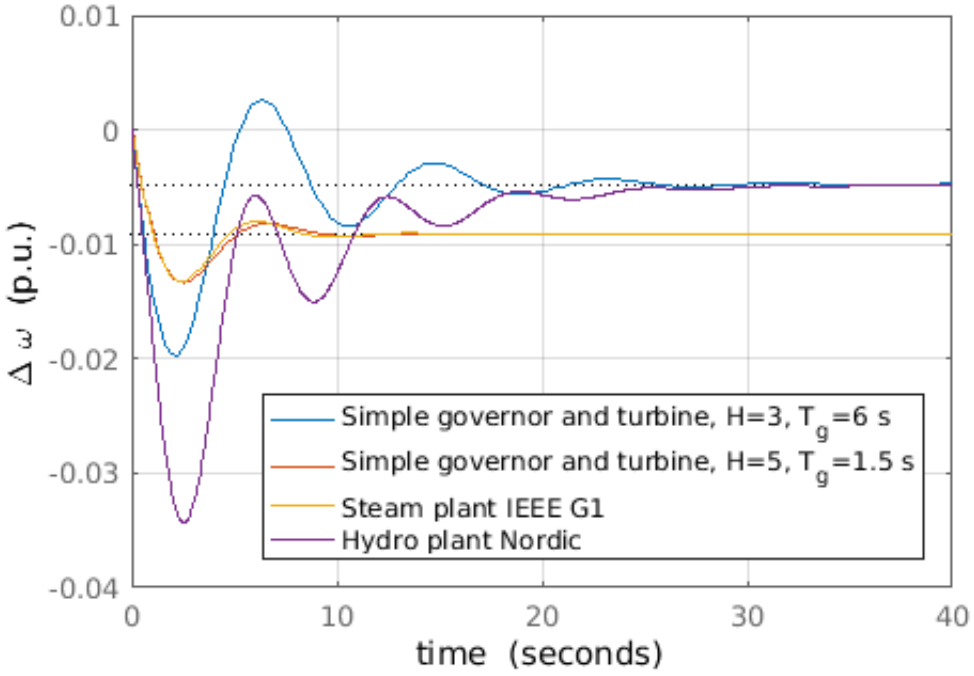


Figure 10: Comparison of step responses for different types of governors and turbines.

## 2.6 Transformers

Transformers are another important part of the transmission system, which are described by complicated physics. A linearised equivalent circuit is given in [12, Ch. 3.2] and presented in Figure 11. For power system analysis a simplification is often sufficient. The entire transformer is approximated by one inductance $X_{eq} = X_1 + \left(\frac{N_1}{N_2}\right)^2 X_2$, where the scaling factor disappears when p.u. is used. This inductance can then simply be merged with the power line.

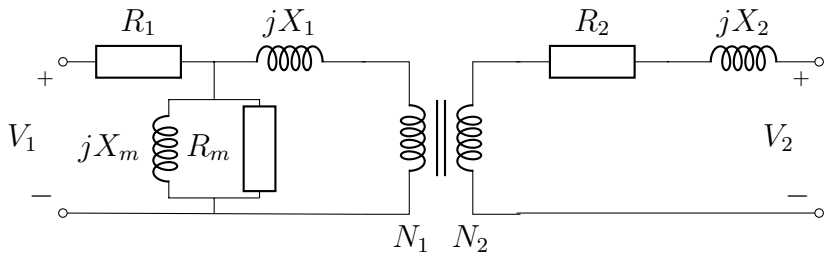


Figure 11: A linear equivalent circuit for a transformer.

## 2.7 Excitation system

The DC field current of a synchronous machine that generates the magnetic field in the rotor is provided by an excitation system. By means of controlling the field current, the terminal voltage and reactive power can be controlled. The voltage also affects the active

power transfer, as given by (2). An excitation system consists of the following parts [3, Ch. 8]:

- Exciter – This is the actuator of the excitation system that provides the field current.
- Regulator – This is the control stage of the excitation system. The input signal is the terminal voltage that is controlled.
- Terminal voltage transducer – This part senses the terminal voltage and converts it to a DC signal.
- Power system stabiliser (PSS) – This provides additional control to damp oscillations and improve stability of the system.
- Limiters and protective circuits – These maintain the exciter and synchronous machine within safe operational limits and are normally distinct circuits.

A model for an excitation system is the IEEE type 1 model [18, Ch. 8]. It is presented in Figure 12. The terminal voltage transducer is not included, the signal $\Delta V_T$ is simply assumed to be available. PSS's and limiters are not used. The regulator is divided into two parts, the stabiliser and the amplifier.

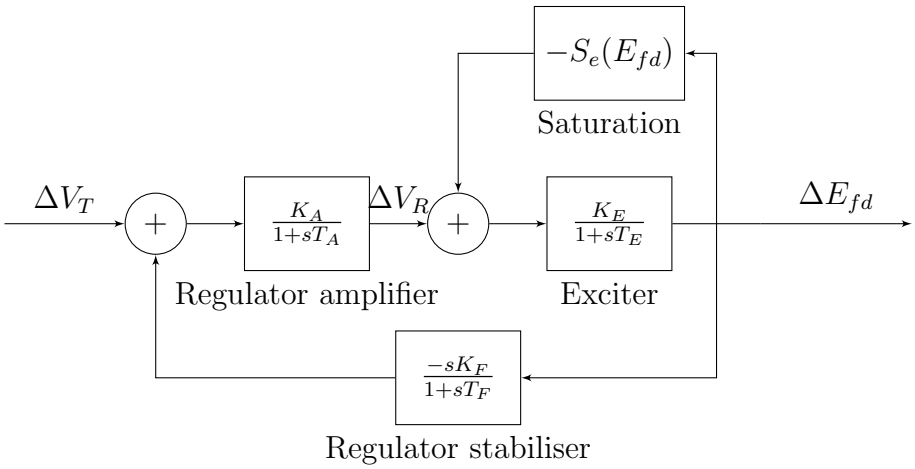


Figure 12: IEEE type 1 exciter system model.

The exciter is typically fast, and a (not too big) disturbance in voltage is most often handled in about a second. Therefore, when not considering fast dynamics, the voltage at a generator bus can be assumed to be at its set point.

## 2.8 System model

A linearised system consisting of above models can be written on state-space form [3, Ch. 12]. Consider a system modelled as a single generator where the governor and the turbine are described by a simple low-pass filter. In combination with the swing equation (1), it becomes the following on state-space form:

$$2H\Delta\dot{\omega} = \Delta P_m - \Delta P_e - D\omega$$

$$\Delta P_m = \frac{-R^{-1}}{1+T_g s}\Delta\omega \quad \xrightarrow{\mathcal{L}^{-1}} \quad \Delta\dot{P}_m = \frac{-1}{T_g}\Delta P_m - \frac{-1}{RT_g}\Delta\omega$$

Written with matrices, this becomes:

$$\begin{bmatrix} \Delta\dot{\omega} \\ \Delta\dot{P}_m \end{bmatrix} = \begin{bmatrix} -\frac{D}{2H} & \frac{1}{2H} \\ \frac{-1}{RT_g} & \frac{-1}{T_g} \end{bmatrix} \begin{bmatrix} \Delta\omega \\ \Delta P_m \end{bmatrix} + \begin{bmatrix} -\frac{1}{2H} \\ 0 \end{bmatrix} \Delta P_e \tag{4}$$

In a system modelled as two generators connected, the angle $\delta$ is also needed in the equation, to account for the transmission of power between the two generators. This gives in total three states for each generator. One angle state can be removed, since only the difference in angle is important. Doing this would remove one eigenvalue at 0, but at the price of symmetry. The resulting system on state-space form is:

$$\begin{bmatrix} \Delta\dot{\omega}_1 \\ \Delta\dot{\delta}_1 \\ \Delta\dot{P}_{m,1} \\ \Delta\dot{\omega}_2 \\ \Delta\dot{\delta}_2 \\ \Delta\dot{P}_{m,2} \end{bmatrix} = \begin{bmatrix} -\frac{D_1}{2H_1} & -k_1 & \frac{1}{2H_1} & 0 & k_1 & 0 \\ 2\pi f & 0 & 0 & 0 & 0 & 0 \\ \frac{-1}{R_1 T_{g,1}} & 0 & \frac{-1}{T_{g,1}} & 0 & 0 & 0 \\ 0 & k_2 & 0 & -\frac{D_2}{2H_2} & -k_2 & 0 \\ 0 & 0 & 0 & 2\pi f & 0 & 0 \\ 0 & 0 & 0 & \frac{-1}{R_2 T_{g,2}} & 0 & \frac{-1}{T_{g,2}} \end{bmatrix} \begin{bmatrix} \Delta\omega_1 \\ \Delta\delta_1 \\ \Delta P_{m,1} \\ \Delta\omega_2 \\ \Delta\delta_2 \\ \Delta P_{m,2} \end{bmatrix} + \begin{bmatrix} -\frac{1}{2H_1} & 0 \\ 0 & 0 \\ 0 & 0 \\ 0 & -\frac{1}{2H_2} \\ 0 & 0 \\ 0 & 0 \end{bmatrix} \begin{bmatrix} \Delta P_{e,1} \\ \Delta P_{e,2} \end{bmatrix} \tag{5}$$

where $k_i = \frac{V_1 V_2 cos(\delta_0)}{2XH_i}$ and $X$ is the reactance of the transmission line.

The same method may also be generalised to an arbitrary number of generators. The modelling of the governor and turbine may also be replaced by any of the previously discussed models. This would lead to more states and more complicated matrices. Different models may be used for different parts of the system and some generators may not have frequency control. More advanced dynamics, e.g. the flux in the generator and the excitation system, can introduce even more states. However, these dynamics are fast and only have a small effect on the overall behaviour and in certain cases. In these cases, it often has the effect of causing damping.

### 2.8.1 Eigenvalues and eigenvectors

As is normally the case with state-space models, the eigenvalues and eigenvectors of the A-matrix provide useful insight into the behaviour of the system [3, Ch. 12]. Knowing these, it is possible to give an approximate description of how the system reacts to an input, i.e. how the frequency is affected by the power. Especially interesting are complex eigenvalues that correspond to oscillating modes. Their absolute values correspond to their undamped natural angular frequencies ($\omega_0$), their imaginary values to their damped natural frequency, and the minus cosinus of their arguments correspond to their damping ratio.

For example, the system in (4) has the eigenvalues

$$-\frac{D}{4H} - \frac{1}{2T_g} \pm \sqrt{\left(\frac{D}{4H} + \frac{1}{2T_g}\right)^2 - \frac{R^{-1}+D}{2HT_g}}$$

Table 2: Modes of a 2-generator system. The three states for the first generator are followed by the three states of the second. For each generator they are in the order: $\Delta\omega$, $\Delta\delta$ and $\Delta P$.

| eigenvalue | absolute value | damping ratio | eigenvector | participation vector |
|---|---|---|---|---|
| $-0.0746 \pm 13.5528i$ | 13.5530 | 0.00550 | $\begin{bmatrix} -0.0002 \pm 0.0345i \\ 0.7994 \\ -0.0073 \mp 0.0001i \\ 0.0001 \mp 0.0258i \\ -0.5992 \pm 0.0019i \\ 0.0054 \end{bmatrix}$ | $\begin{bmatrix} 0.2859 \mp 0.0023i \\ 0.2851 \pm 0.0012i \\ 0.0007 \\ 0.2141 \mp 0.0004i \\ 0.2137 \pm 0.0016i \\ 0.0004 \end{bmatrix}$ |
| $-0.1428 \pm 0.6389i$ | 0.6546 | 0.218 | $\begin{bmatrix} -0.0003 \pm 0.0014i \\ 0.7069 \mp 0.0002i \\ -0.0064 \mp 0.0014i \\ -0.0003 \pm 0.0014i \\ 0.7073 \pm 0.0002i \\ -0.0064 \mp 0.0014i \end{bmatrix}$ | $\begin{bmatrix} -0.1938 \mp 0.0912i \\ -0.0357 \\ 0.2261 \pm 0.1063i \\ -0.2587 \mp 0.1217i \\ 0.0357 \\ 0.2263 \pm 0.1065i \end{bmatrix}$ |
| -0.1425 | 0.1425 | 1 | $\begin{bmatrix} 0.0001 \\ -0.1715 \\ -0.6860 \\ -0.0001 \\ 0.1715 \\ 0.6860 \end{bmatrix}$ | $\begin{bmatrix} 0 \\ 0.0011 \\ 0.4988 \\ 0 \\ 0.0011 \\ 0.4989 \end{bmatrix}$ |
| 0 | 0 | – | $\begin{bmatrix} 0 \\ -0.7071 \\ 0 \\ 0 \\ -0.7071 \\ 0 \end{bmatrix}$ | $\begin{bmatrix} 0 \\ 0.5 \\ 0 \\ 0 \\ 0.5 \\ 0 \end{bmatrix}$ |

If it is not overdamped, this corresponds to the (undamped) natural angular frequency $\omega_0 = \sqrt{\frac{R^{-1}+D}{2HT_g}}$ and the damping ratio $\zeta = \frac{\frac{D}{4H}+\frac{1}{2T_g}}{\omega_0}$. Therefore, it can in this case be concluded that the frequency of the step response is proportional to $\sqrt{\frac{1}{H}}$.

The eigenvectors give the activity of the mode in each state, which is a measure on how large effect the mode has on this state. For an oscillation, the absolute values of the eigenvector give the magnitude of the oscillation in the states, and the arguments give the phase.

In the case with 2 generators in (5), it is too difficult to calculate the eigenvalues analytically. A numerical calculation with $D = 1$, $T_g = 7$ and $R = 0.05$ for both generators, $X = 0.5$ and $H_1 = 3$ and $H_2 = 4$ gives the eigenvalues and eigenvectors presented in Table 2.

The corresponding step response is given in Figure 13. The step response consists of two overlaid sinusoids, each corresponding to one pair of eigenvalues.

There are two complex eigenvalues pair. The first corresponds to a fast oscillation

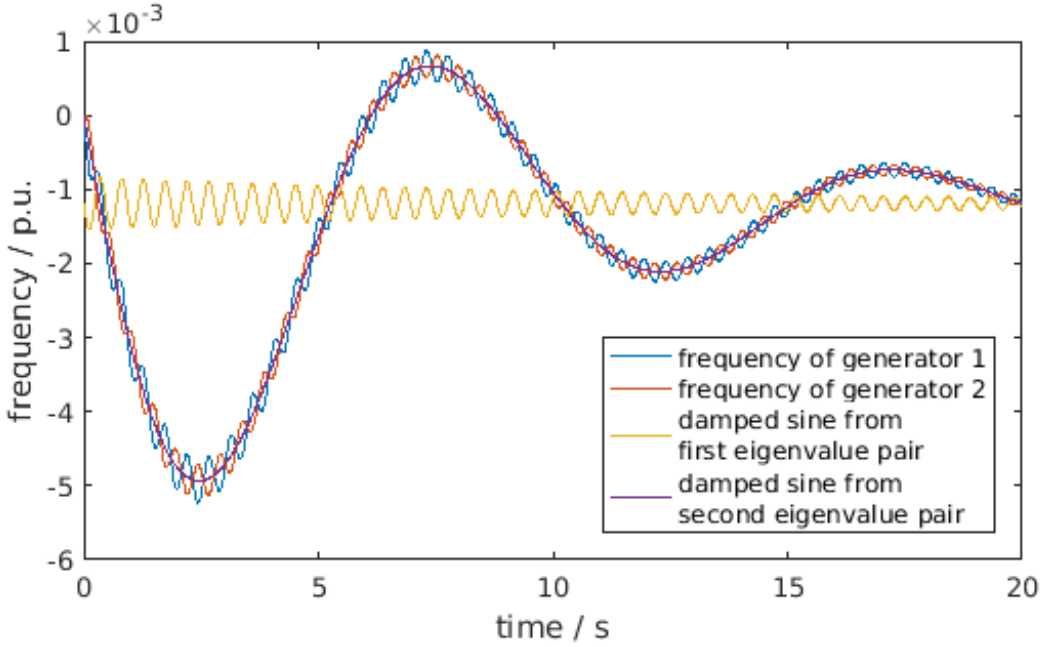


Figure 13: The step response for two connected generators.

between the generators. This can be seen by the high natural frequency of the eigenvalue and the low damping, both matched in the step response. In the corresponding eigenvector, the states of the two generators have opposite signs, meaning that there is a phase difference of 180°.

The second eigenvalue pair corresponds to the slower, larger more damped mode. Here the generator masses move together as one and this is therefore called the rigid body mode. Once again, the eigenvalue and the step response match. In the eigenvector, both generators have the same sign and similar size, which means that they oscillate in phase.

The non-oscillatory (real) eigenvalue seems to correspond to the difference in power between the two generators, which decays to zero with the time constant 0.1425. This is not very interesting.

The eigenvalue 0 corresponds to the fact that the absolute angles drift when the frequency is below nominal, but only the relative angles matter and this does in no way affect the system.

The scaling of the different variables in the eigenvectors depends on the units used. To rescale them and get a measurement of how much each state participates in a node, the columns of the participation matrix $\mathbf{P}$ can be used. It is found as $\mathbf{P} = \mathbf{\Psi}^T \circ \mathbf{\Phi}$, where $\mathbf{\Phi}$ is the matrix with the right eigenvectors as columns, $\mathbf{\Psi} = \mathbf{\Phi}^{-1}$, and $\circ$ denotes the elementwise product. These vectors are dimensionless and normalised such that the sum equals 1.

Using this, it can for example be seen that the governors practically do not participate in the oscillation between the generators. This means that the realisation of the governor and turbine does not affect this oscillation.

It also shows that the second mode is an oscillation between the rotor speed and the governor and turbine, without the angle. They have their respective output and input connected, which explains why they oscillate.

It should also be noted that the first generator participates more in the oscillation between the two generators. Looking at the eigenvector, the generator with $H = 3$ has $4/3$ times the activity of the generator with $H = 4$ in the frequency and angle. This is due to its lower $H$ which means that the same difference in energy results in a larger change in frequency in this generator. This can be shown by looking at the expression for rotational energy $E_r$:

$$E_r = \frac{J\omega^2}{2} = \frac{HS\omega^2}{\omega_0^2} \Rightarrow \frac{dE_r}{d\omega} = \frac{2HS\omega}{\omega_0^2} \Rightarrow d\omega = \frac{dE_r}{2HS\omega/\omega_0^2}$$

## 2.9 Variability of load

The load power has variations over time, which leads to variations of the frequency. An example of how the frequency varies under normal operation is shown in Figure 14. These variations will be used for estimation. The noise characteristics are not necessarily the same at all times of the day and year.

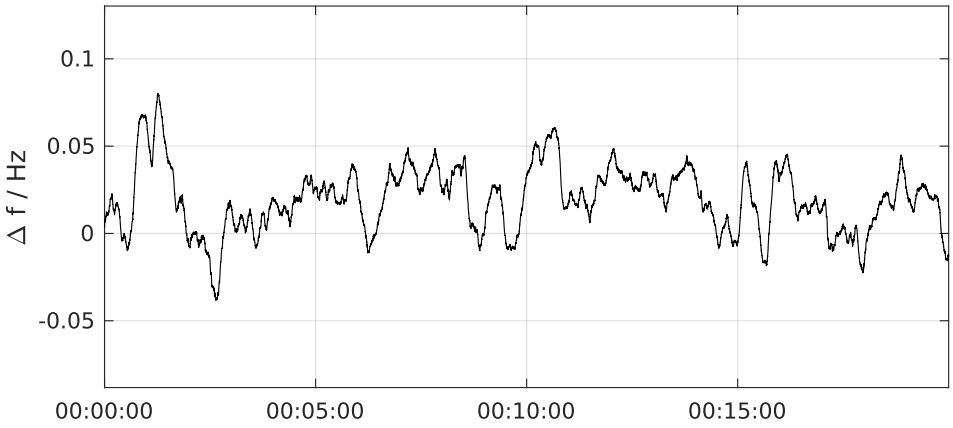


Figure 14: Frequency deviations from 50 Hz during 20 minutes on June 1, 2005, measured in Lund.

The program ARISTO [19] is considered to have a realistic noise model and is used to model this. The model is based on an ARMA-model [20]:

$$y(k) = -a_1 y(k-1) - a_2 y(k-2) + b_0 e(k) + b_1 e(k-1) + b_2 e(k-2) \tag{6}$$

where $y$ is the load variation, $e$ is white noise with standard deviation $K_n$ and $k = nT_s$. The parameters are listed in Table 3. Unfortunately, this model is based on a low sampling time, a few seconds, leaving the question of what the noise characteristics are above the Nyquist frequency of this model unanswered. The way ARISTO handles it is by zero-order hold interpolation between the noise levels, i.e. only updating the power every $T_s$ second and keeping it constant in between. It may be noted that this model corresponds well to a continuous model of white noise filtered through a first order filter with corner frequency $0.15/T_s$. In Figure 15 the spectrum of the stochastic load noise in ARISTO is shown and compared to a continuous low-pass filter. As can be seen, both interpolations are similar, with the difference that the zero-order hold interpolation in ARISTO gives rise to notches and valleys. It must be considered very dubious that such irregularities

Table 3: Parameters for the ARISTO model of stochastic load variations.

| **notation** | **name** | **typical range** |
|---|---|---|
| $K_n$ | noise level | 0.02 – 0.1 |
| $T_s$ | sampling time | 1 – 3 |
| $a_1$ | filter constant | -0.7 |
| $a_2$ | " | -0.14 |
| $b_0$ | " | 0.22 |
| $b_1$ | " | 0.075 |
| $b_2$ | " | 0 |

exist in a real spectrum, and especially if several loads are combined with different $T_s$ and are out of sync. Then the continuous extrapolation is probably a more realistic model.

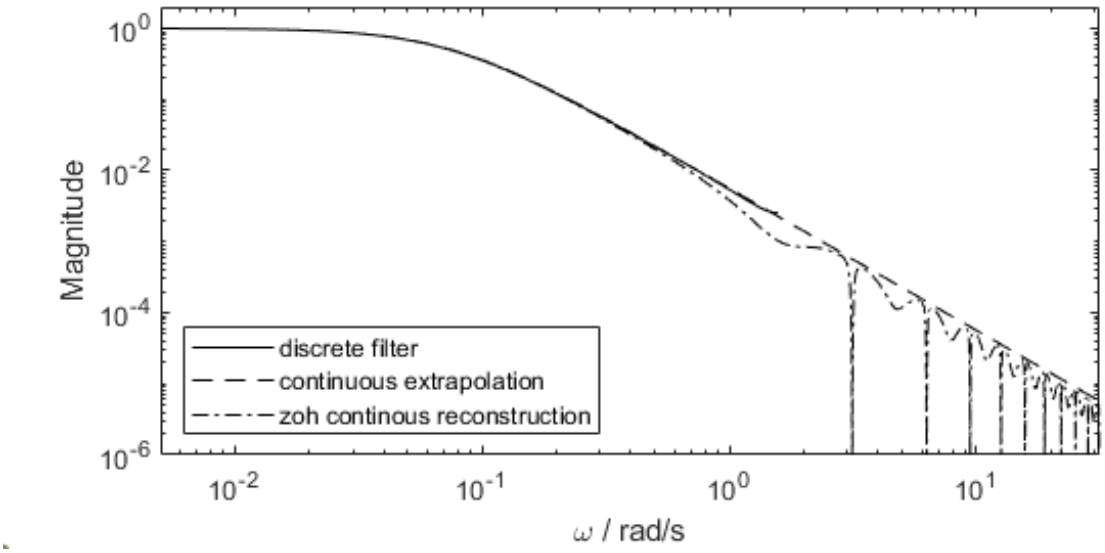


Figure 15: Spectrum of the stochastic load variations in ARISTO.

Another way to model the stochastic load variations is to calculate the spectrum of measured grid frequency. Doing this shows that it varies approximately as low-pass filtered white noise with corner frequency 0.1 rad/s, and on top off that some oscillations (presumable from modes). This is illustrated in Figure 16. The roll-off after the corner frequency is 40 dB/decade.

Unlike the spectrum in Figure 15 which is calculated from the power, this is calculated from the frequency. That means that the power noise is filtered through the system. Based on the hydro model in Figure 7, the spectrum of the system transfer function is flat until $\approx 1$ rad/s, where there is a bump due to the rigid body mode, and then it falls with 20 dB/decade. To explain the roll-off in Figure 15, a steeper roll-off is needed than in the ARISTO model, at least for frequencies $< 1$ rad/s. A simple model is therefore a second order low pass filter with corner frequency 0.1 rad/s. However, for higher frequency where the system transfer function provides a roll-off of 20 dB/decade, only 20 dB/decade is needed in the noise, as in the ARISTO model. Therefore, the 40 dB/decade-model is less reliable for frequencies significantly above 1 rad/s.

The frequency measurements also show the magnitude of the stochastic variations. The fast frequency deviations rarely reach 0.1 Hz, as the regulations stipulate, but peak values of 0.05 Hz deviations from the mean is not uncommon. When simulating, the magnitude of the power variations can be chosen such that the deviations are of this size.

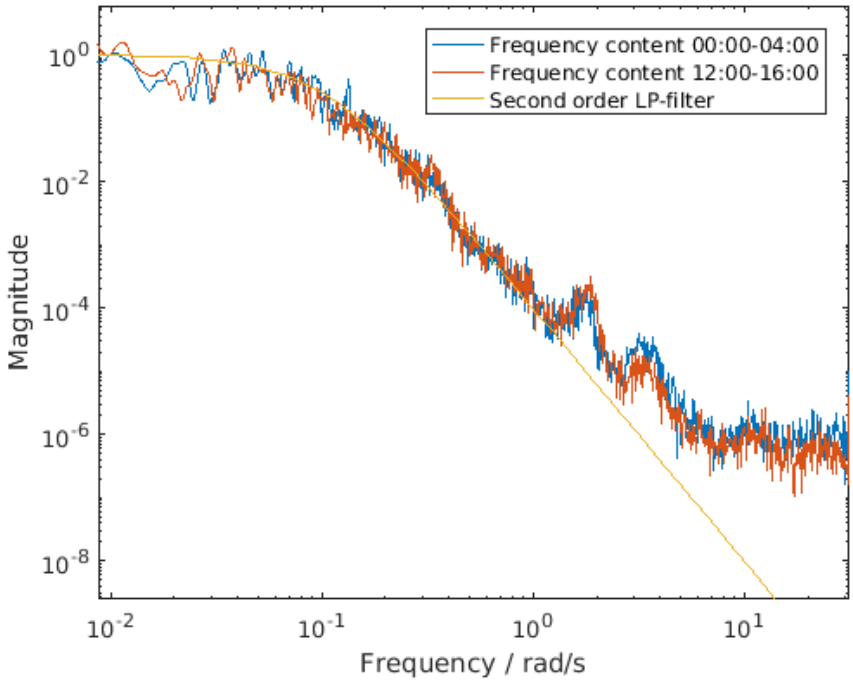


Figure 16: Spectrum of measured ambient frequency variations on June 1 2005. Notice the peaks due to oscillatory modes.

Another possibility is to purposefully vary the power balance. This can be achieved by for example HVDC links which are controllable. However, these links are few and it will not be possible to choose where the disturbance occurs. Therefore, it might not be guaranteed that all modes in the system are excited.

The induced disturbances will most likely be step disturbances, due to the wide frequency content and since they are easy to cause. If control permits, other kinds of disturbances could also be considered, e.g. white noise which also has wide frequency content. The choice of disturbance also depends on what the system operator can accept.

If a HVDC link is used to create a disturbance, the input signal can be known. Therefore, the task is of a different nature than if the input signal is unknown. Nevertheless, the proposed method still works. It should be noted that it also opens up for a wider range of methods, such as those earlier proposed in literature [7, 8, 9]. The possibilities this leads to will not be further considered in this thesis.

## 2.10 Measurements

The method employed in this thesis can rely solely on frequency measurements. This is one of its main advantages. Frequency varies little in a given geographical area and across different voltage levels. Therefore, measurements could theoretically be done more or less anywhere in the approximately right area. In contrast, voltage may be heavily affected

by a weak grid, by load close to the measurement point and transformer settings. To measure power flow, more advanced equipment installed at the right position is needed. Still, there may be some local disturbances caused by short circuits, topology changes, and energisation of transformers among other phenomena [21]. These often have high-frequency characteristics and can be filtered away.

Phasor measurement units (PMUs) are standard equipment for measuring frequency among other things in a power system. Measurements from a reasonable amount of PMUs can be assumed to be available.

All measurements have limitations and are subject to noise from disturbances, inaccuracies in the measurements and other things. Most simply, this is modelled as white measurement noise. Typically, the signal is filtered in some way to smoothen it [21].

The sample time of the measurements is most likely determined by the equipment. Nevertheless, high sampling rates are not necessarily desired, and the measurements should rather be downsampled. This is typically what is done in previous research on mode identification (e.g. in [22] and [23]). Faster sampling rates means fewer cycles for measuring the frequency and larger error, while adding little if the sampling already is significantly faster than the frequencies of interest. Its purpose would then mainly be to sample high-frequency noise without aliasing in order to filter it away. Standard sampling rates are for PMUs 10, 20, 50 and 100 Hz for a 50 Hz system [24], but other equipment might use other sampling rates. Still, somewhere around 10 Hz is a reasonable value also for equipment used for local control, and if the sampling rate is higher it is possible to downsample.

An expected accuracy of the measurements should be around 10 mHz, i.e. a maximum error of 5 mHz [21, 24]. However, it is of less importance to know the true frequency, what matters is the change of frequency. Therefore, accuracy is not the main interest but rather the precision. A number on that is typically less available. It is quite possible that the precision would be close to the resolution of the measurement equipment. This could be 1 mHz for a commercial PMU.

Some other measurements of dynamic parameters are also necessary to construct the model. These measurements correspond to the steady state around which the system is to be linearised. The values in question are: power output of generators (at least those used in control), phase angles and/or power flows between areas and possibly some voltages. It might seem like this contradicts the previously stated advantage of the method that it does not require power measurements. However, these measurements are not necessarily done continuously, and a larger error can be tolerated. The small variations in steady state are not necessary to detect, but rather the total value, leaving space for larger measurement errors. The values are also typically available through a state estimator [25].

# 3 The dependency of the modes on system parameters

To use the eigenvalues of the system matrix for parameter estimation, it is useful to understand how the values of the parameters affect the modes. Unfortunately, the matrix quickly grows too large to calculate the eigenvalues analytically. Equations of the fifth order or higher are famously impossible to solve in the general case [26], meaning that the characteristic equation of system matrices of systems with five or more states cannot be solved for the eigenvalues. Therefore, approximations and empirical studies are necessary.

The analysis starts with a simple governor and turbine model, and then proceeds to the more complicated Nordic frequency model for hydro governors from section 2.3. The rigid body mode and inter-generator modes are considered separately. The former is present in systems with only one generator, making it a natural starting point. When more generators are added, inter-generator modes arise as well.

To illustrate how the modes are affected by the parameters, root-locus plots are used. They show how the eigenvalues move when a parameter changes.

## 3.1 Simple governor and turbine

The earlier presented system where the governor and turbine were modelled as one low-pass filter is a useful starting point. Even in this simple case, analytical methods fail when there are two or more generators. The system then has six states (although one may be removed), and the eigenvalues cannot be found analytically. However, it is possible to find approximate formulae for the eigenvalues empirically.

### 3.1.1 Rigid body mode

As already noted in section 2.8, the oscillation angular frequency in the case of one generator was $\omega_0 = \sqrt{\frac{R^{-1}+D}{2HT_g}}$. The structure of this expression is logical. A larger $H$ makes the dynamics slower, since more mass needs to be accelerated and decelerated. A larger $T_g$ makes the power response slower, and likewise the oscillations. The stationary frequency after a disturbance is determined by $R^{-1} + D$. If this term is larger, then the power response is more powerful, resulting in faster oscillations. The square-root can be explained by the fact that the energy is proportional to $\omega^2$.

It would be useful to generalise this to two or more generators. In that case there is one mode corresponding to the dynamics of the frequency of the centre of inertia, i.e. all generators together in phase, called the rigid body mode. In Figure 13 this is the large, slow oscillation. The mode can be described by generalising the expression for one generator. Its frequency can be well estimated by the expression (7).

$$\omega_0 = \sqrt{\left(\sum_i \frac{(R_i^{-1} + D_i)S_i}{2T_{g,i}}\right) \frac{1}{\sum_i H_i S_i}} \tag{7}$$

The sum $\sum_i H_i S_i$ is a measure of the total inertia of the system.

Equation (7) was confirmed by Monte-Carlo simulations of 100 systems with 5 generators. For each system a random set of parameters were generated. The parameters were in the following intervals: $H \in [0.5, 16]$, $S \in [0.5, 4]$ $D \in [0, 4]$, $T_g \in [5, 15]$ and

$R \in [0.02, 0.1]$. It was checked if the system was stable, otherwise it was discarded and replaced by another system. For each system the actual rigid body eigenvalue was found from the system matrix and it was compared to the value given by equation 7. This gave a mean error of 0.23%. The largest error was 0.69%.

### 3.1.2 Inter-generator oscillation

The oscillation between two generators can be approximated by (8). It can also be derived analytically by setting up a four-state system without governors or damping. The rationale for excluding the frequency control is that it was seen in section 2.8 that it did not participate in the inter-generator oscillation. It can then be confirmed empirically in simulated systems with governors and damping.

$$\omega_0 \approx \sqrt{\frac{2\pi f V_1 V_2}{2X}\cos(\delta_0)\left(\frac{1}{H_1}+\frac{1}{H_2}\right)} \tag{8}$$

As stated, the governor and turbine dynamics are not present in (8) and do not affect the oscillation frequency noticeably. This is due to the fact that the oscillation is too fast for the governors to react. It is also worth noticing that the lowest inertia has the highest influence on the frequency. However, the lower the inertia on one side, the lower the activity of the mode. That is, as the inertia of one generator decreases towards zero, the frequency of the oscillation increases towards infinity, but at the same time its activity decreases towards zero and the mode disappears. Without any inertia there is no oscillation.

When there are more than two generators involved in the oscillation, the simple expression does not work. A source of difficulty is that the generators do not participate equally in the oscillation. There are two groups of generators, at approximately 180°-phase difference, but although generators in one group are in phase, they may oscillate with different amplitude. To further complicate the issue, the participation in the oscillation changes when the parameters, including $H$, vary. An exception is if the generators are sufficiently closely connected to be modelled as one, i.e. having (almost) the same frequency.

An example of a root-locus plot for a system with 3 generators where the eigenvalues are plotted as $H$ changes is shown in Figure 17 and 18. The rigid body mode is still described by equation (7), but the dependence on $H$ of the inter-area modes is clearly non-linear and complicated. The same thing is true for the mode activity. It is normalised by multiplying the activity with $H_i$ for each node and dividing by the sum of the absolute values of all. This gives equal amount of normalised activity for each group that is oscillating against the other.

The mode frequency seems to correlate somewhat linearly with $\sqrt{\sum_i \frac{NA_i}{H_i}}$, where $NA_i$ is the normalised activity, a generalisation from equation (8), but the deviations from linearity are non-negligible. There does not seem to be any simple formula describing the modes in this case.

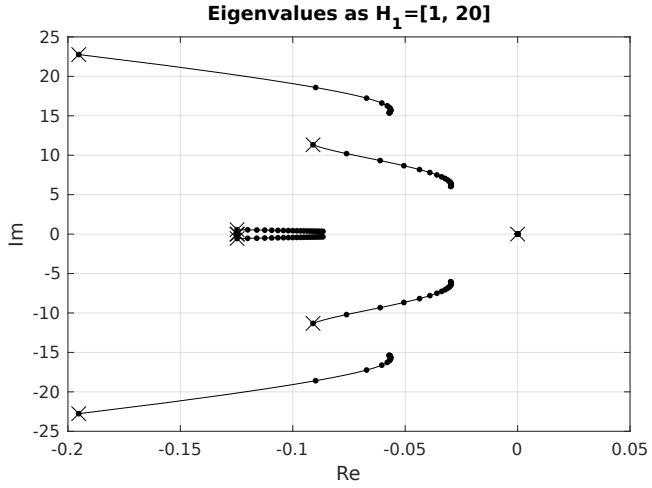


Figure 17: Root-locus plot for a system consisting of three generator, with $H_2 = 4, H_3 = 7, D = 1, R = 20, T_g = 8$. Generator 2 is connected to the other generators with $X$=0.4 p.u., while generators 1 and 3 are not connected. The crosses mark the lowest parameter values. Dots mark integer values of $H_1$.

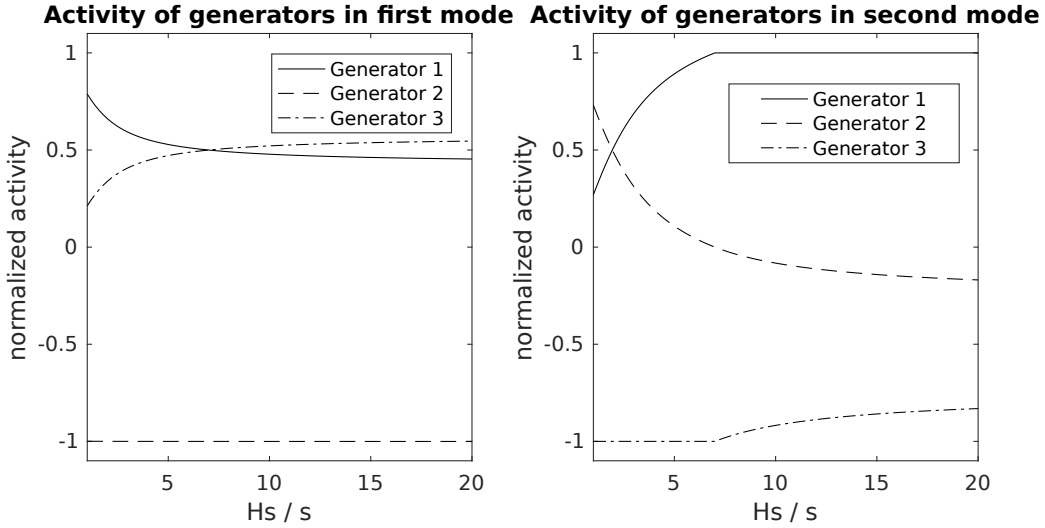


Figure 18: The change of activity in the inter-generator modes of a three generator system as $H$ changes.

## 3.2 Hydro plants for frequency control

The model presented in 2.3 will be used here.

### 3.2.1 One-generator system

Root-locus plots for a one-generator system are shown in Figures 19 and 20. There are four eigenvalues, two real and one complex pair. The largest real eigenvalue has close to no effect on the step response. This can be seen by calculating the transfer function, removing it, and confirming that the step response looks the same. The other three, however, are not too different in magnitude, although the complex pair seems to be of

larger importance in most cases. If the system contains many generators, the activity is the same in all generators for both the complex pair and the real eigenvalue. Calculating the transfer function and removing the other eigenvalues gives the centre of inertia-response. Therefore, it can be said that all are rigid body eigenvalues. The complex pair is more important and will also be shown to be easier to estimate.

One important observation is that the relation is highly non-linear and it was not possible to determine any formula describing it. Some qualitative remarks can nevertheless be made. A higher $H$ clearly means a lower frequency, at least to a certain extent before the imaginary part flattens out for high $H$. This is the same as seen previously. The damping ratio is also improved initially, but for sufficiently large $H$ it decreases. Therefore, when it is most important to estimate $H$, i.e. when $H$ is small, the damping ratio is low. This is an important observation, since it is typically easier to estimate eigenvalues with low damping ratio.

Varying $D$ probably gives the strangest result of all parameters. The complex eigenvalues vary in a quite unpredictable way. A more important conclusion is that for larger $D$, the real eigenvalue becomes more dominant, and stops any oscillation in the step response. This corresponds to what one might expect given that $D$ is the damping of the generator. Due to behaviour as this, it should be noted that it is hard to read the step response from the root-locus plots.

An increasing $T_W$ worsens the damping ratio, and even risks leading to instability, while it also slows down the system. Both effects are expected, the former since it means moving a zero further into the right half-plane and the latter since it means an increasing time constant of the pole.

A higher $K_p$ means a faster oscillation, but worsens the stability, as is often the case with P-controllers. But with a too small $K_p$ the system oscillates more as well, due to insufficient control, and the best result is given with a $K_p = 3 - 4$.

The most important contribution of $K_i$ is to make the slower real mode faster. This means that the frequency reaches its final value faster, as is typically the case with and purpose of I-controllers. It may also decrease the damping ratio as an adverse effect.

$T_S$ mostly affects the faster mode which has little effect on the step response. More interestingly, a large $T_S$ makes the oscillation slower and less damped. This is what can be expected of a delay.

The most important effect of $R$ on the step response is that it determines the final frequency error, which is not well reflected in the modes, which change little as $R$ is varied. The damping ratio increases somewhat with larger $R$ which corresponds to less control response.

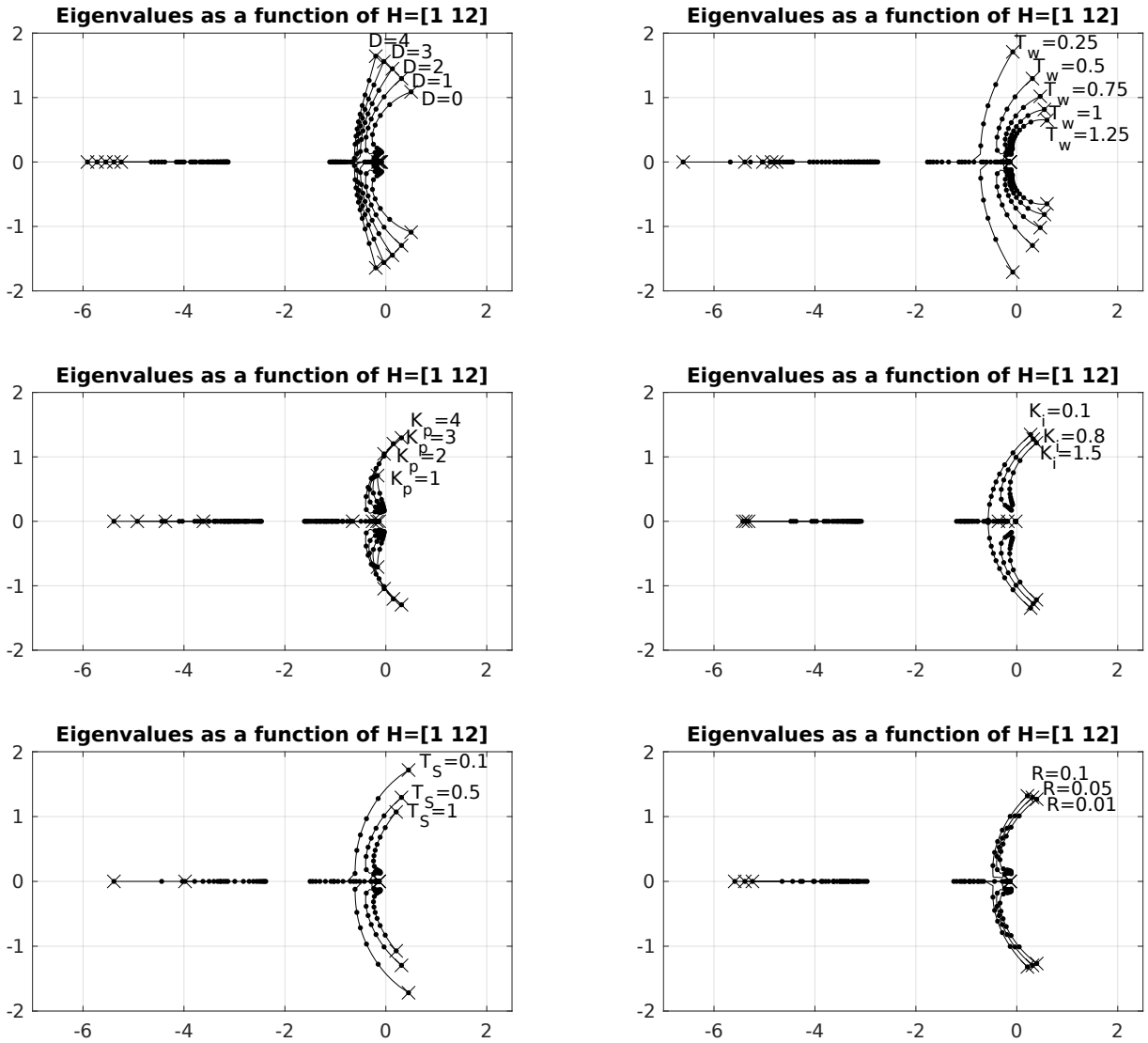


Figure 19: Root-locus plots for a system consisting of one generator, with varying $H$, and the nominal values $D = 1, R = 0.05, K_i = 0.6, K_p = 4, T_S = 0.5, T_w = 0.5$. The circles mark the lowest parameter values. Dots mark integers values of $H$.

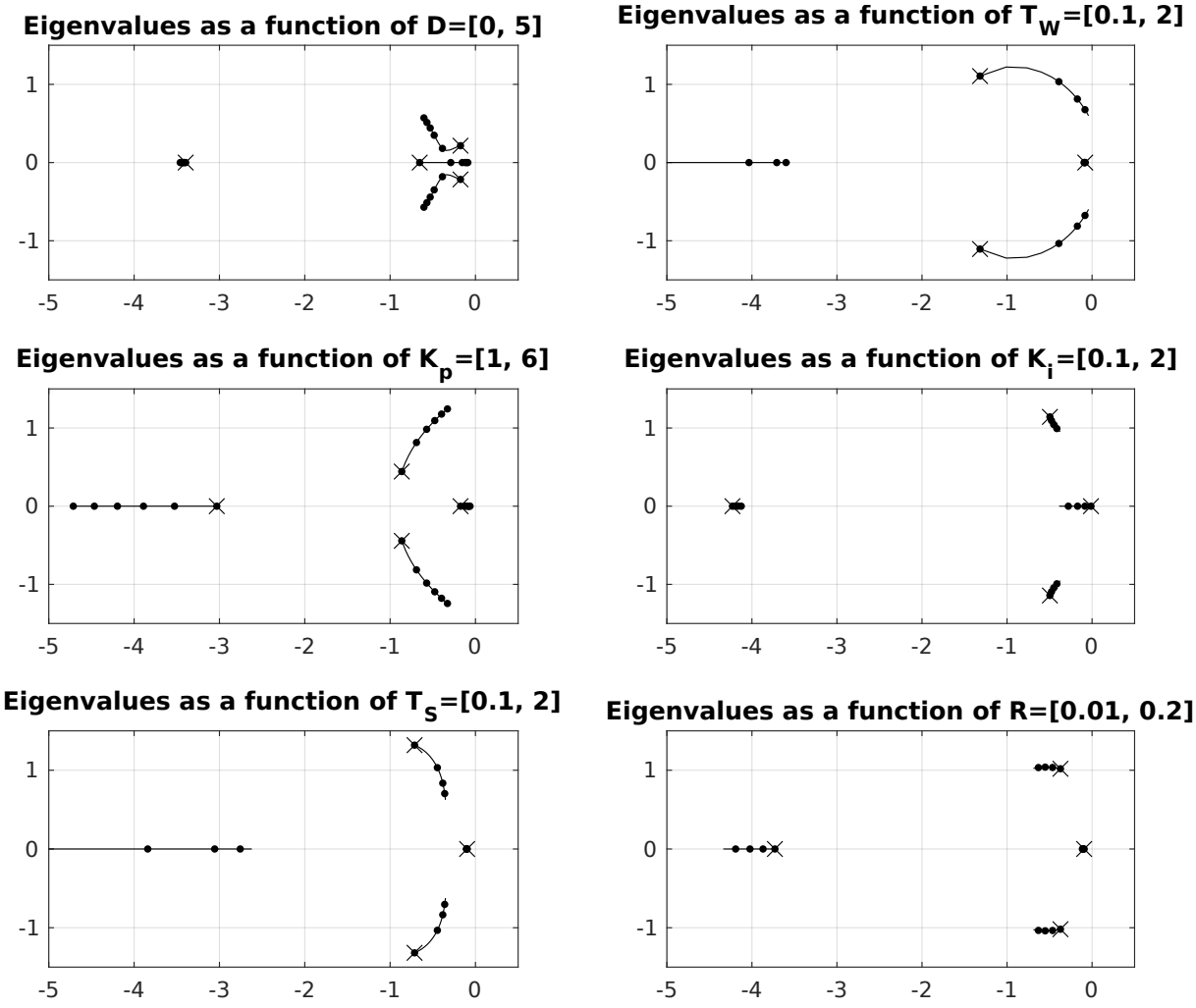


Figure 20: Root-locus plots for a system consisting of one generator, with the nominal values $H = 3, D = 1, R = 0.05, K_i = 0.6, K_p = 4, T_S = 0.5, T_w = 0.5$. The crosses mark the lowest parameter values.

### 3.2.2 Two-generator system

When a two generator system is simulated, inter-generator oscillations also appear. Root-locus plots for varying $H$ are shown in Figure 21.

As stated earlier, the inter-area mode is too fast to be heavily affected by the control, and the result does not noticeably vary from what was previously found. Equation (8) still describes the frequency quite well. It can also be noticed that the damping ratio is worsened, although the relationship is complicated.

It can be seen in the right plot that the rigid body mode including both generators is very similar to that of only one generator. It is also seen that the distribution of the inertia is not important. Only looking at this mode, it is almost as if there were only one generator.

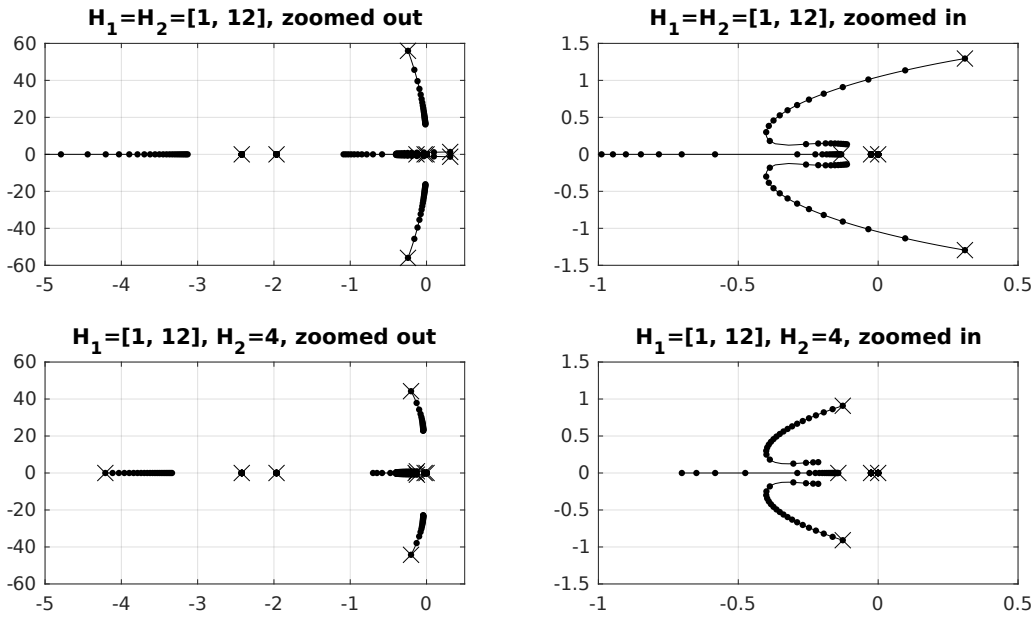


Figure 21: Root-locus plots for a system consisting of two generators, with varying $H$. In the top plots both generators have the same varying $H$, in the bottom plots only $H$ of the first generator is varied. $D = 1, R = 0.05, K_i = 0.6, K_p = 4, T_S = 0.5, T_w = 0.5$ for both generators. The crosses mark the lowest parameter values. Dots mark integers values of $H$.

## 3.3 Steam plants for frequency control

In Figure 22, a root-locus plot for varying H has been plotted for a one-generator system where the turbine and governor are given by the IEEE type G1 model. The parameters are $K = 10$, $T_1 = 0.1$ s, $T_2 = 0.5$ s, $T_3 = 0.3$, $T_1 = 0.6$ s, $T_2 = 0.5$ s, $T_3 = 0.8$ s, $T_4 = 1$ s, $K_1 = 0.3$, $K_2 = 0.25$, $K_3 = 0.3$ and $K_4 = 0.15$. The main interest is the rightmost eigenvalue pair. Just as for the simple model and the hydro plant model, its imaginary part decreases with inertia.

## 3.4 Conclusions

Although this reasoning contributes to the understanding of the systems dynamics, it only leads to concrete formulae for the simplest governor model. This is still interesting for understanding, and the behaviour of the more complex model does seem to have similarities to this simple system. It does not seem possible to extract a concise and effective formula for the eigenvalues for systems with hydro governors, and still they are fairly simple. What this section then shows, is the general impact of the parameters. Some investigations and attempts have been made to find expressions for the relations, but without success. Therefore, a better approach is to find the correspondence between parameters and eigenvalues numerically.

Nevertheless, there are important conclusions to be drawn from this study. One is that the rigid body mode is not affected to any larger extent by the distribution of the inertia, only the total inertia. Another conclusion is that a larger $H$ means slower oscillations, typically it is somewhat proportional to $1/\sqrt{H}$.

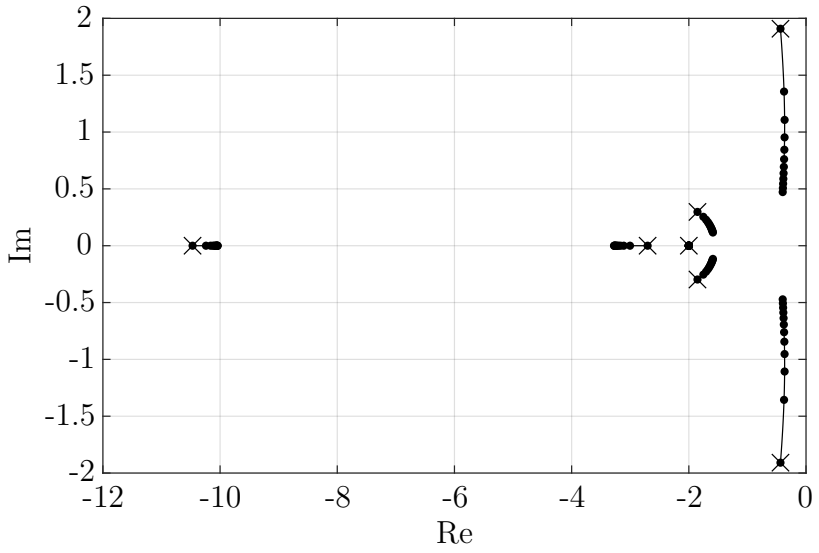


Figure 22: Root-locus plot for a system consisting of one generator controlled by the IEEE type G1 turbine and governor model. $H$ varies from 1 to 12. Dots mark integer values of $H$.

The analysis here may also be useful to determine the sensitivity to model errors. The method is based on finding $H$ by matching the modes of a model to measured modes. If some parameters are wrong, it will move the theoretical mode, and the plots show how much and in which direction. This will be further analysed later on.

Equation (8) for inter-generator modes is also potentially useful even for systems with more complicated governors. It is limited to systems with two generators, which are rare, but also has some merit for oscillations between two distinct areas. However, it does not consider voltage control that may impact the mode.

# 4 Estimation of electromechanical modes

Mode estimation can be done in several ways. The measurement signal can be the frequency, but it can also be the power flow between two areas or the phase angle, although only the frequency is considered in this thesis due to time limitations. The estimation can be done from a large disturbance or from ambient frequency variations, each case requiring its own methods and posing its own challenges. The former is discussed in section 4.3 and the latter in section 4.4. With the proposed inertia estimation method, any mode estimation can be connected to the next step, and mode estimation does not necessarily have to be done as here.

The large difference in dynamics between the rigid body mode and the inter-generator modes also motivates separate treatment, which is done in section 4.5 and 4.6, respectively.

Estimating modes in a power system is an area where ample research has been conducted [23]. Mostly the interest has been focused on estimating highly oscillatory modes that endanger the stability of the system, and then the most important parameter to estimate is the damping ratio. Estimations of the rigid body mode have hardly been done at all. In this project, the focus is different. Modes with higher damping ratio are of interest as well, and there is no reason to focus on the few modes that are most dangerous for stability. Rather, it is better to estimate as many as possible. The damping ratio is not the main interest, frequency is at least as important. In fact, frequency is even more important for two reasons. Firstly, it is shown in chapter 3 that changes in $H$ tends to give rise to stronger changes in the frequency of the mode, i.e. vertical more than horizontal lines in the root-locus plots. Secondly, frequency can be estimated more accurately than damping [23, p. 2-31].

One method must not necessarily be used in all cases. One method might handle the slow and more damped rigid body eigenvalue well, while performing bad on the fast and weakly damped inter-area eigenvalues, while the opposite is true for another method. Then it is obviously advantageous to use the best one in each case. Furthermore, different methods could be used for damping ratio and frequency estimates.

## 4.1 Simulation

To test and compare the methods, simulations were used. Using real data for this would be very difficult or impossible since it is not known what the true values are, when in a simulation they are readily available.

To ensure that the result is valid in a more general context and not just in one case and decrease the risk of having the result affected by chance, the Monte Carlo method is used, and many random systems are tested. The parameters of each system are set randomly, and it is verified that the system is stable. Then a random signal with power variations is generated as input to the system and its response is simulated. The mode estimation method investigated is run with the simulated grid frequency, and the resulting estimation is compared to the actual mode found from the system matrix. The result from all these simulations are considered together to evaluate the accuracy of the method.

The grid frequency measurements will, as always, not be perfect, and neither will the system supply a perfect step response. The normal operational disturbances will remain during a step disturbance, and the response of the system to it might give rise to new disturbances. This is included in the simulations and modelled according to section

2.9 and 2.10, i.e. the load variations are white noise that is low-pass filtered, and the measurement noise is white noise with the amplitude 1 mHz.

## 4.2 AR(MA)(X)-models

Many estimation algorithms are based on AR or ARMA-models. This means that the measured signal $y(k)$ is calculated as a linear combination of the previous values of $y$ and an unknown white noise $e$:

$$y(k) + a_1 y(k-1) + ... = b_0 e(k) + b_1 e(k-1) + ...$$

When $b_i = 0,\ \forall i \neq 0$, it is an AR model, otherwise an ARMA. If an input is added on the right-hand side, i.e. $c_0 u(k) + c_1 u(k-1) + ...$, it becomes an ARX or ARMAX-model.

To estimate an ARMA-model, different methods are possible. Some popular examples are Yule-Walker, least square and the prediction error method (PEM). Details on these methods are beyond the scope of the thesis, instead the reader is referred to a book on system identification, e.g. [27]. Typically PEM gives the best result, but is comparatively computationally expensive [23, p. 2-10]. It should therefore be preferred when possible.

For AR-models, recursive methods are also of interest in real time applications, where they save computational time. This is mostly relevant for the case when estimations are made from ambient noise. Recursive methods are not inherently different, and the result from recursive and non-recursive methods should be similar. Except computational efficiency, recursive methods' use of forgetting factors might also be valuable. Values from the past are less relevant than recent values, if the time span is large enough for the system parameters to have changed. If they have changed, but not too much, past values might be useful to a limited extent, but not as much as new values, hence why the forgetting factor would be useful. It might also be the case that the computational gain is limited, for example if it is sufficient to calculate the parameters only occasionally or the used measurement time is not too long. In this thesis recursive methods will not be studied.

## 4.3 Estimation from step disturbance

Disturbances in the power balance in the shape of a step occasionally occur in power systems. It could happen due to unintentional failure of a generator, a HVDC connection, a transmission line or something similar. A disturbance could also be purposefully created to analyse the system, e.g. with a HVDC connection. In all these cases, the step disturbance occurs at one specific node. It makes it easy to model, but may not activate all modes enough. Modes where the disturbed generator does not participate will have little excitation.

To keep the disturbances as small in magnitude as possible, it is advantageous to repeat small disturbances many times instead of using one large step, i.e. using a square wave signal. Both the rising and falling edge can be used for estimation in the same way. To minimise the impact on the power balance, the square wave should have the average power zero, i.e. be one half of its amplitude above the original power half its cycle and one half of its amplitude below the original power the other half of its cycle. A reasonable frequency for the square wave is one disturbance in 30-60 s, to let the last step response fade away.

Three methods to estimate the modes from a step will be considered: Prony's method, eigenvalue realisation method (ERA) and matrix pencil method (MPM). There are others, but these are the most established methods [23, p. viii-ix]. All methods might be used in combination with low pass filtering to remove some measurement noise. It is known beforehand that the rigid body mode will have a frequency $< 1$ Hz, and anything above that should be safe to filter away.

### 4.3.1 Prony's method

Prony's method is a way to decompose a step or impulse response into decaying sinusoids [28]. For a signal $y(t)$, this means finding $P$ different $B_i$ and $\lambda_i$, such that:

$$y(t) \approx \sum_{i=1}^{P} B_i e^{\lambda_i t}$$

Typically, this is done in discrete time, and the formulation becomes:

$$y(k) \approx \sum_{i=1}^{P} B_i \zeta_i^k, \text{ where } \zeta_i = e^{\lambda_i \Delta t} \tag{9}$$

The idea is similar to that of Fourier analysis, but with the difference that it permits non-zero damping.

The method for Prony analysis is the following. First the data is fitted as an impulse response to an ARMAX-model (or just ARX), i.e. find $a_i$ and $b_i$ in the expression

$$\frac{Y(z)}{X(z)} = \frac{b_0 + b_1 z^{-1} + ... + b_q z^{-q}}{1 + a_1 z^{-1} + ... + a_p z^{-p}}$$

where $X(z)$ is an impulse and $Y(z)$ the measurements. This expression is then expanded in to its partial fractions, i.e.

$$\frac{B_1}{z^{-1} - \zeta_1} + .. + \frac{B_p}{z^{-p} - \zeta_p} \tag{10}$$

where $\zeta_i$ are poles.

These are the sought values in (9), and the continuous eigenvalues are found as $\lambda_i = \frac{ln(\zeta_i)}{\Delta t}$. The parameters $B_i$ give the amplitude of their respective modes.

The order of the ARMAX-model is a parameter that must be decided. It should be greater than the order of the actual system to also fit noise, otherwise the noise will disturb the fitting of the actual modes, and underfitting must be avoided with some margin. However, this means that modes that are fitted to noise must be sorted out.

Prony's method can be generalised to use several inputs, in accordance with [29]. It is achieved by using an AR-version of the method. When estimating the parameters, all signals are stacked, as if they were from various observations of the same process. The differences in the signals are achieved by letting $B$ in equation (9) vary.

### 4.3.2 Eigenvalue realisation algorithm

The eigenvalue realisation algorithm (ERA) is popular in many fields, including power systems study, as it has solid mathematical foundation and is considered robust [23,

pp. 1-7−1-11]. For example, in [30] it was found to have a performance comparable to Prony's method. It is also possible to generalise the algorithm such that it uses multiple measurement signals. The algorithm is as follows [23, pp. 1-7−1-10]:

First, Hankel matrices $H_0$ and $H_1$ are constructed from the measurement signal $y$ where $r = N/2 - 1$:

$$H_0 = \begin{bmatrix} y_0 & y_1 & \cdots & y_r \\ y_1 & y_2 & \cdots & y_{r+1} \\ \vdots & \vdots & \ddots & \vdots \\ y_r & y_{r+1} & \cdots & y_{N-1} \end{bmatrix}, \quad H_1 = \begin{bmatrix} y_1 & y_2 & \cdots & y_{r+1} \\ y_2 & y_3 & \cdots & y_{r+2} \\ \vdots & \vdots & \ddots & \vdots \\ y_{r+1} & y_{r+2} & \cdots & y_N \end{bmatrix}$$

Then singular value decomposition is performed on

$$H_0 = U\Sigma V^T = \begin{bmatrix} U_n & U_z \end{bmatrix} = \begin{bmatrix} \Sigma_n & 0 \\ 0 & \Sigma_z \end{bmatrix} \begin{bmatrix} V_n^T \\ V_z^T \end{bmatrix}$$

where $n$ is the number of modes to be estimated. Only the $n$ largest singular values will be used, the rest are discarded as noise. The matrix $A = \Sigma_n^{-1/2} U_n^T H_1 V_n \Sigma_n^{-1/2}$, and its eigenvalues $\zeta$ correspond to the discrete poles of the system while the continuous eigenvalues can be found as $\lambda = \frac{ln(\zeta)}{\Delta t}$.

### 4.3.3 Matrix pencil method

The matrix pencil method (MPM) is comparatively new in the study of power systems, but has shown to be useful. For example it is claimed in [31] that it may perform better than Prony. The algorithm is the following [23, pp. 1-10−1-11]: The Hankel matrix $H_0$ and $V_n$ from its singular value decomposition are found as for ERA. From $V_n$, $V_1$ and $V_2$ are created, where $V_1$ contains all but the last row of $V_n$ and $V_2$ all but the first row. Then $Y_1 = V_1^T V_1$ and $Y_2 = V_2^T V_1$ are defined. Finally, the discrete pole $\zeta$ are found as the generalised eigenvalues of the matrix pair $\{Y_2; Y_1\}$ which can be converted to continuous eigenvalues as above.

### 4.3.4 Sorting out wrongly identified modes

All methods have in common that they detect more modes than there actually are. This is due to the fact that some headspace is needed to make sure that the sought modes are included in the estimate. It is also advantageous to estimate the noise as modes, in that way it will be excluded from the estimate of the real modes. The disadvantage is of course that the interesting modes must be found among many falsely identified modes.

All methods give a value on the magnitude of the modes. Modes fitting to noise can be expected to be smaller than actual modes, if the noise level is not too high. This gives a way of doing a first sort. However, the largest modes are not necessarily those sought after, among other things due to strong noise.

At least the measurement noise is expected to have high frequency. Modes in the power system rarely have a frequency above a few Hz, which also gives a method for filtering out uninteresting modes. Furthermore, inter-generator modes do not have too large damping ratio, and if they have, they will probably not be possible to estimate accurately. The rigid body mode on the other hand is expected to have relatively high

damping ratio, but it is also known to be slower. Therefore, a sorting might let through modes that either has low damping ratio or are slow.

In [28] it is proposed to calculate the Prony analysis for various model orders. The idea is that the modes for noise will vary more when the model order changes than the actual modes, and therefore the true modes can be identified as those that show up on the same place in all model orders. This method is not applicable to MPM and ERA, since the first modes will be the same regardless of how many are estimated from their residual.

## 4.4 Estimation from ambient noise

There is a constant change of power balance in the power system due to the change in load. This constitutes a weak noise that excites the system. Using it, a model can be constructed and modes extracted. Ideally, the noise should be white, which is not reasonable to expect. It rather has low-pass characteristics, as discussed in section 2.9. This means that it might not excite the system completely, which may cause problems. It also makes modelling more difficult, and the noise characteristics might be estimated as a part of the system. However, the noise will probably not be oscillatory, meaning that oscillatory modes should still be possible to distinguish from the noise.

### 4.4.1 AR-model

From measurements of the frequency, an AR or ARMA-model can be constructed. The poles of this model should correspond to the modes of the system [23, p. 2-8 − 2-10]. If the resulting expression is expanded into its partial fractions as previously, not only the poles will be found, but the numerator also gives a value on how large the activity of the frequency in the mode is.

The above procedure can be repeated for all individual measuring points. The final estimate can then be calculated as the (weighted) average of all individual estimates. The result will be slightly different for different measurement points. Most noticeably, the estimations of inter-generator modes depend on their activity at the measuring point. It is logical that more activity in general means better estimates, and no activity obviously means no estimate. It is therefore reasonable to weigh the contribution of a measurement point to the average estimate by activity.

It is also possible to treat all measurement points simultaneously, as if they came from different experiments. This is most interesting for the rigid body mode were the activity is the same at all measurement points.

## 4.5 Estimation of rigid body mode

### 4.5.1 Estimation from ambient noise

Estimating the rigid body mode from ambient noise is an especially difficult task, since it typically has high damping ratio and its slow characteristics might be mixed up with the variations due to power fluctuations. Therefore, the result is expected to be worse than for inter-generator modes.

Since the damping ratio is high, there is no clear frequency peak in the spectrum, and spectral methods can be disregarded. Instead, ARMA and state-space methods must be

used. Several model orders can be used to decrease the risk of an unfortunate selection of order, and then either the mean or the median of them be calculated.

To test how capable the estimation was, a one-generator model with a hydro governor and turbine according to section 2.3 was simulated in Matlab. The parameters were in the following intervals: $H \in [1, 8]$, $D \in [0.5, 3.5]$, $T_S \in [0.2, 0.5]$, $K_p \in [2.5, 5]$, $K_i \in [0.3, 0.7]$ and $T_W \in [0.4, 0.8]$, while the droop was $R = 0.05$. The estimations were based on frequency data from 1000 s with the sampling rate 10 Hz. The results are presented in Figures 23 and 24.

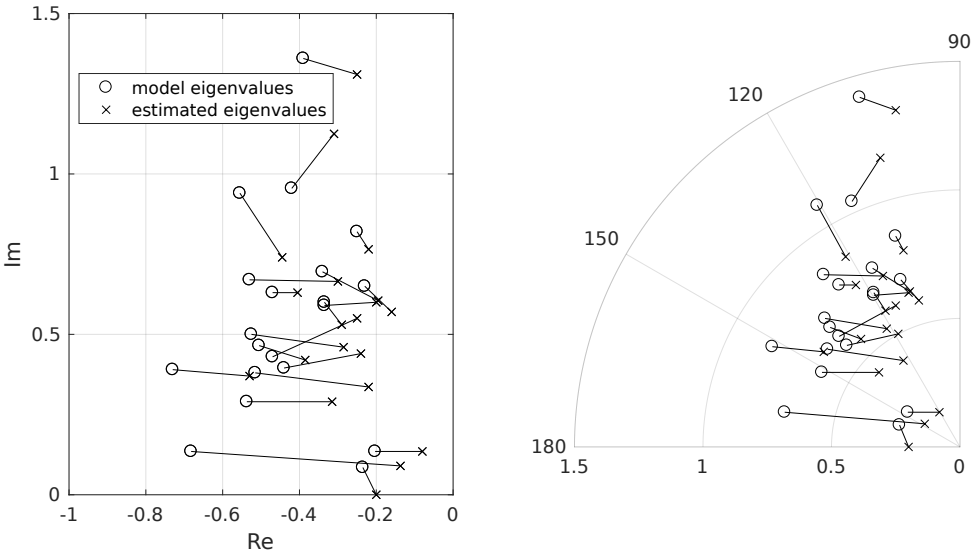


Figure 23: Estimated rigid body eigenvalues from ambient noise, using the median of AR models of several orders. Only one eigenvalue of a conjugate pair is shown. The left and right image is the same, but in different coordinate systems.

The fluctuations in power were simulated as white noise low-pass filtered with the cut off-frequency 0.1 rad/s. White measurement noise was added, but was too small and high-frequent to affect the result more than marginally. This also means that the amplitude of the power fluctuations was of little importance, as long as it was much more than the measurement noise. Instead the limiting factor was its frequency content. Both the power variations and the measurement noise were chosen to be realistic in amplitude and frequency content.

It was determined that the best way to estimate the mode was to use several AR processes estimated with Matlab's function `ar`. The least-square method was used to estimate the parameters, although the choice did not seem to matter very much and Yule-Walker and the forward-backward approach gave approximately the same result. The model orders used were 60-120 with steps of 5. This is much higher than the order of the system model, which was only five, but the system model also has zeros that must be approximated with many poles. An ARMA model worked as well, but did not improve the result, and was more computationally costly. Using n4sid did not give satisfactory results.

To handle the many model orders, the median was taken. It is not entirely obvious that this is better than the mean, but the median seems to have a small advantage. An advantage of taking the median is that it is less sensitive to outliers than the mean. Often

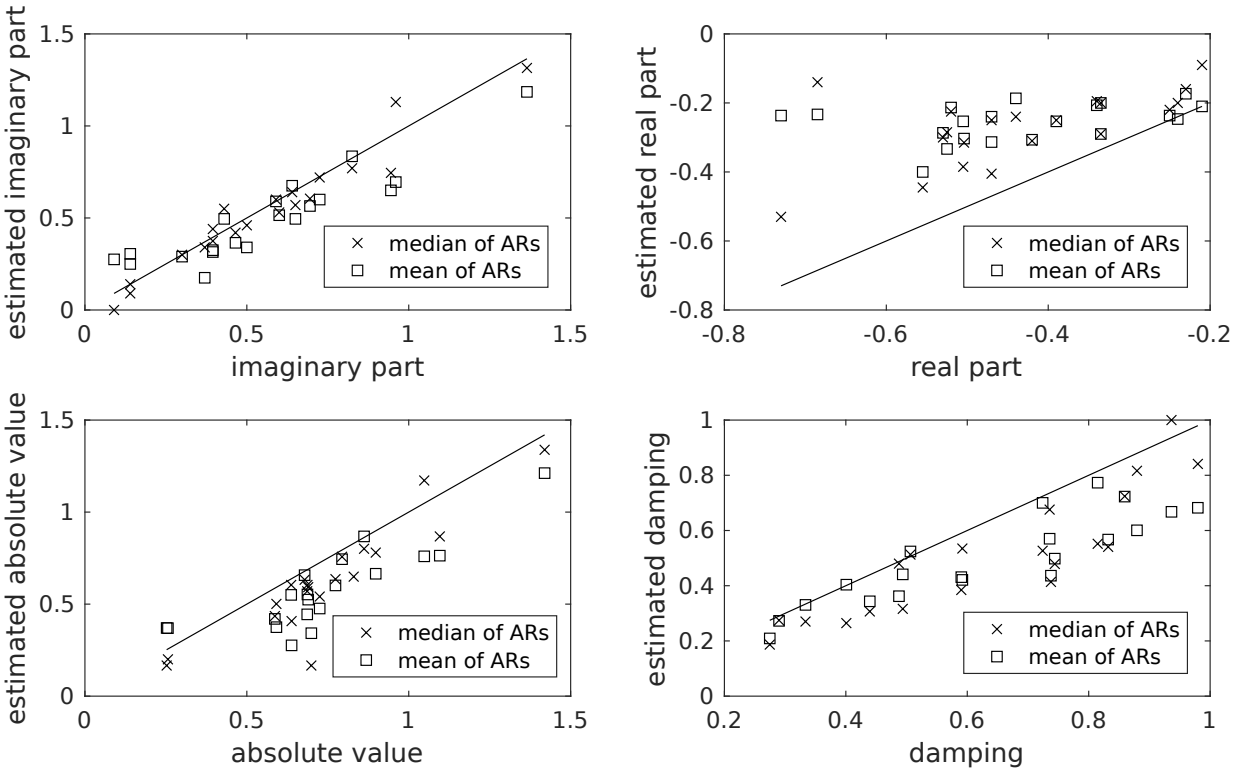


Figure 24: Estimated rigid body eigenvalues from ambient noise on the y-axis vs. eigenvalues of the model on the x-axis. This figure presents the same cases as Figure 23. The line indicates ideal estimation, i.e. the estimated value is the same as the value from the model.

it is preferable to sort out outliers and then calculate the mean, however, it was noted that if one model order gives an extreme outlier it is quite possible that another model order also gives a similar outlier. It might even be unclear which cluster is the estimate and which is the outlier. Therefore, the median may be a more robust choice.

The imaginary part of the estimated eigenvalues was often close to the actual. There were, however, some values somewhat off, putting the robustness of the method into question. This was especially true for cases with low damping ratio. A plausible explanation is that the mode was hidden behind the low frequency of the exciting signal. For the low damping cases, the estimations were good, often only a few percent error in the imaginary part. Disregarding the two eigenvalues with the highest damping ratio (0.98 and 0.95), the standard deviation of error in the imaginary part was 12%, with a few values increasing it significantly.

The real part was on the other hand almost always underestimated. It did even improve the accuracy to multiply the real part by 1.5, however, this solution is completely ad hoc and dubious due to the lack of theoretical motivation or even possible speculation. Instead, it is sounder to conclude that the imaginary part is reliably estimated and the real part less so (which remains true even if a multiplication by 1.5 is performed).

Using the ARISTO noise model instead, the problem becomes another. Estimation is still possible, even easier, but the method surprisingly becomes slightly different. Instead of an AR-model, an ARMA-model performs much better. Model orders between 28 and 40 were used with step size 2. The results are shown in Figures 25 and 26. The errors

were normal distributed with mean close to zero. The standard deviation of the relative estimation error of the non-zero imaginary parts was 24.6%, but for those with a damping ratio $< 1/\sqrt{2}$, it was only 8.8%. The standard deviation of the relative estimation error of the real parts was 30.3%, and not lower when the damping ratio was low.

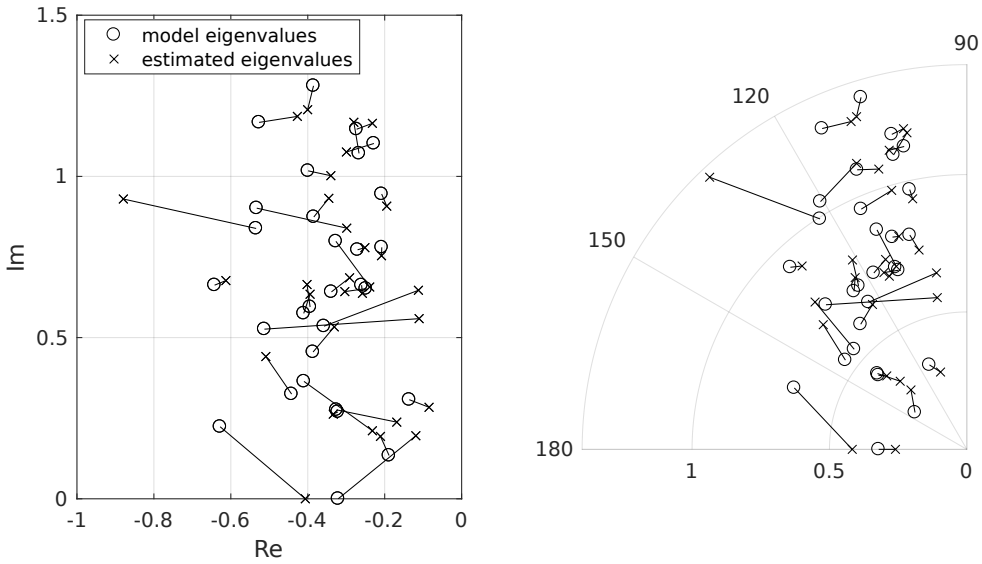


Figure 25: Estimated rigid body eigenvalues from ambient noise, using the median of ARMA models of orders 28-40. The left and right image is the same, but in different coordinate systems.

Since only the rigid body eigenvalue was considered, the result should be possible to generalise to a system consisting of many generators. The rigid body eigenvalue is mostly decided by the governor and turbine; electric dynamics are typically too fast to affect the mode and are consequently of less importance to model.

### 4.5.2 Estimation from step response

If the ambient estimation is not good enough, there is also the possibility to create a step disturbance. This is expected to be better for estimating the rigid body eigenvalue, since it determines the main behaviour of the step response, and the high damping ratio is less of a problem since the measurements are only for a short period of time anyway.

It is certainly possible to get a good estimate of the rigid body mode with a step disturbance. The challenge is instead to estimate it sufficiently accurately with the smallest possible disturbance. Naturally, causing large disturbances in the power system, although controllable and brief, is not desired.

For different step magnitudes, Monte-Carlo simulations with 100 unique systems with two generators were used to estimate the estimation error. Only one generator had a governor, to simulate the fact that not all generation participates in the frequency control. The base power of the generators, and thus the share of the system with frequency control, was random. The variation in load power was simulated as previously and acted as a noise here. The average error is presented in Figure 27.

For ERA and MPM a small trick was used. It was noted that they occasionally were completely wrong, but did detect the global mode, just not as the most significant. These

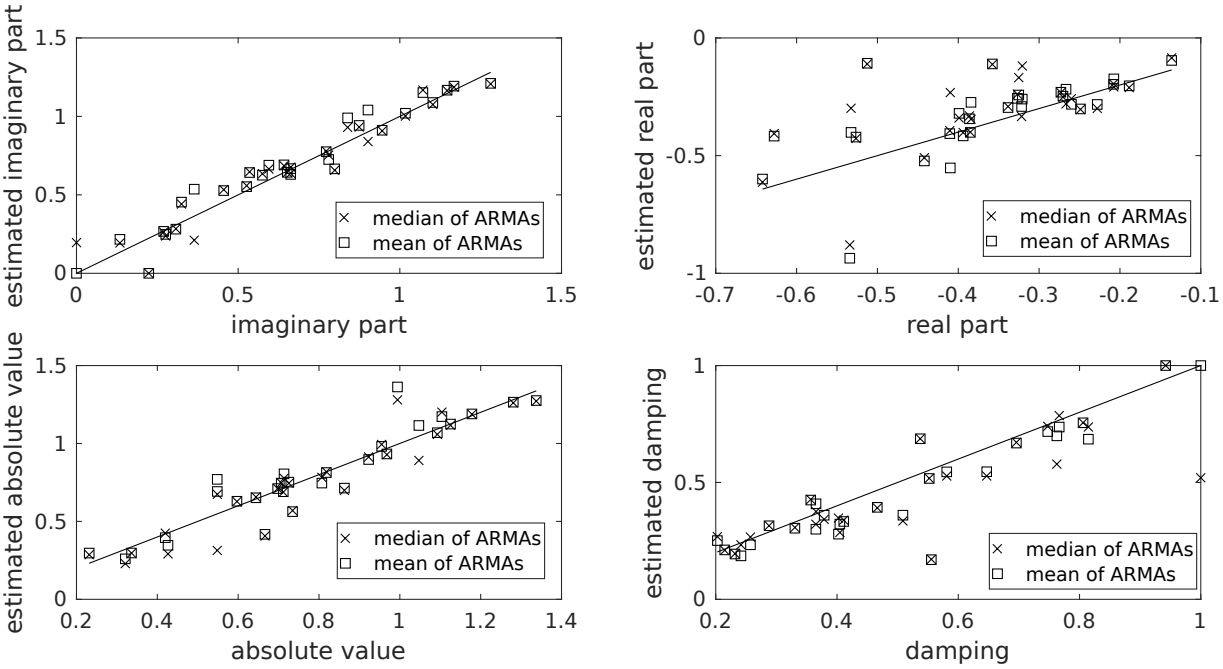


Figure 26: Estimated rigid body eigenvalues from ambient noise on the y-axis vs. eigenvalues of the model on the x-axis. This figure presents the same cases as Figure 25. The line indicates ideal estimation, i.e. the estimated value is the same as the value from the model.

errors would worsen the average drastically. To sort them out, it was simply checked if there was a second mode that was closer to the Prony estimate, then that was used instead. Therefore, the values plotted in Figure 27 are not what ERA and MPM could achieve alone. Still, there were only one or two candidates for the global mode, so they are not copying Prony directly, just use it as a guideline when the estimates were non-conclusive.

In this test the similarity between all methods was striking. There is no difference and their estimates are similar. No clear improvement was seen when averaging the estimates of the different methods. The difficulty in the estimation is to handle the power variations that intermix with the step response, rather than to pick a good method.

The error decreases as the magnitude of the step increases. This is of course completely natural, since it improves the signal to noise ratio. Unlike the ambient estimation, both the real and the imaginary part can be estimated with not too different accuracy.

As previously, there is a tendency that large damping ratios cause larger error. This is clearly seen when comparing the error of all systems to only those where the global mode had a damping $< 1/\sqrt{2}$, which is also plotted in Figure 27.

The error is not normal distributed. There are a few outliers where the methods give estimates far off, giving a bad average. If it would be possible to exclude the cases with large errors, the improvement would be large.

The number of generators is expected to have little influence on the estimates. If it has any sizeable effect, it could be a small improvement since it supplies more measurement points. This tendency is seen to some extent, but gives no drastic improvements.

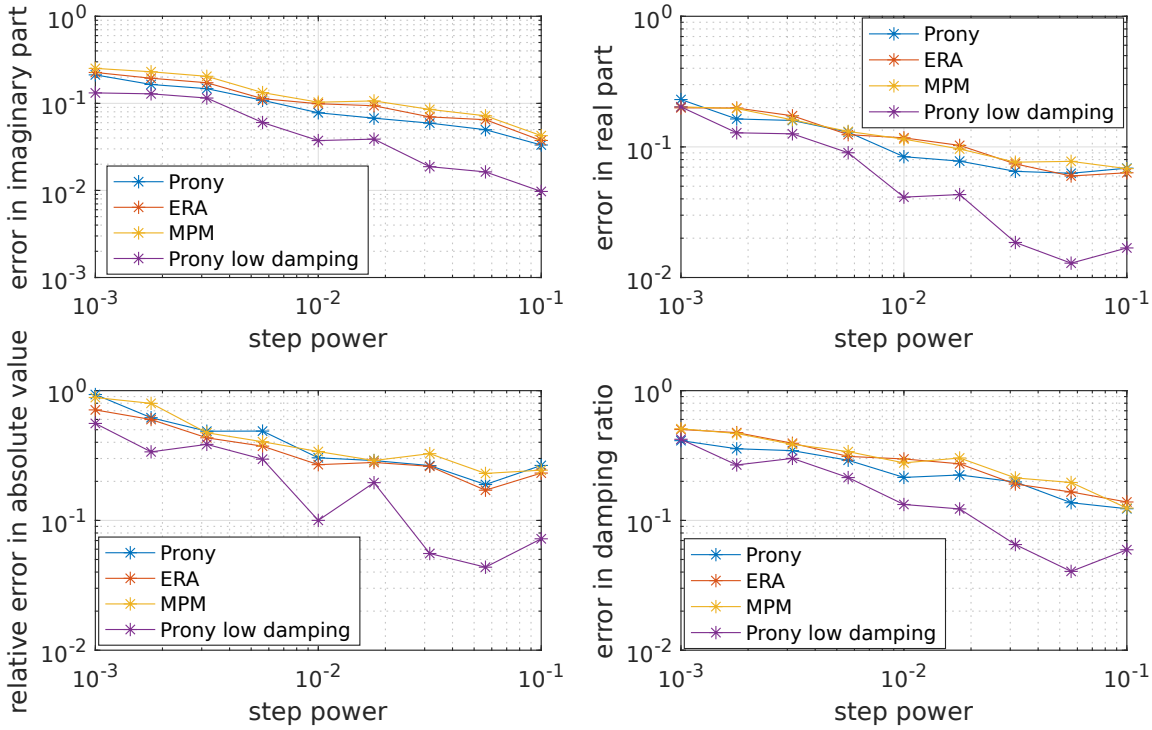


Figure 27: The average error for different methods at different step magnitudes. The x-axis shows the step magnitudes in proportion to total base power of the system. "Prony low damping" only includes those estimates with Prony where $\zeta < 1/\sqrt{2}$.

### 4.5.3 Combining several step responses

Three methods for combining several step responses were considered. One is to average the frequency measurements from all of them, a second to adapt the method to use several inputs, and a third to estimate the modes for each step and average the mode estimates. The results from this is shown in Figure 28 for 10 steps. The methods were run on 40 random systems. Computational time set this limit. This is not enough to remove all dents in the curve, but should suffice for evaluation. As can be seen, the best method is averaging the frequency. Adapting Prony's method to use several inputs worked as well, but averaging is also simpler, and therefore it seems to be the best option. Adapting ERA to many inputs on the other hand, gave clearly worse results than using the average frequency. It cannot with absolute certainty be excluded that no mistake was made in the implementation, but regardless it did not seem like a path worth pursuing.

Using the averaged frequency response also gives a clear theoretical answer to how much of an improvement is achieved with $N$ steps, it reduces the noise by $1/\sqrt{N}$ and permits decreasing the step size with the same factor. This means that the curve for the estimation only using one step should be identical to the estimation using average frequency, but shifted $1/\sqrt{10} = 3.16$ to the right. This is not clearly seen in the Figure 28, but is still plausible. The discrepancy can be explained by the fact that too few iterations were run (due to computational limitations). Another explanation is that for high levels of noise, most methods may resort to occasional random guesses, and then they will have the same accuracy (although all methods are better than pure random

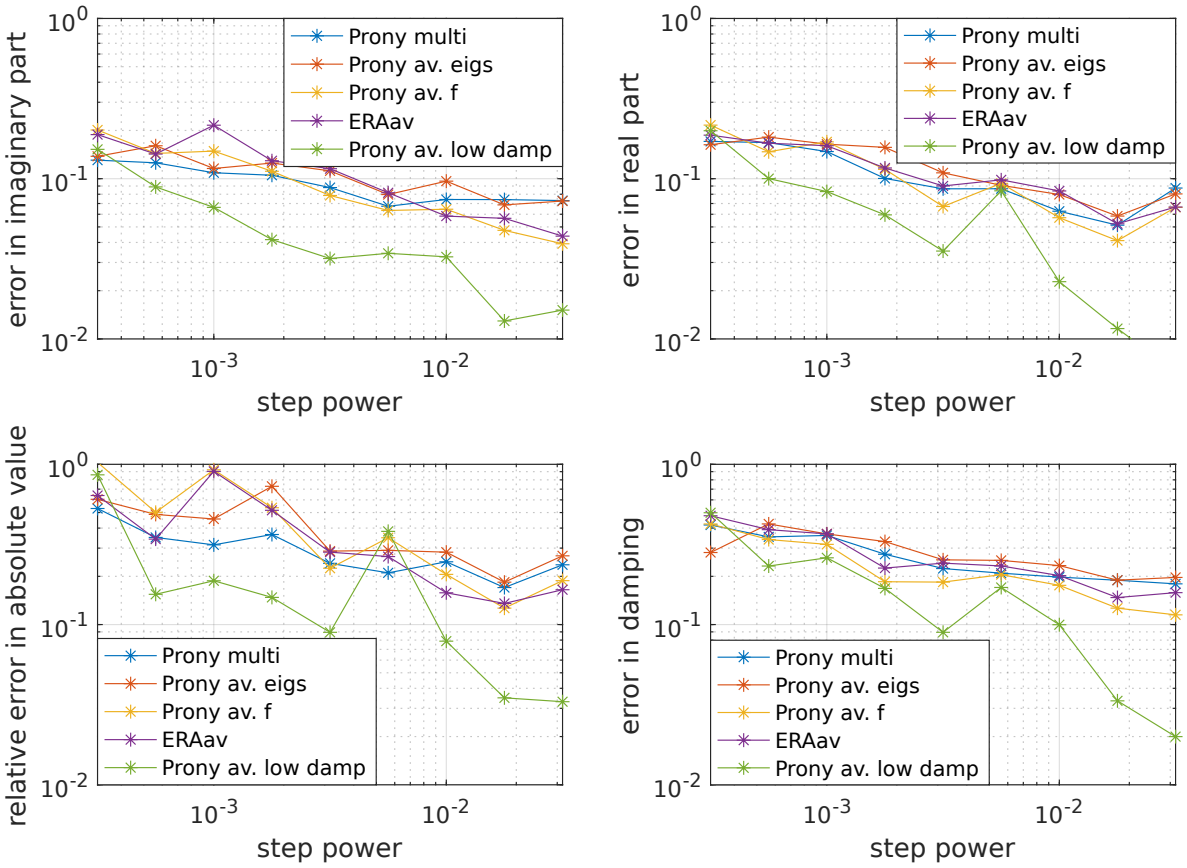


Figure 28: The average error for different methods at different step magnitudes. Ten steps are used. The case only using the first step is included as reference. The x-axis shows the step magnitudes in proportion to total base power of the system.

guessing for the lowest step magnitude).

### 4.5.4 Discussion

Based on the simulations, estimation from ambient noise works well when the damping ratio is small enough. For the simulated systems, this was often the case, due to the fact that it was regulated by a hydro power plant which is difficult to get well damped. It cannot be expected to get an equally good result for a system with the frequency control done by thermal plants. It should also be noted that the measuring time influences the result. It could be possible to measure longer and get better results.

In the simulated systems, it was shown that the rigid body mode could be estimated from ambient conditions with a standard deviation of the error slightly above 10%. To reach a similar accuracy with a step response, a disturbance of the magnitude of at least 1% of the system power would be needed. This is a sizeable disturbance that is not necessarily possible. For the Nordic system, with a total power of 40-70 GW, this would mean 400-700 MW. It is within the capacity of a HVDC link and not completely impossible, but definitely not desired. However, if many steps are combined, it would be possible to reach the result with disturbance with the magnitude of a few thousandths of

the system power, i.e. a few 100 MW. It should also be kept in mind that a low inertia situation would give rise to a larger step for the same disturbance, meaning that not even that large steps may be required.

Still, the mode estimations from steps are not very impressive, and based on the study in this thesis, it is hardly motivated to induce step disturbances, considering the small improvement compared to ambient measurements. In the case of step disturbances, another method for inertia estimation might be superior, i.e. simply looking at the initial rate of change of frequency (RoCoF). However, there might be unintentional disturbances that can be used. These are larger than what can be induced, and a single, or a few, may suffice. In this case, the method still provides an advantage compared to calculating the RoCoF, since it does not assume knowledge of the power imbalance.

Regardless of the choice of method, there are a few outliers that worsen the result significantly. If they can be sorted out, the results would improve significantly. This could be possible using system knowledge, previous estimates etc.

## 4.6 Estimation of inter-generator modes

In this thesis, only the estimation of inter-generator modes from ambient noise is considered. This is the area where most value is expected from the inter-generator modes. Although the modes do appear in a step response, they are weak in comparison to the rigid body mode, making them difficult to distinguish. If step responses are available, the global mode can already be estimated in a fairly accurate and robust manner, decreasing the need for the inter-generator modes. In the ambient noise, however, a low damping ratio is more important for successful estimation, giving an advantage to the inter-generator modes.

In previous research, inter-generator modes have been successfully estimated with high accuracy. For example, in [22] four modes were detected from ambient noise in a real system and compared to estimates from a step response. The differences in frequency estimates were merely a few percent while the damping estimates had larger differences. The damping ratio of these modes were between 10 and 30 %, which is not especially low for inter-generator modes, meaning that estimation is possible even for slightly higher damping ratios.

### 4.6.1 Mode shape estimation

For the inter-generator modes, the mode shape, i.e. the activity of each generator in the mode, is useful to know. The activity is here the activity in the frequency, but it could be in other states as well, e.g. the angle. An area with large inertia will have less activity than an area with small inertia when the same power oscillates between them. For the rigid body oscillation all generators are equally active. A simple way is to use the estimate of the magnitude of the mode ($B$ in (10)) from the different measurement point. There are, however, other and better methods.

One is the transfer function method [23, p.2-20]. One measuring point is chosen as reference. Then transfer functions are constructed such that $G_{kl}(s) = \frac{Y_l(s)}{Y_k(s)}$, where $\mathcal{L}^{-1}\{Y_k(s)\} = y_k(t)$ is the measurements at the reference generator and $\mathcal{L}^{-1}\{Y_l(s)\} = y_l(t)$ is the measurements at another generator. This can be done using Matlab's function `arx`. This function is evaluated at the eigenvalue, and the result describes the relative activity

between the two generators as well as the phase.

Another variant of this method is to only use the imaginary part of the eigenvalue, i.e. evaluating the function at $s = i\omega$ where $\lambda = \sigma + i\omega$. This is equivalent to calculating the frequency content with a Fourier transform and then comparing the values of both signals at the frequency $\omega$, which should be the frequency of the oscillation. This works when the damping ratio is low and $\lambda \approx i\omega$, an assumption that is rather reasonable when inter-generator eigenvalues are considered. Nevertheless, caution is necessary, since in [32] it is only recommended to use this method when the damping ratio $< 0.05$. Still, it has clear advantages. The method turns out to be much faster computationally than the transfer function method since a fast Fourier transform (FFT) can be used instead of estimating a transfer function.

Other methods, e.g. subspace methods, exist, but are not discussed here [33].

### 4.6.2 Estimation from ambient noise

In Figure 29 modes are detected in 20 Monte-Carlo simulated 4-generator systems from ambient noise. The system parameters were randomly generated an laid in the following intervals: $S \in [0.5, 6.5]$, $H \in [1, 6]$, $D \in [2, 11]$ (this is high, but it compensates for the fact that voltage dynamics and PSSs which would increase the damping are not modelled) and $X_{ij} \in [0.8, 1.6]$ with 50% probability to be zero. The noise model is white noise filtered through a first order low-pass filter with the corner frequency 0.075 rad/s (based on the ARISTO model). The eigenvalue is estimated as the average from 5 ARMA models of the orders 22, 24, 26, 28, 30.

The imaginary part of the eigenvalues could be estimated with high accuracy, although it was occasionally not possible to identify all three modes. Most of the time the error was below 1% and the standard deviation of the relative error was 1.3% and 1.5% for the two first modes and 1.1% for the third mode when it was identified. The damping was less reliably estimated. This is a well-known phenomenon and expected. Still, the result was quite good, achieving $< 10\%$ error about half of the time, and the standard deviation of the relative error was 9.3%, 15% and 19% for the three modes.

The mode shape estimates did less consistently give good results. Most of the time they did, but not always, especially for higher damping ratios. In this case it was not obvious that the transfer function method gives better result, and it seems to have a comparable performance to the frequency method.

A similar simulation was run with 8 generators. This meant 7 inter-generator modes. In general, 5 modes could be estimated, but occasionally only 4, and sometimes 6 or 7. The estimates of the imaginary part of the eigenvalues were still excellent. For the best 5 eigenvalues, the standard deviation of the percentual error was 1-4%. For the damping, it was 25-40%, sometimes being completely wrong, even for the modes that were confidently estimated. More worrying was the observation that the mode shape was less reliably estimated. Usually, two modes were possible to estimate decently, with an error 0.05-0.15 (error calculated as $\sum_{i=1}^{4} |NA_{i,est} - NA_{i,true}|$, where $NA_i$). For the third and fourth best, the estimate could be anywhere between 0.10 and 0.5. That the fifth mode shape was accurately estimated was an exception, and for at least two mode shapes the estimates were highly inaccurate.

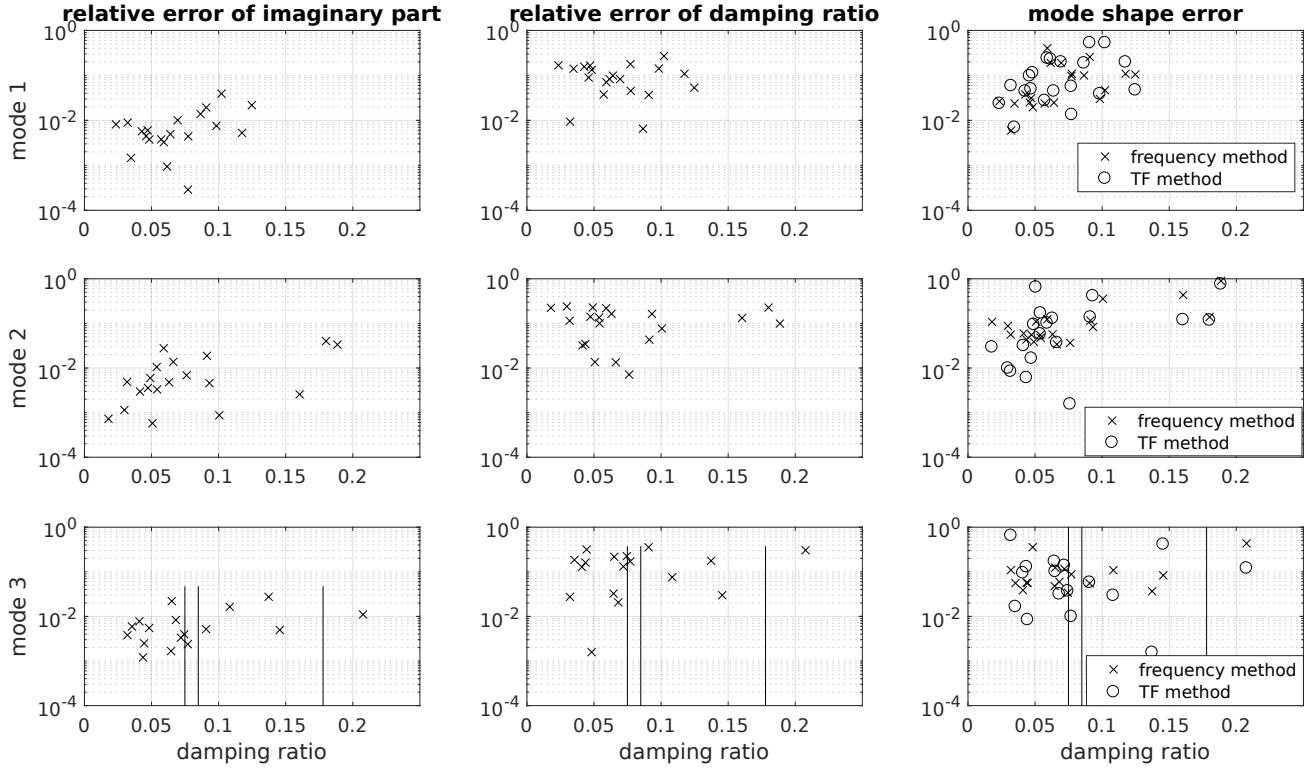


Figure 29: Estimation of inter-generator modes in 20 4-generator systems. The lines mean that a mode there could not be reliably detected. The modes with damping 0.075 and 0.18 that could not be detected because another mode was very close. The detected modes are sorted in order of estimated activity. The shape error is calculated as $\sum_{i=1}^{4} |NA_{i,est} - NA_{i,true}|$, where $NA_i$ is the normalised signed activity. By randomly generating a mode shape, this error is on average 1.32.

## 4.7 Discussion

The inter-generator modes were possible to estimate with a few percent error in the frequency. The estimates of the damping ratio were much less accurate. This is in line with previous research. However, it was not always possible to detect all modes, especially when there were many.

The choice of using the damping on the x-axis in Figure 29 was due to the expectation that the error should be larger for higher damping. This was to some extent true, as can be seen in the figure, at least for the imaginary part and the mode shape. Still, it seems possible to get decent estimates in most of the span of damping ratio tested, although high damping ratio jeopardises the reliability of the estimates, especially of the mode shapes.

The weakness does on the other hand seem to be the mode shape estimation. The mode shape can be used for both identifying inter-generator modes and as a basis for inertia estimation, where the second use requires higher accuracy. The shape of a few modes could be accurately estimated, but not much more, and the estimates were not as accurate as the estimates of the imaginary parts. A possible reason for the inaccurate estimates of the mode shapes, especially for the 8-generator system, is that there were too many modes with too much damping, resulting in wide lobes that increases the activity

at the (complex) frequency of another mode. For the 8-generator systems the frequency method performed noticeably worse than the transfer function method, which is consistent with this hypothesis since the frequency method does not evaluate the function at its peak. Therefore, the transfer function method still is preferable, even if no clear advantage was seen in the 4-generator systems.

Possibly, even better results could be achieved than what was done in this quite basic study. There are many more methods that are not considered here, e.g. the entire family of state-space methods. This is true for the estimation of the eigenvalue as well as the mode shape.

## 4.8 Some attempts on mode estimation from real data

The method proposed in this work has not been used on real frequency data. Due to limitations in time and data, this has not been possible. When real data is considered, it is not possible to know the true values of modes, making the evaluation of the method difficult.

One way to tackle this is to use step disturbances. An estimate can be made from the step disturbance, as well as from the time before the disturbance. Ideally, they should match. However, there are problems which this method. First it assumes that the system is identical before and after the event, which is not necessarily true. Secondly, it will not be known which method provides the best answer if they diverge. However, the rigid body mode is known to be estimated quite well from the step response and can serve as a reference. Inter-generator modes cannot be as reliably estimated. One is probably possible to estimate, and visible in the step response, but not necessarily more accurately than from ambient noise. The main purpose in this section is therefore to estimate the rigid body mode from noise and compare the estimate to the presumably more reliable estimation from the step response.

Five events were considered, from May and June 2005. For the analysis, PMU data recorded in Lund were used. They were performed with 50 Hz sampling rate and were downsampled to 10 Hz. This decreases the high frequency noise and no useful estimation is lost since 10 Hz is much more than the expected frequency of the modes. The same methods as previously were used for mode estimation. For the ambient estimation, measurements from 10 minutes were used, and for the step estimation 40 seconds.

The results for estimating the rigid body mode are presented in Table 4

As can be seen, the estimates from ambient measurement and the step response corresponded quite well for the first two events, and decently for the fifth. For the third and the fourth event they corresponded badly.

It is unclear why the two bad estimates were bad. Regardless, it could be noted that some things could be made to improve the correspondence. For example, for the June 2 event, an AR-model could be used for estimating from the ambient measurements (model orders 80 to 160 with step size 5). Then the estimates were $-0.1578 \pm 0.1558i$ and $-0.1614 \pm 0.1610i$ for the median and mean respectively, having an imaginary part much closer to what was estimated from the step response. The same modification did not work for the May 28 event, where the result remained more or less the same.

It was also possible to reconstruct the step response from the estimates and compare the shape to that of the actual measured step response. This is shown in Figure 30 for two events. For the left event the correspondence is very good, even for the ambient estimation.

Table 4: Estimation of rigid body mode from real frequency measurements for five events.

| Case | Time | Step estimation (Prony) | Ambient estimation (ARMA, median) | Ambient estimation (ARMA, mean) |
|---|---|---|---|---|
| 1 | 2005-05-24 22:11 | $-0.0784 \pm 0.1177i$ | $-0.0779 \pm 0.1229i$ | $-0.0772 \pm 0.1172i$ |
| 2 | 2005-05-27 22:24 | $-0.1017 \pm 0.1297i$ | $-0.1128 \pm 0.1255i$ | $-0.1052 \pm 0.1333i$ |
| 3 | 2005-05-28 21:52 | $-0.0898 \pm 0.1316i$ | $-0.0944 \pm 0.0775i$ | $-0.0854 \pm 0.0748i$ |
| 4 | 2005-06-02 10:06 | $-0.0987 \pm 0.1843i$ | $-0.1775$ | $-0.1876$ |
| 5 | 2005-06-14 23:04 | $-0.1183 \pm 0.1065i$ | $-0.0773 \pm 0.0900i$ | $-0.0775 \pm 0.1124i$ |

For the right event the correspondence is not quite as good. What the difference between the two cases is, is not known. It is possible to speculate that the correspondence is good for the first event since it is caused by a HVDC line being disconnected. A disconnected HVDC line may have less influence on the system, while a disturbance due to a generator being disconnected leads to system changes.

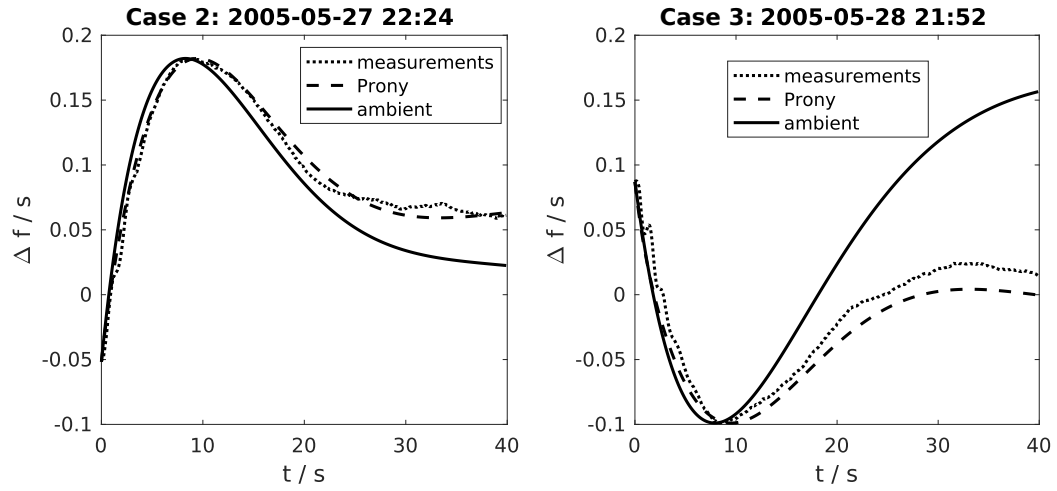


Figure 30: Frequency measurements from two events as well overlaid with reconstructed step responses from the rigid body mode. The step responses are scaled to have the same magnitude. The left step response was due to the exporting HVDC line Skagerrak 3 between Norway and Denmark being disconnected. The right due to Ringhals B2 being disconnected.

One may also notice that the time of the minimum corresponded quite well to that predicted by the ambient estimation, something noted in all cases. The reason and implications of this are unclear. Possibly it could open up for another method of inertia estimation by focusing on the time of the minimum instead of the modes. In Figure 2 it is seen that this also depends on the inertia.

Furthermore, it was noted that the estimate was very sensitive to the data used. Using the measurements from a few minutes earlier could give a different result, and even

such things as mean subtraction and how it was done could affect the result significantly. Therefore, it is maybe not wise to draw further conclusions than that estimates of the rigid body mode from real measurements is a formidable challenge, much more difficult than for the simulated systems that have been investigated in this thesis. A speculative explanation for the worse performance compared to theory is that there is a backlash in the governor, making the dynamics non-linear. The results presented are thus most likely overly optimistic. Further studies are needed in this area.

# 5 Inertia estimation from modes

Since the sensitivity analysis of the modes determined that the dependencies were highly non-linear and complicated, it is not plausible to find an algebraic expression to solve for $H$. Therefore, numerical methods must be used. To investigate the possible methods for this and evaluate their accuracy, estimations are done on various systems with varying $H$.

To perform the numerical estimation, a system model is needed from which modes can be calculated. This is discussed in section 5.1. To find the parameters such that the calculated modes match the measured is a non-trivial optimisation problem even with a system model. Aspects of this is discussed in sections 5.2 and 5.3.

A basic division can be made between the inter-generator modes and the rigid body mode, since both the possibilities to estimate them and the use to estimate the inertia from them differ. They are studied separately, the rigid body mode in section 5.4 and the inter-generator modes in section 5.5. Ideally the information from them is combined to give the best possible estimation, hopefully surpassing the accuracy of each individually. This is investigated in section 5.6.

## 5.1 System modelling

If the eigenvalues of a system are given and the structure of the system is known, its parameters can be estimated numerically. First the system matrix of the system is constructed. It will include some known parameters and some unknown parameters, where $H$ is in the latter category. Then the task can be formulated as finding values for the unknown parameters such that the modes of this system matrix coincide with the measured modes. This means minimising an objective function that takes the unknown variables as input and gives the difference (in some sense) between the calculated and estimated eigenvalues as output. The activity of generators in a mode might also be included in the objective function.

Instead of constructing the system matrix manually, a simulation software can be used. This allows for easy implementation of more features and decreases the risk of mistakes. In the project, PowerFactory was used for this.

To construct a model, a large range of parameters must be known. Those that are not known can be set as unknown in the model and estimated as well. Obviously, the task will be easier the more parameters are known. Fortunately, the system operator (or system operators in the Nordic case as each country has its own) does have access to certain system information and models.

$H$ will inevitably be unknown, and in the simulations also $D$ will be assumed to be unknown.

For the rigid body mode, knowledge of the governors and the turbines is needed. Dynamic models of governors and turbines and their parameters can be assumed to be known for larger power plants, but to a considerably less extent for smaller power plants. For electrical motors they are not known at all. However, large power plants have larger impact on the system than small. The system operator can also be expected to have access to a model describing at least the total governor and turbine responses of the entire system in some configuration [4, p. 45]. However, some parts of the system may be out of service, which would affect the accuracy of the model.

When the rigid body mode is considered, only the frequency of the entire system and not of individual generators is of interest. In this case, it is possible to simplify the system into only having one frequency and model it as if all generators are connected to the same node. This reduces the number of states of the system, but risks worsening the estimations. Doing this, transmission lines and transformers are not explicitly modelled and may even be ignored. Even if the simplification is not made, it can be noted that these parameters matter little and exact knowledge of them is not needed. It may be taken even one step further, and modelling the system as only having one generator. The total inertia is what determines the mode, and there is little or no gain in differentiating how the inertia is distributed among individual generators. However, merging all generators in all aspects might be exaggerated. It might be wiser to have different generators in the model, but set the inertia and some other parameters to the same in all of them. Most problematic is the summation of different governors, who may give rise to frequency control that cannot be described well by one simple model. Nevertheless, a model of the power system with only one generator is often a decent approximation for analysing the primary frequency control. In reality, it is more probable that the entire frequency control is merged into one or a few models.

To estimate faster inter-generator modes, knowledge of more dynamics is needed. This includes voltage regulators and power system stabilisers (PSSs). Both are designed by humans and their structure and parameters should be possible to know. The generator machine parameters should also be known. These are static, and it seems reasonable to assume that there is some knowledge of them.

Transmission lines are static and their parameters should be well known, but they may be in service or not, something that is most likely known. The power flow in them is on the other hand variable and affects the point around which the system is linearised. The same is true for the voltages and bus angles. It is possible to continuously estimate these states with a state estimator [25], which can be assumed to be available in the control room. Regardless, these states are used for linearising, meaning that they are not too sensitive to errors and very frequent updates are not needed.

More can be assumed to be known for larger power plants, and less for smaller, but smaller power plants have less control and affect the system behaviour less. It would however be good if the model could handle uncertainties in these parameters as well.

## 5.2 Mode matching

There is also the problem of matching the numerically calculated and the measured modes. If a calculated mode corresponds to a measured one, but is compared to another mode, it might give a much larger error than there actually is. If they are paired incorrectly, the gradient of the error may also be incorrect. An illustration of how this could affect the estimation is shown in Figure 31. The frequency, damping and mode shape, i.e. the activity of the generators, all change with the parameters. Therefore, the matching will also change, causing discontinuities in the objective function. This may contribute to creating local minima, making the optimisation problem more difficult.

The rigid body eigenvalue should stand out clearly as having the most activity in the frequency. This is not necessarily true for the inter-generator modes, but they should form a rather distinct group, with low damping and in a limited frequency interval. However, matching the different inter-generator modes is not trivial.

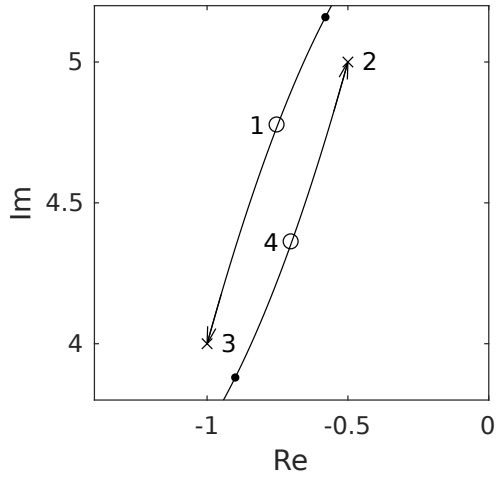


Figure 31: An illustration of how incorrect mode-matching could trap the optimisation algorithm in a local minimum. The example is not based on any real system. The measured eigenvalues are marked with crosses, and the calculated with circles. As a parameter varies, the calculated eigenvalues move along the black lines. If 1-3 and 2-4 are matched, the error is decreased by changing the parameter in the direction of the arrow, and the calculated eigenvalues will after a few steps coincide with the measured. This means that the perfect match in parameters has been found. If 1-2 and 3-4 are matched instead, the error is decreased by changing the parameter in the opposite direction of the arrow. The modes will after a few step get stuck in the local minimum marked with dots.

The matching for the inter-generator modes is performed in the following way. For each pairing an error is defined based on how close the two modes are in some respect, then the objective is to find the matching that minimises the total error. If there are more measured than calculated eigenvalues (there will always be $N-1$ calculated eigenvalues but all $N-1$ modes will rarely be possible to detect), dummy states can be added that has the cost zero for matching with all. Adding the dummy states means that only the theoretical modes that match the measured modes best are used, the remaining match with dummy states and are discarded. This matching problem is well-known, and a solution is to use the Hungarian algorithm [34]. It is implemented in the Python module scipy as scipy.optimize.linear_sum_assignment.

The error can be defined based on three aspects: the imaginary part of the eigenvalue, the damping and the mode shape. The damping is difficult to estimate, and may say little about the mode anyway, and is therefore not used. The imaginary part provides more useful information and can be accurately estimated, but the mode shape is believed to be the most consistent property of a mode for different parameter values.

In the optimisation routine in this work, the matching is made with the Hungarian algorithm, mainly focusing on the mode shape. The cost for matching a measured and calculated mode is defined as: $25 \cdot ||\boldsymbol{a}_m - \boldsymbol{a}_c|| + 2 \cdot |\omega_m - \omega_c|$ where $\boldsymbol{a}_i$ is the vector of the signed, normalised activity of the mode, and $\omega_i$ its imaginary part.

## 5.3 Optimisation

When an objective function has been defined, it is to be minimised. If there are many parameters, the dimensionality of the problem makes it too computationally costly to

evaluate all possible parameters. Therefore, an optimisation method must be used to minimise it. The minimisation problem is common, but potentially difficult.

The most computationally costly operation is to evaluate the error function, since the system matrix (which is very large for a realistic model) must be constructed and its eigenvalues found. This is especially true when PowerFactory is used for this. Although the internal operation of PowerFactory is not known, it is probable that it for each change of parameter needs to recalculate the load flow and linearise the system again. If the system matrix can be constructed directly in for example Matlab, much computation time would be saved, but this is not done due to the complexity of the task.

Most methods are based on the gradient of the objective function, and it is also used in this project. Since it is not possible to calculate the gradient of the function analytically, numerical methods must be used. The most basic method, which is also used in this project, is to evaluate the objective function at two close points, calculate the difference and divide by the distance. This requires two evaluations of the objective function. The procedure must be repeated in all directions, i.e. once for every unknown parameter.

When the gradient is determined, a line search is performed to find how far in the descent direction the objective function is minimised, i.e. finding a suitable step size. A simple way of doing this is to take a (too) long step, evaluate the objective function, and decreasing the step size until a smaller error is achieved, and then continue to decrease the step size until the error starts to grow again, then a minimum in that direction has been found and is used as the start of the next step. How fast the step size is to be decreased is an act of balance between accuracy and faster computation. If the step size is decreased too slowly, many function evaluations are needed, slowing down the program, but if it is decreased too fast there is a risk of missing an interesting point. It has been concluded that a good rate of decrease is to make the step between 50 and 80% as large as the last iteration. If the error is very large, e.g. 100 times larger than the previous error, time can be saved by decreasing the step size more drastically, 5 or 10 times.

There are more sophisticated methods for line search. However, they are mainly targeted at finding the exact minimum in the descent direction. This might not be necessary, instead a "good enough" result might be sufficient, and the inaccuracy compensated by calculating the gradient at the new point and taking another step. This procedure is repeated until the method converges and the error stops decreasing. The procedure was terminated when the error was $>98\%$ of the error in the previous iteration.

More advanced methods for optimisation exist. What has been described is a first order method. Second order methods such as Quasi-Newton exist as well. They are intended to handle the case when the minimum lies in an almost orthogonal direction to the gradient at most point. The problem can be visualised as a long valley with a small incline, where the minimum lies in the end of the valley, and the optimisation method moves sideways, up and down the walls of the valley. Some attempts showed, however, that second order methods did not improve the result much. Rather, the problem seems to be local minima and discontinuities, something that second order methods do not solve.

To avoid local minima, several initial values must be tried. Then the estimate with the smallest error from all runs is chosen. An alternative is to use the average estimation from all runs weighted by the error instead of the single best result, which is done in this work. This is intended to decrease the variability and exclude strange outliers. Naturally, more runs with different initial values increase the probability to find the minimum, but the computational cost also increases quickly. The problem is especially pertinent for

large, complex systems. If the system only has two generators, one run was found to almost always be enough to find the minimum, but for larger systems more runs were needed. Due to computational limits, the number of runs were held in the range 5-10. It should be noted, however, that these computational limits could be relaxed for actual estimation rather than for evaluation purpose. For evaluation purpose the program must be run many times to determine average performance and robustness.

It is also necessary to a check that the result found by the minimisation algorithm is reasonable (e.g. positive $H$). This was achieved by using a penalty for values outside a reasonable range. An extra term is added to the objective function, e.g. $k \cdot \max(0, -H)^2$, where $k$ is a large number.

There are some parameters for the optimisation algorithm that must be decided. Those are:

- initial step size (varies a lot, select such that it always needs to be decreased, but still reaches a minimum before time-out);
- factor for decreasing step size (0.5-0.8);
- limit stop the algorithm from working too long on decreasing the step size or taking new steps (10-15 steps has been used, it seems rare that more is beneficial unless the initial step size is too large);
- stop criterion (the error is $> 0.98$ times the previous error);
- multiplier to compensate the difference in scale between $H$ and $D$ (multiplying the gradient with respect to $D$ by 10 has shown to improve the results);
- the step size to calculate the gradient ($10^{-4}$);
- the number of different initial values to try (mostly limited by computational power, about 5 should usually be enough, but more increases robustness).

The simplified pseudocode for the optimisation procedure is presented in appendix A.

## 5.4 Inertia estimation using the rigid body mode

The simplest method for estimation is to only use the rigid body mode. Any information about inter-generator modes is discarded. Since less information is used, it is probable to mean less reliability and accuracy.

What is won, is of course simplicity. Some parameters, such as the connections between nodes, is no longer necessary. Most importantly there is no need to estimate the inter-generator modes or model them. Since they require modelling of the voltage dynamics, this simplifies the modelling greatly.

In this case, only the inertia constant of the entire system can possibly be estimated, and not those of the individual parts. Nevertheless, this is the most important value from a system perspective, and only estimating the total inertia is still satisfactory.

In this section, two systems will be considered. First, the IEEE 14-bus system with five generators is considered in subsection 5.4.1. To this system hydro governors and turbines were added. In subsection 5.4.2 the IEEE 39-bus test system with ten generators is considered, a system dominated by steam plants. Finally, the sensitivity to errors is discussed in subsection 5.4.3.

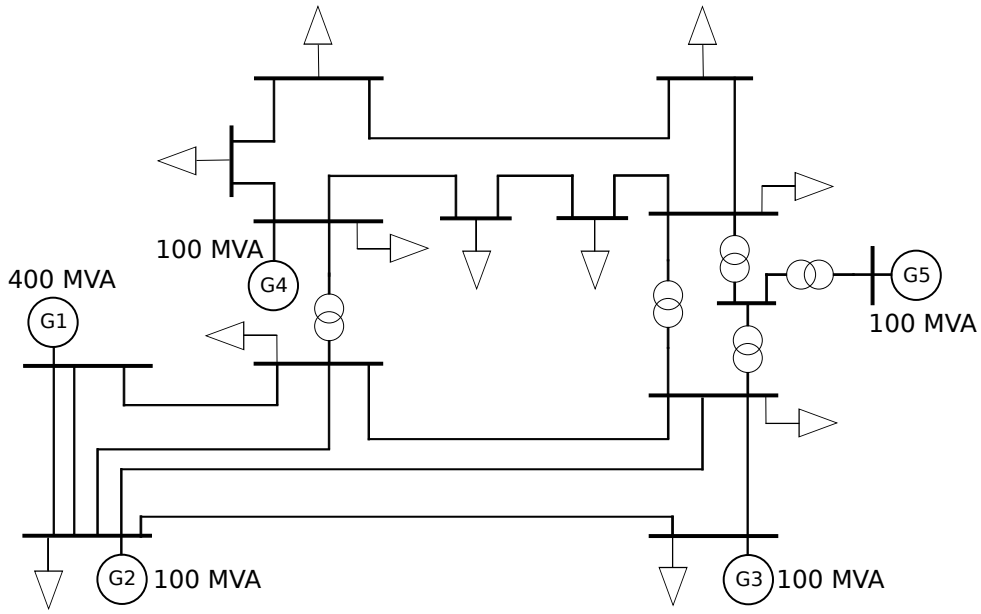


Figure 32: Single line diagram for the IEEE 14-bus system.

### 5.4.1 Five-generator system

The 14-bus IEEE test system is a simplified model of the power grid in the American Midwest in 1962 with five synchronous machines. Three of the synchronous machines are compensators that do not generate active power while only two are generators. However, both categories have inertia, and therefore there is little need to distinguish between them. It may also be noted that one generator represents half of the base power of the system, making it asymmetric. A single line diagram of it is shown in Figure 32. There is an existing PowerFactory model for this system, but unfortunately it does not feature control. Therefore it has been manually added, with hydro governors and turbines according to the model presented in 2.3 and voltage exciters of IEEE Type 1 (see section 2.7). The inertia has also been changed to test many scenarios.

It was quickly determined that if both the real and the imaginary part of the rigid body mode was known, the total inertia could be very accurately estimated, with an error $< 1\%$, even with the damping $D$ of the generators unknown. Alternatively, if the damping of the generators were known and only the imaginary part used, it was also possible to determine the total inertia with high accuracy, albeit not exactly, with a few percent error. However, none of these cases is very realistic. As has been concluded previously, the real part of the mode is difficult to estimate accurately (see section 4.5), and the damping is unlikely to be known. Therefore, a more realistic scenario is to only use the imaginary part and have the damping unknown, and in that case the estimates are no longer almost exact. For the first two cases there were as many unknown parameters as variables, meaning that it could be solved uniquely, while in the latter case there were two unknown ($D$ and $H$) and only one measured parameter (the imaginary part).

The optimisation was run on this system, only using the imaginary part of the rigid body eigenvalue. The results are shown in Figure 33. For lower values of the inertia, the results were good, with only a few percent error or less. Running the optimisation method more times with different initial values generally improved the result, but was computationally costly, as previously discussed.

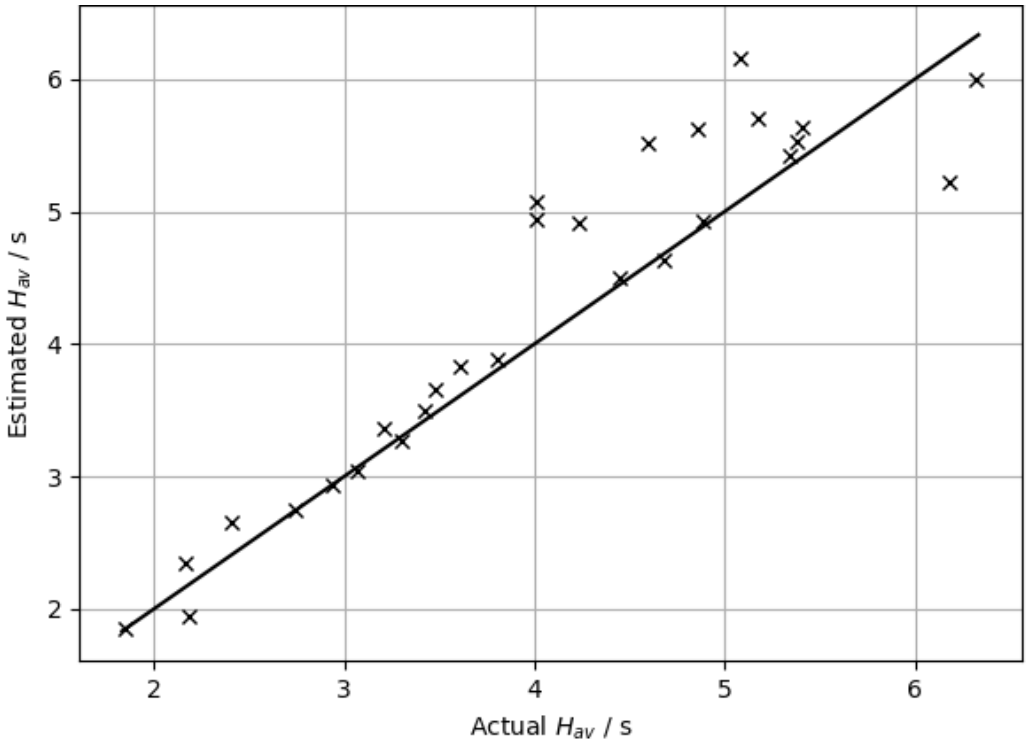


Figure 33: Estimated inertia versus actual inertia in the 14-bus system.

For higher values of the inertia, the results were less reliable. The explanation was that the mode was well damped or overdamped, meaning that it had no imaginary part or only a small one. Therefore, less information was available for the estimation.

If only the imaginary part is used, the problem reduces to a one-dimensional regression problem thanks to the fact that the individual inertia is not important for the rigid body mode, only the total inertia of the system. Therefore, the imaginary part of the rigid body mode can be plotted against the total inertia. With only one parameter, it is computationally possible to do exhaustive calculations and find the function from the inertia to the imaginary part of the rigid body eigenvalue. This can be achieved by fitting a polynomial to a set of calculated points. Using this function, the inertia can quickly be estimated by evaluating the function for a measured value of the imaginary part of the rigid body mode. This is shown in Figure 34. In this figure, the damping was also assumed to be unknown, this explains most of the spread around the fitted line. With the damping unknown, the standard deviation of the percentual error was estimated to 8.8%, with the damping known, it decreased to 2.3%.

As seen in Figure 34, the error was also smaller for smaller inertia values, and for large enough values, the curve flattens out and the imaginary part is no longer useful to distinguish between the high inertia values. This is similar to what was seen in Figure 33. As was seen in the root-locus plots in Figures 19 and 21, an increasing $H$ decreases the imaginary part to a certain point where it stops, and the real part changes instead. Before the curve flattens, the result is significantly better. The standard deviation of the relative error when $H_{av} = \frac{\sum_i H_i S_i}{\sum_i S_i} < 4$ s was only 5.5 % with the damping unknown. This is shown in Figure 35 where the error is plotted against the sum of all inertias. The dip at $\sum H_{av} = 5$ s is explained by the fact that this was the estimate when the imaginary part had reached the constant value. Since it is most important to estimate the inertia

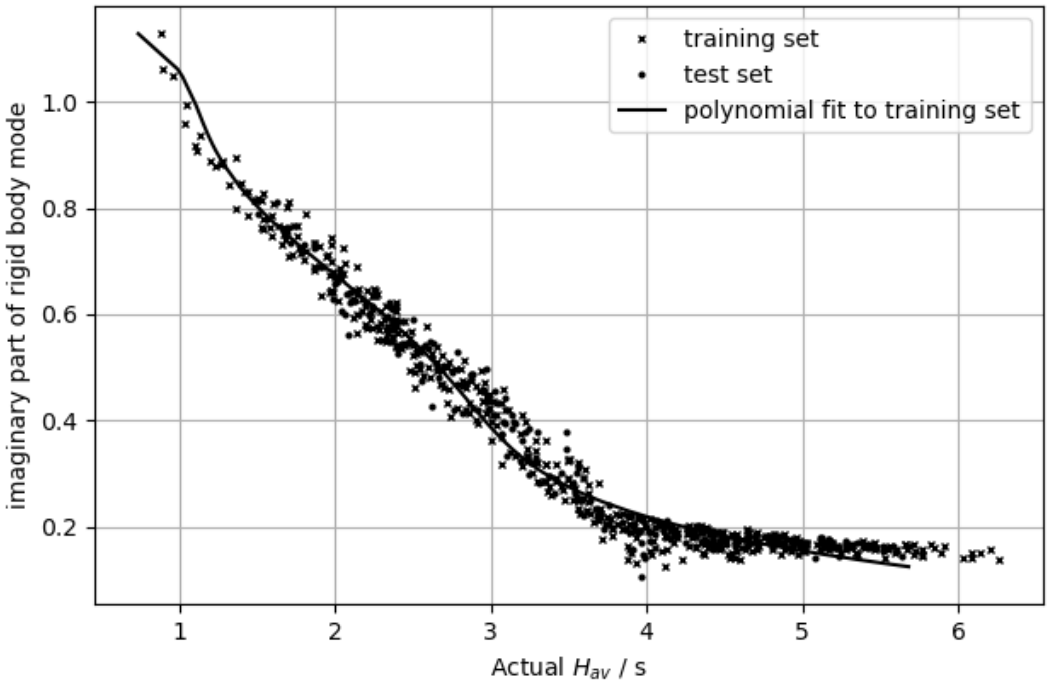


Figure 34: The imaginary part of the rigid body mode vs. the total inertia of the IEEE 14-bus test system. The damping was allowed to vary between 0 and 1.5 p.u.

correctly when it is low, the increase in the error for high values is not necessarily very serious.

### 5.4.2 Ten-generator system

The 39-bus IEEE test system is a simplified model of the New England power system. It has 10 generators, 19 loads, 34 lines and 12 transformers. Unlike the 14-bus test system, the PowerFactory implementation has governors and voltage controllers implemented. The voltage regulators are IEEE type 1 (see section 2.7). One generator has no governor (since it is an equivalent of the rest of the Eastern Interconnection power system), one is a hydro plant and the remaining are steam plants with the IEEE type G1 steam turbine and governor model described in section 2.4.

It can be noted that this system is weakly controlled, due to the lack of governor in the largest generator and weak droop in the governors, giving less power per Hz deviation from nominal frequency. Hence, the modes are slower and more damped. It also means unrealistic difficulty for the mode identification. The steam plants have the droop $R = 0.2$, which is very high, and strangely, the hydro turbine has the droop 0.05, and is therefore compensating for a disproportional amount of the disturbance. The governors were therefore modified, such that all had the droop 0.1. This is still quite much, meaning that mode and inertia estimation is difficult. To give a smoother frequency response with the higher droop, the governor was sped up, with the parameters $K = 10$, $T_1 = 0.1$ s, $T_2 = 0.5$ s, $T_3 = 0.3$ s. The last modification makes the mode less oscillatory and the inertia estimation more difficult.

The same procedure was applied to this system, and the result was similar to that of the IEEE 14-bus test system. The imaginary part of the eigenvalue is plotted against the

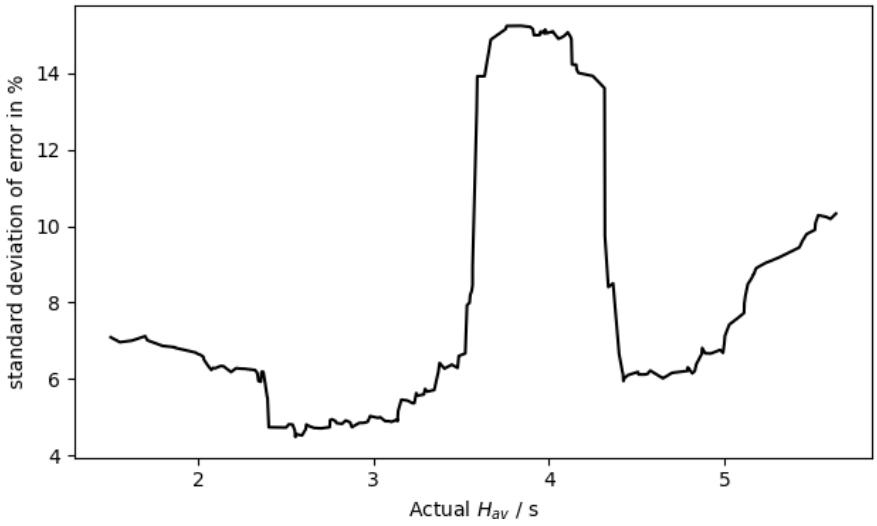


Figure 35: The error of estimating the imaginary part of the rigid body mode vs. the total inertia of the IEEE 14-bus test system.

total inertia in Figure 36. The qualitative appearance is the same as in Figure 34, and the slightly different shape is explained by the different governors. The deviation from the fitted polynomial line was 5% for the entire set, with the damping unknown. This is not different enough from the IEEE 14-bus test to suspect any noteworthy differences. The reason for the slightly lower error was most likely that the average damping varied less (since there were ten generators to average over instead of five). The error seemed to depend the same way on the inertia, with increasing error for larger inertia. The derivative of the curve, i.e. how sensitive the inertia estimation was to measurement error in the mode, looked the same, with slightly lower values. The conclusion that can be drawn for this, is that the results are not too dependent on the system.

### 5.4.3 Sensitivity to error

In reality, there will always be measurement and model errors, and therefore it is important to know how these affect the estimation of $H$. Two kinds of errors are considered, errors in the measured modes and errors in the model parameters. Furthermore, there might be errors in the model structure, something considered too difficult to analyse here.

First, it is considered how an error in the estimation of the imaginary part of the modes propagates to an error in the estimation of the inertia. This can be found by taking the derivative of the fitted polynomial. The derivative explains how much the estimated inertia changes for a change (or measurement error) in the eigenvalue. The relative error, i.e. how many percent error in $H$ is caused by a given percent error in the estimated imaginary part, can be found by normalising the expression, giving $\frac{dH/H}{d\omega/\omega}$. In Figure 37 the propagation from the relative error in the estimated imaginary part to the relative error in the estimated inertia is plotted. The magnification of the error goes from 2-3 for very small inertia values, meaning that the relative error doubles or triples, to 0.5 for higher, meaning that the error is halved. The sensitivity is larger for the 39-bus system for unknown reasons. For very high values for the 14-bus system this plot is not useful, due to the inherent error when the curve flattens out. The error propagation for low

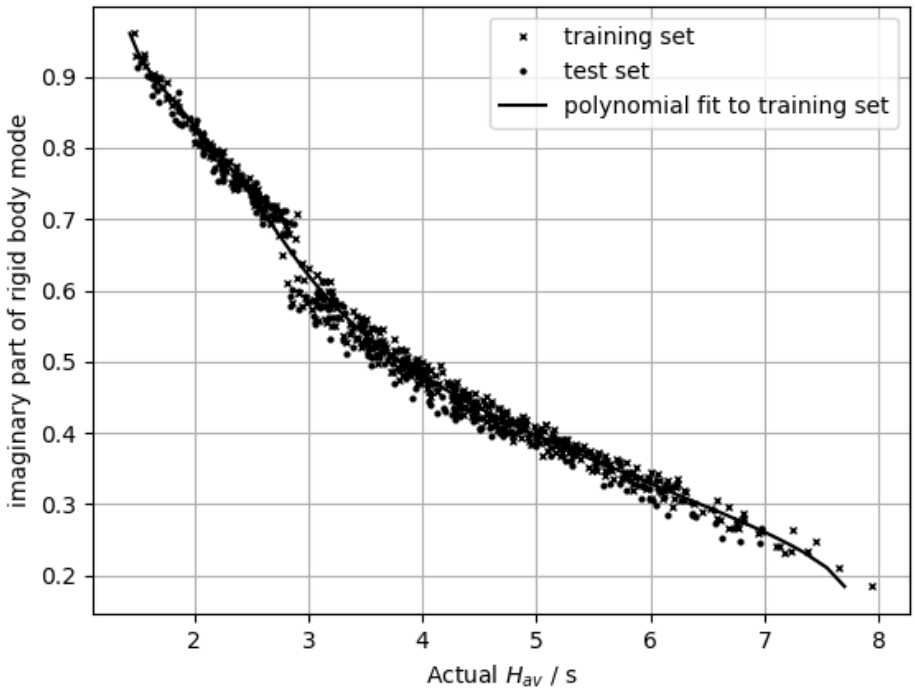


Figure 36: The imaginary part of the rigid body mode vs. the total inertia of the IEEE 39-bus test system. The $D$ for the generators was allowed to vary between 0 and 1.5 p.u.

inertia values is an unfortunate result, but it must be kept in mind that the estimations are better when the imaginary part is large (and the damping low), and these two effects may to a certain extent cancel out, meaning that the characteristic of the curve cannot definitely be deemed neither detrimental nor beneficial.

Secondly, there is the error from incorrect model parameters. This is investigated by using the model of a hydro power plant, which is assumed to be the only factor impacting the rigid body mode. This allows for a simplification using only one generator and a single bus grid. Derivatives are used in a similar manner, i.e. how much the estimated $H$ changes as one parameter changes. Assuming that the imaginary part alone is used for estimation, this can be written as $\frac{dH}{dK} = \frac{dH}{d\omega}\frac{d\omega}{dK}$, where $K$ is the parameter. The introduction of $\omega$ means that the calculation is done in two steps, first it is considered how the parameter affects the imaginary part, then how the imaginary part affects $H$. This can be normalised to get the relative error propagation: $\frac{dH/H}{dK/K} = \frac{dH/H}{d\omega/\omega}\frac{d\omega/\omega}{dK/K}$. Setting up the system matrix in Matlab, this was done by numerical differentiation, giving the result in Figure 38.

As can be seen, the most serious error propagation is to be expected from $T_w$, $K_p$ and possibly $T_S$. For all but $T_w$ in some cases, the error propagation is below 1, i.e. the relative error in the parameter is reduced when estimating the inertia. The other parameters maintain rather moderate values for anything but extreme values. It should be kept in mind that all values here are not necessarily reasonable for a governor. It must also be kept in mind it is in no way taken into consideration how accurately the parameters are known, giving the error to be multiplied by the factors in Figure 38.

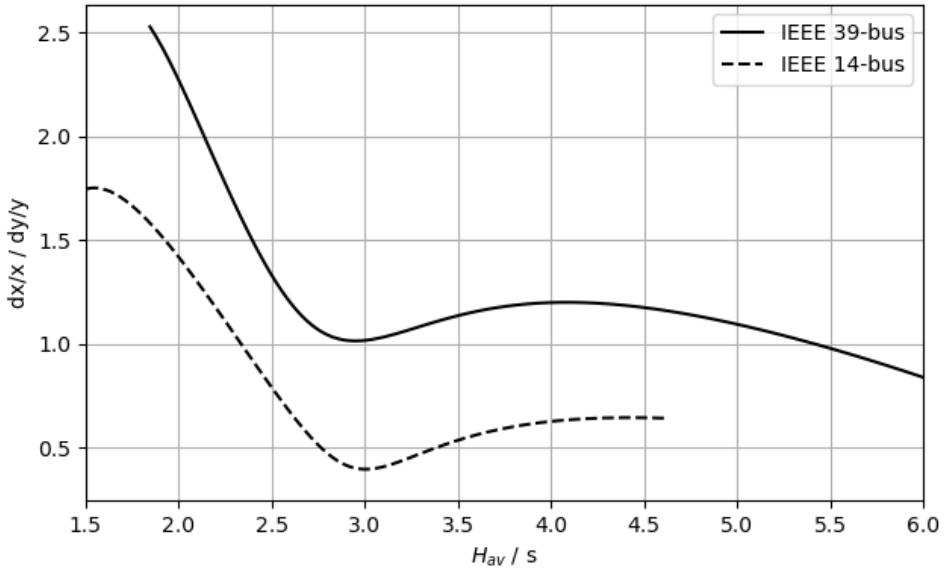


Figure 37: How much the relative error in the imaginary part is magnified when estimating the inertia, using the curve from Figure 34.

## 5.5 Inertia estimation using inter-generator modes

Using the inter-generator modes instead of the rigid body mode has some inherent difficulties. To estimate the inertia $J$ of the entire system, it is most important to accurately estimate $H$ in generators with a high base power, meaning that the same $H$ translates to a larger inertia $J$. These generators also have the largest influence on the rigid body mode. The same is not true for inter-generator eigenvalues. It is not necessary for a generator to be active in any detected mode (or the activity is very small), making it difficult to deduce the inertia from that mode. Nevertheless, that a generator is not active in a mode also constitutes information.

As noted in chapter 3, the frequency of the oscillation between two generators is to a higher extent determined by the generator with lower inertia, as seen in equation (8). This would mean that the $H$ of the smaller generator would be more accurately estimated, while it is more important to accurately estimate the $H$ of the larger generator. If the difference in size is too large, the mode will be difficult to detect at all, and as a consequence probably not be possible to use in the estimation.

The possibilities to tackle this problem are the following:

- have enough modes such that all generators are somewhat active in at least one mode;
- combine with the rigid body mode for estimation;
- exclude the generator without activity from the estimate. This could be useful if the inertia of this generator could be known in some other way. For example, the physical values could be known for a large power plant.

Furthermore, not all modes will be possible to estimate, as seen in section 4.6. Only a few can be assumed to be accurately estimated. The estimates of the imaginary part of the modes are quite accurate, but the damping estimates have large uncertainty. The

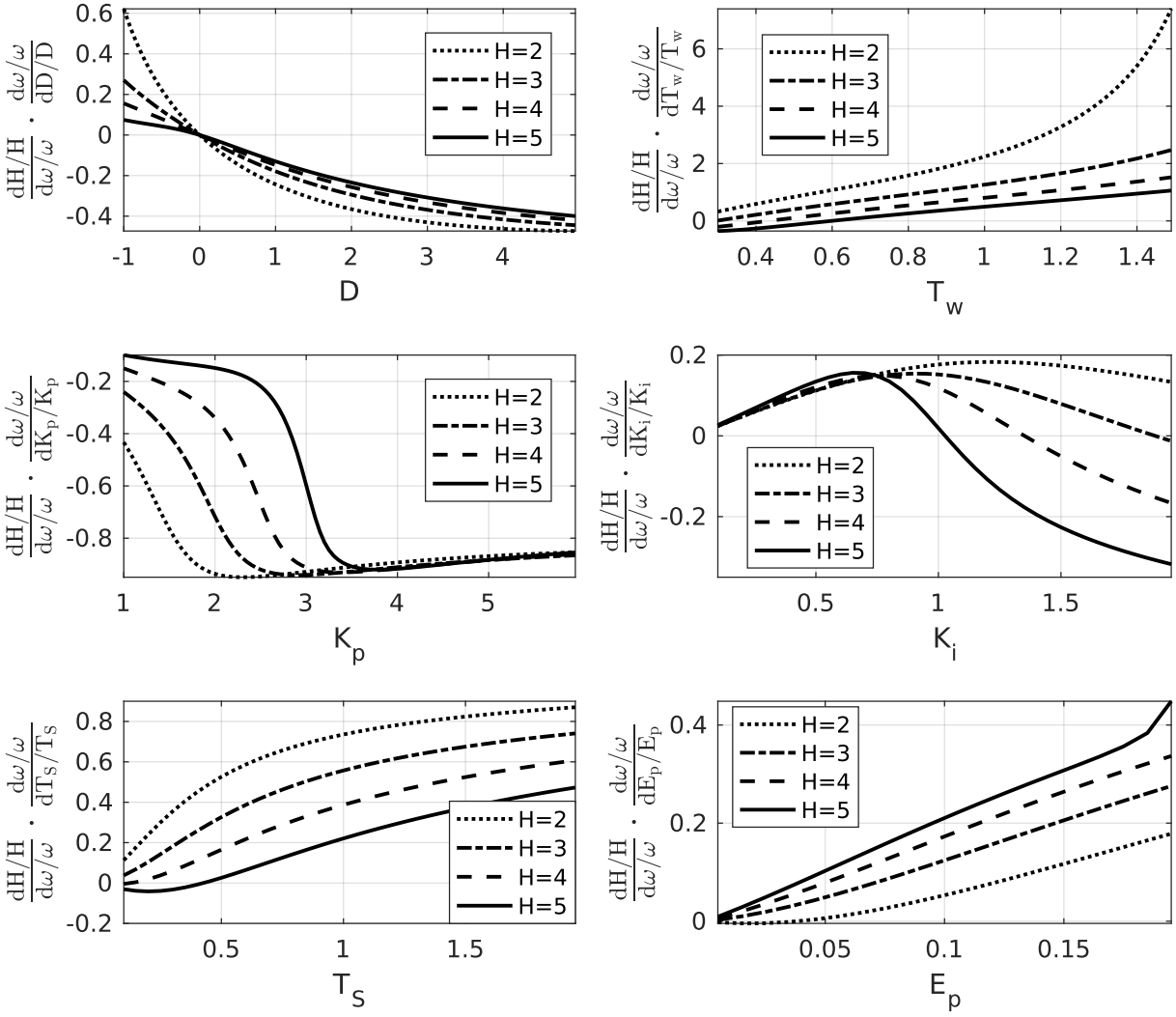


Figure 38: How much the relative error in a model parameter is magnified when estimating the inertia, using the imaginary part of the rigid body mode. Nominal values are $H = 3s, D = 1, R = 0.05, K_i = 0.7, K_p = 4, T_S = 0.5s, T_w = 0.5s$.

mode shapes can be estimated for a few modes, but the estimates are often somewhat inaccurate.

In this section, various systems will be considered. First, some initial investigation is performed on a simple two-generator system in subsection 5.5.1. The complexity is then increased, first with a three-generator system in subsection 5.5.2, then with a two-area system with four generators in subsection 5.5.3, the IEEE 14-bus test system with five generators in subsection 5.5.4 and finally the IEEE 39-bus test system with 10 generators in subsection 5.5.5. Some remarks on the sensitivity to errors are made in 5.5.6.

### 5.5.1 Two-generator system

A simple system consisting of two generators was constructed in PowerFactory. A single-line diagram is shown in Figure 39. The generators had hydro plant models (although this should not matter) and automatic voltage regulators (AVRs). Whether the system only had two buses or additional buses with load did not matter for the result. This system only had one inter-generator eigenvalue which made the task easier. It had on the other hand 4 unknown parameters, $H$ and $D$ for both generators.

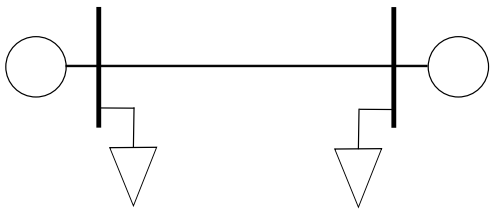

Figure 39: Single-line diagram of the two-generator system.

Only the imaginary part of the eigenvalue was initially used to estimate $H$ since it was the most likely to be well measured. Nevertheless, it was determined that the optimisation algorithm was able to estimate the system inertia with good accuracy, typically with only a few percent error. Sometimes the error was larger though, typically due to a large difference in inertia between the two generators. $D$ was not estimated very accurately, but that is of less importance for this project. That is not very surprising, since the damping is linked to the real part of the eigenvalue and an incorrect estimate of $D$ does not affect the imaginary part noticeably. Adding the real part to the estimation did not even improve the result, and it is a reasonable decision to leave it out all together, given the uncertainty in its estimation.

Although the total system inertia was accurately estimated, the individual $H$ of each generator was not. The expression of the oscillatory frequency from $H$ is symmetrical for $H_1$ and $H_2$, as can be seen in (8). It could identify the case where the inertia was distributed between the generators correctly (and it occasionally did), but it could also find its mirror, where generator 1 had the $H$ of generator 2 and vice-verse. Still, this is not necessarily a major problem, since the total inertia is typically more interesting.

If the mode activity was included in the estimation the accuracy increased. The distribution of inertia was also correctly estimated. What the mode activity in this simple case describes is how much the same amount of transferred power affects the electrical frequency, which directly depends on the ratio of the inertia of the two generators.

### 5.5.2 Three-generator system

A simple three-generator system was constructed in the same way as the two-generator system above. A single-line diagram is shown in Figure 40. The purpose of this was to confirm that the results could be generalised to larger systems. That it was still possible to estimate the inertia accurately is shown in Figure 41. In this case two inter-generator modes existed and were used, once again only the imaginary part of the eigenvalue was used.

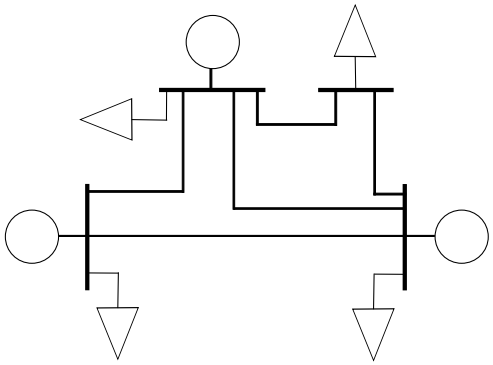

Figure 40: Single-line diagram of the three-generator system.

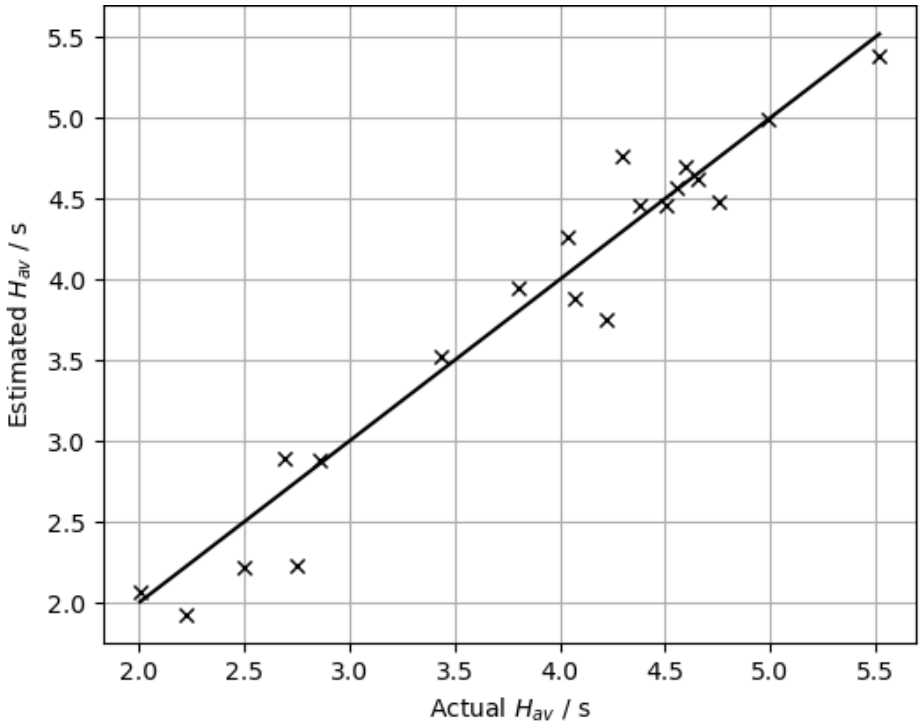


Figure 41: Estimated inertia versus actual inertia in a simple 3-generator system.

A worrying observation, however, was that if one generator had a much larger power base than the other two, the error increased. When they are of similar size, the error typically remains within a few percent. When one generator represents more than half the system base power, the error often reaches 10-20%. The large generator stands for a disproportionately large share of the error. If it is excluded from the estimate, the error

decreases. It should be kept in mind that normally if the error is randomly distributed among the generators, excluding one generator is expected to increase the relative error[1]. Partially the increased error due to power concentration can be mitigated by including the shape in the estimation. This can be seen in Figure 42. Even better would be if the inertia of the large generator was known, then the error for the remaining two generators is typically $< 1\%$.

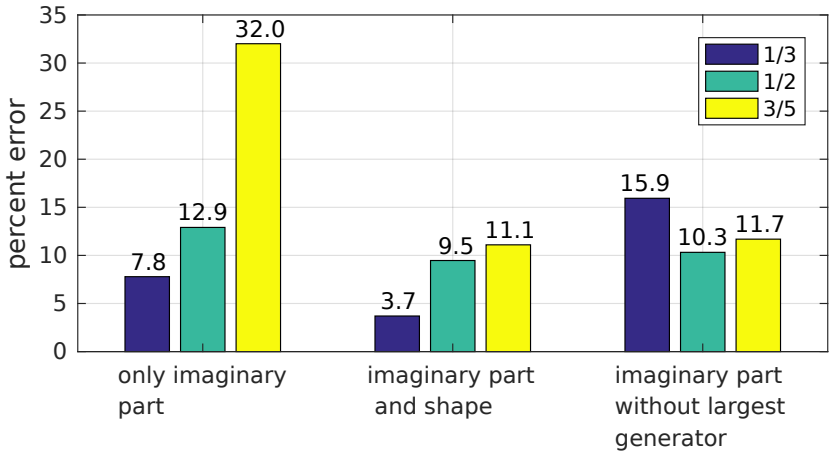


Figure 42: The estimated standard deviation of the percentual error for the three-generator system for different levels of concentration of the power. The standard deviation is calculated from 20 runs.

### 5.5.3 Two-area system

Since it is not always possible to estimate all inter-generator modes in a system, it would be preferable to be able to estimate the inertia from only a few. The principle is illustrated with the system presented in [3, p. 813] and shown in Figure 43. The system has four generators and is divided into two areas with two generators in each. It has three inter-generator modes, one between the areas and one within each area. The goal is to use only the inter-area mode to estimate the total inertia. An attempt to do this is shown in Figure 44. The imaginary part and the mode shape were used for estimation. Beside the inertia constants, the damping for each generator was also assumed to be unknown.

The most important parameter was the imaginary part of the mode. Focusing only on this parameter, the problem becomes a one-dimensional regression problem. In Figure 45, the imaginary part of the eigenvalue is plotted against the total inertia. The correlation is clear, and $H$ can be predicted simply by reading this graph. For $H_{av} > 4$, the standard deviation of the relative error was around 8%, while for $H_{av} = 2 - 3$ it was 14%. In this case the damping was set to be unknown, but it does not explain the deviations from the trend line, since the results remained even when the damping was known. The performance only using the imaginary part of the rigid body eigenvalue is slightly worse than if the mode shape is also used, especially for lower values of the inertia, showing that it may be worthwhile to include the mode shape.

[1] If $\mathrm{E}(X) = \mathrm{E}(Y) = \mu$, $\sigma(X) = \sigma(Y) = \sigma$, and $X$ and $Y$ are independent, then $\mathrm{E}(X+Y) = 2\mu$, $\sigma(X+Y) = \sqrt{2}\sigma$ and $\frac{\sigma(X+Y)}{\mathrm{E}(X+Y)} = \frac{\sigma}{\sqrt{2}\mu} < \frac{\sigma(X)}{\mathrm{E}(X)} = \frac{\sigma}{\mu}$.

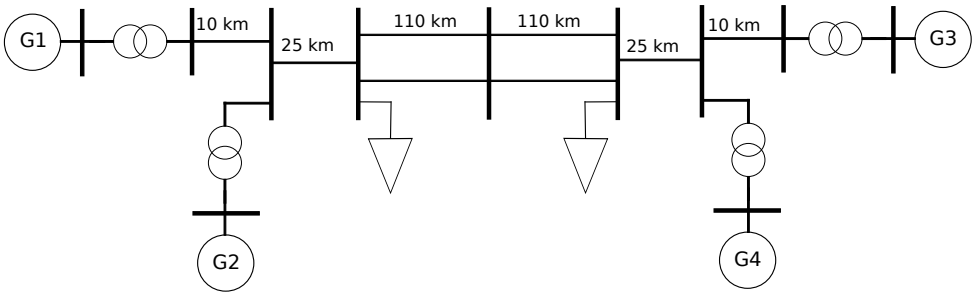


Figure 43: The two area system from [3].

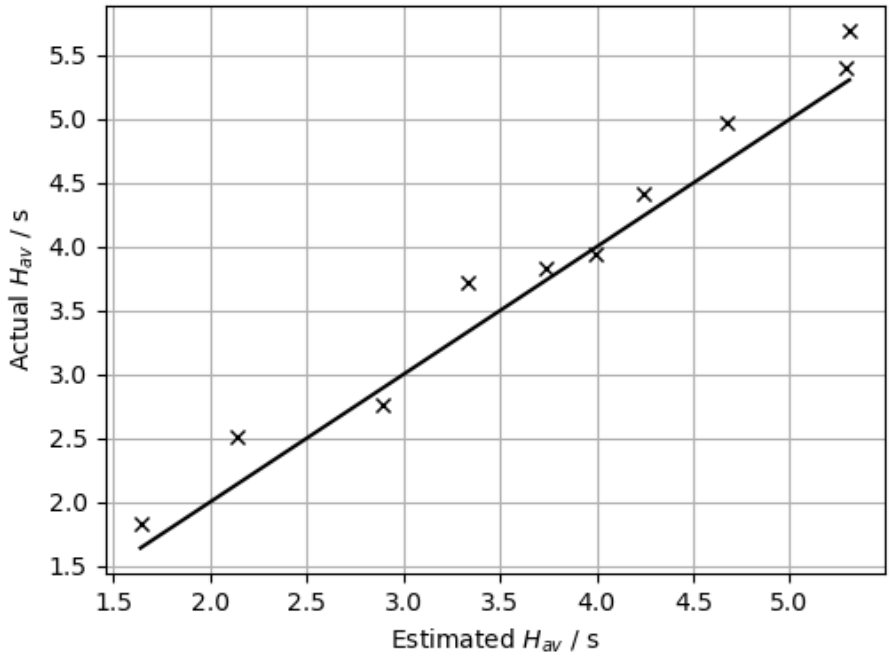


Figure 44: Estimated inertia versus actual inertia for the two-area system in [3]. The standard deviation of the relative error was 8.38%.

### 5.5.4 Five-generator system

The inertia of the previously mentioned IEEE-14 bus test system proved much harder to estimate with the inter-generator eigenvalues. It was very difficult to achieve good results without using the mode shape. It may even be impossible, since the optimisation algorithm did not seldom find solutions with the correct eigenvalues, but with the incorrect inertia. This problem was further exacerbated when not all four inter-generator modes were used. The explanation for this is most likely failed mode matching. At least a partial explanation of the failed mode matching is the increased number of modes. With the mode shape included, the result improved. In that case it was also possible to estimate the inertia of individual generators. This worked even if the mode shape was only used

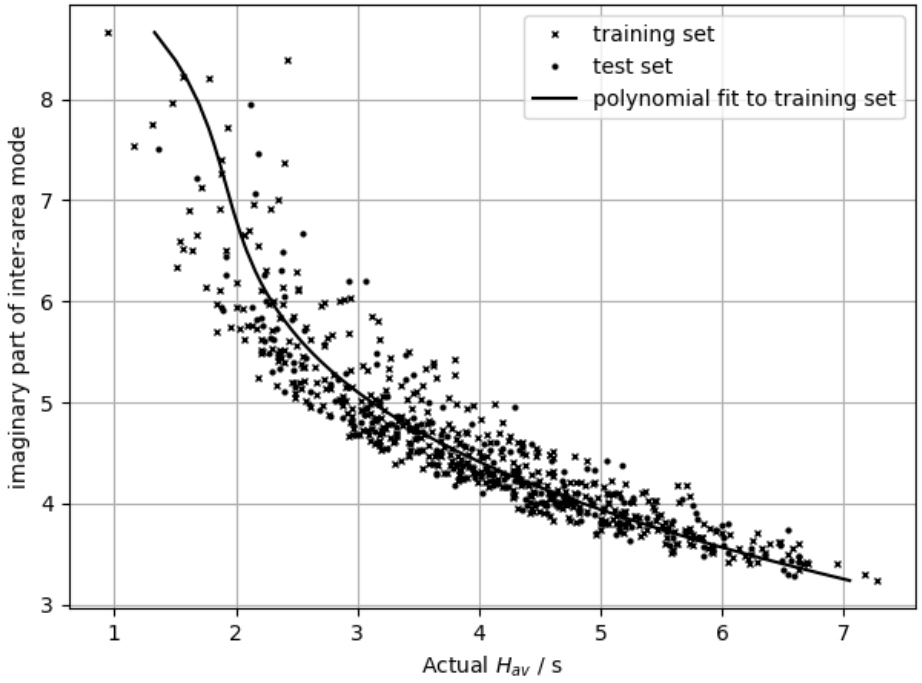


Figure 45: Inertia vs. the imaginary part of inter-area mode for the two-area system in [3]. Estimating the inertia from the imaginary part gave an error with the percentual standard deviation 10%.

for matching. The objective function to minimise in this case was:

$$\frac{w_{Im}}{N-1}\sum_i |\mathrm{Im}\{\lambda_{i,est}-\lambda_{i,meas}\}|^2 + w_{activity}\left(\sum_i \frac{\sum_j |NA_{i,j,est}-NA_{i,j,meas}|}{N(N-1)}\right)^2$$

where *est* stands for estimated (numerically calculated), and *meas* for measured, $\lambda_i$ are inter-generator eigenvalues, $NA_{i,j}$ is the normalised activity of generator $i$ in mode $j$, $N$ the number of generators and $w$ where weights. The values used were $w_{Im} = 50$ and $w_{activity} = 2000$.

Simulations were run using all four inter-generator eigenvalues as well as only the three and two most distinguished. In Figure 46 the actual vs. the estimated total inertia is plotted. The standard deviations of the relative errors were 2.7%, 7.4% and 7.3% when 4, 3 and 2 modes were used. That is, the error increased when not all modes were used in the estimation. However, this is the result after sorting out a few cases where the minimum value of the objective function was too high. This was most likely due to an unlucky choice of initial values and could be fixed by running the script for longer. That these estimates were bad was determined without any information about the actual inertia or error. Some estimates that actually were quite good (mostly due to luck) were also sorted out.

A problem occurred if all generators did not participate in at least one mode. Then the estimate of $H$ for that generator was worse. The effect was stronger the fewer modes used for estimation. Consider the following two illustrative examples. One is of a successful inertia estimation, and one of a less successful. It should be noted, however, that it is not always as clear-cut as in these two cases.

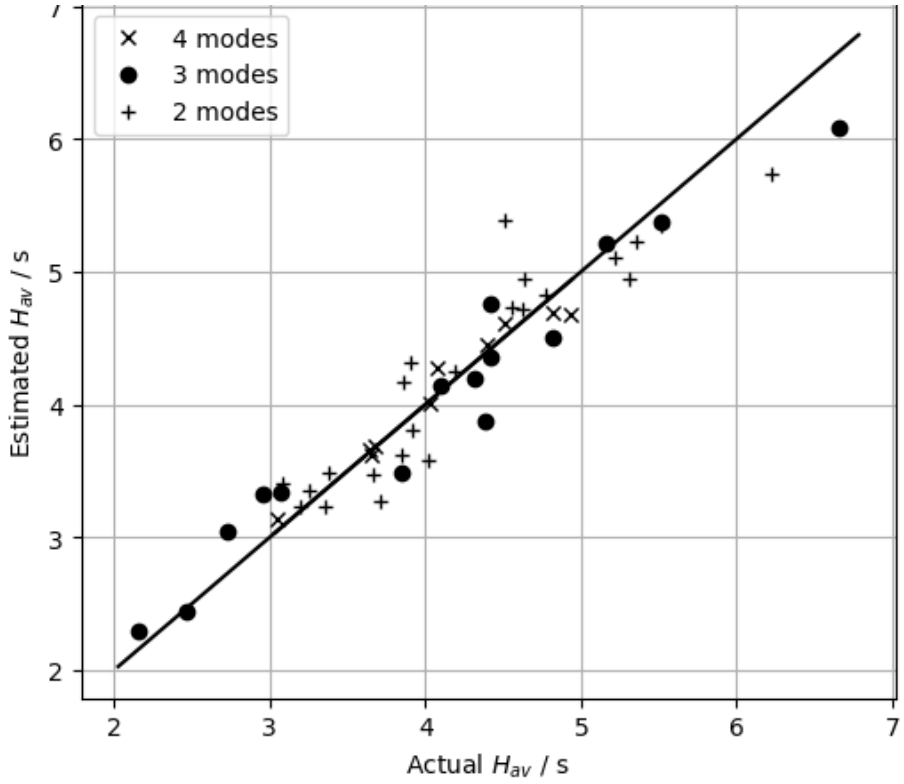


Figure 46: Actual vs. estimated total inertia for the IEEE-14 bus test system, using the imaginary part and the mode shape.

A successful identification using two modes was performed on the set $[H_1\ H_2\ H_3\ H_4\ H_5] = [6.63\ 2.69\ 4.18\ 6.05\ 2.30]$. The identified $H$ were $[6.55\ 2.68\ 4.38\ 5.23\ 2.29]$. The error in the total inertia was 100.58 MVAs, that is 2.38%. The error in $H_4$ explains 82% of this error. This is by no means chance, as is seen looking at the modes. One mode was $-1.75 \pm 16.07i$, with the shape $[0.15\ -0.64\ 0.12\ 0.02\ 0.07]$, while the second was $-0.88 \pm 11.99i$ with the shape $[0.03\ -0.02\ -0.27\ -0.06\ 0.62]$. Generator 4 has low activity in both modes, making it harder to estimate. That the estimation of $H_4$ was not worse may to some extent be attributable to luck. Generator 1 also has weak activity, but at least some activity in the first mode, especially considering it has four times as large base power as the other. On the other hand, generator 2 and 5 have large activity in modes 1 and 2 respectively, and consequently the estimates of their inertia was excellent.

A less successful identification was performed on the set $[H_1\ H_2\ H_3\ H_4\ H_5] =$ $= [1.77\ 4.76\ 6.46\ 2.47\ 1.12]$. The identified $H$ were $[2.08\ 4.11\ 9.65\ 3.39\ 1.09]$. The error in the total inertia was 466.43 MVAs, that is 21.3%. Most error was due to $H_3$, although there also were sizeable errors in $H_1$ and $H_4$. One mode was $-1.16 \pm 17.29i$, with the shape $[-0.13\ -0.01\ -0.01\ -0.15\ 0.69]$, while the second was $-1.61 \pm 13.99i$ with the shape $[0.67\ -0.19\ -0.01\ -0.12\ -0.02]$. The activity of generator 3 was extremely low in both modes, which explains the difficulty to estimate it. As a consequence, the error due to $H_3$ was 68% of the total error. (The errors in the other generators partially cancel out, the error in $H_3$ was 68% out of 129% in total). It is also not possible to expect a very accurate estimate of $H_4$. On the other hand, $H_5$ should be accurately estimated, which it was, but so should $H_1$, which was not exactly the case. It may be speculated

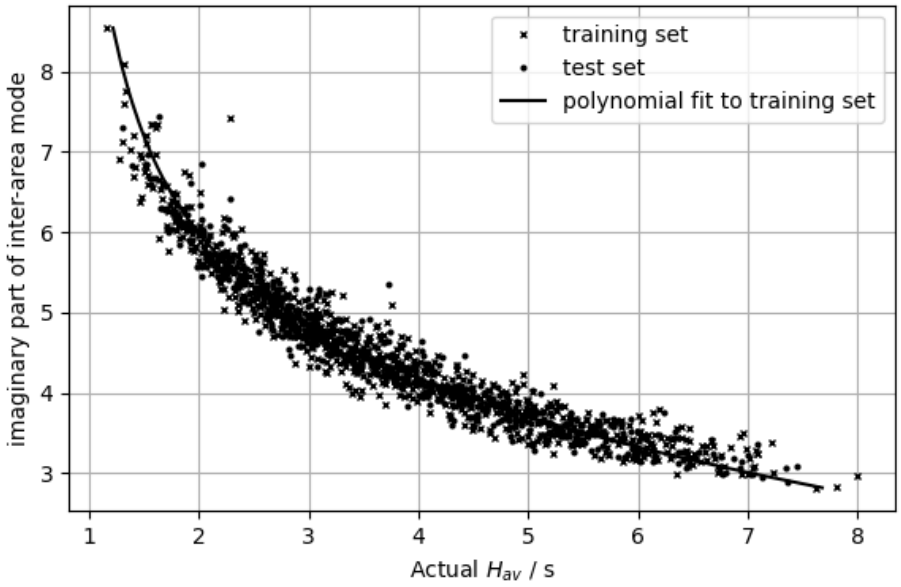


Figure 47: The imaginary part of the inter-area mode between the New England network and the rest of the Eastern Interconnection vs. $H_{av}$.

that the difficulty with the others makes the entire optimisation more difficult and the error propagates. It should also be kept in mind that the size of generator 1 increases the difficulty, and its contribution to the error. There is also a limit to the reasoning with activity, and not all blame can be put there. In this case the error of the objective function was also comparatively large, meaning that the optimisation did not achieve the best possible result, and this estimate could be identified as less reliable.

### 5.5.5 Ten-generator system

The previously mentioned IEEE-39 bus test system was also studied. It should be noted that one generator represents the connection to the rest of the North American power system. This generator is disproportionately large and represents alone the majority of the base power and as a consequence, often the majority of inertia (depending on its $H$).

There is one mode between the large generator and the remaining generators in New England that all have different, but similar activity. This mode in itself gives a lot of information about the inertia. In Figure 47, the imaginary part is plotted for different inertias. The damping was also allowed to vary, but it had no noticeable effect on the accuracy. The standard deviation of the percentual errors of the training set, evaluated at the polynomial, was 8.6% and for the test set 8.7%. The error did not clearly depend on the inertia.

More information is available in the mode shape. A two-dimensional regression was made using only the normalised activity of the large generator in the mode beside the imaginary part. This improved the result slightly, decreasing the standard deviation of the percentual error to 6.6% and 6.8% for the training and test set, respectively. The error distribution is shown in Figure 48. However, it is not certain that it is worth including the mode shape. The main factor determining the estimate is the imaginary part while the shape only explains a part of the residual error. Quite small errors in the mode shape can cancel out the benefit, about an error with the standard deviation 10%. If the mode

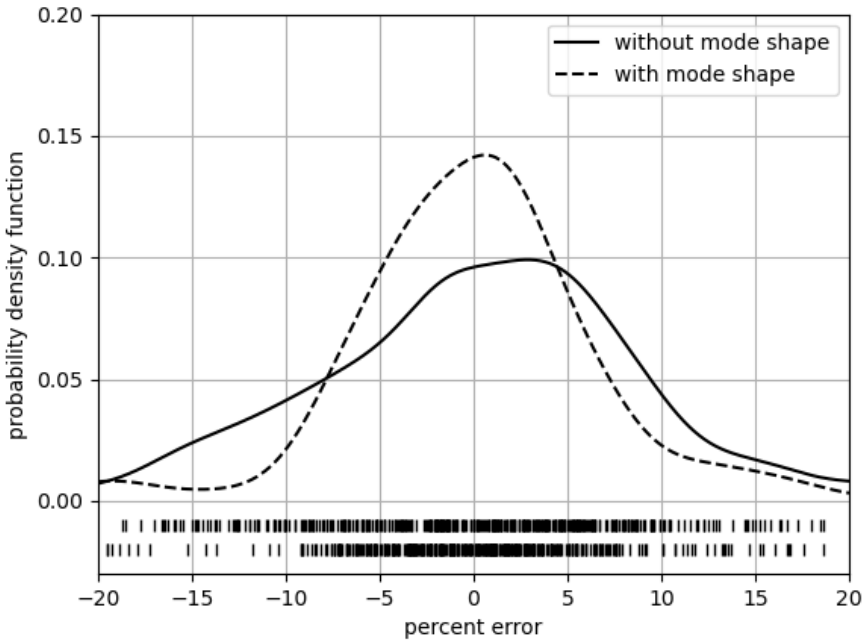


Figure 48: The distribution of errors when one inter-area mode is used for inertia estimation. The marks at the bottom indicate individual values, the upper without the mode shape, the lower with it.

shape cannot be more accurately estimated, it is not worth including.

### 5.5.6 Sensitivity to errors

Two types of errors can affect the estimation. The first is the error in the mode estimation. This is the only case considered here. The other is the error in the model. This includes system parameters as well as errors in the model structure or lack of elements in the model. Since there are many parameters that must be taken into consideration when calculating the inter-generator eigenvalues, the potential errors are likewise many. In fact, these errors may be so many and difficult to correct that they render the method useless, using inter-generator modes. To determine if that is the case is beyond the scope of this thesis.

The simplest case to consider in order to understand the sensitivity is the two-generator system. If an error was added to the eigenvalue, $H$ was incorrectly identified. The optimisation algorithm still worked and did find the $H$ that corresponded to the incorrect eigenvalue. It was noted that an error in the mode frequency $\omega$ resulted in an approximately twice as large percentual error in $H$, which is illustrated in Figure 49. This relationship was very clear when only $H$ was unknown, when also $D$ was unknown, there was a larger uncertainty, although the general tendency remained. A non-rigorous explanation can be given in the following manner. The frequency is approximately given by $\omega = \frac{c_1}{\sqrt{H}}$ according to chapter 3, where $c_1$ is a constant:

$$\frac{d\omega}{dH} = \frac{-0.5c_1}{H^{3/2}} = \frac{-0.5\omega}{H} \iff \frac{dH}{H} = -2\frac{d\omega}{\omega}$$

This of course puts extra demands on the accuracy of the estimated eigenvalues.

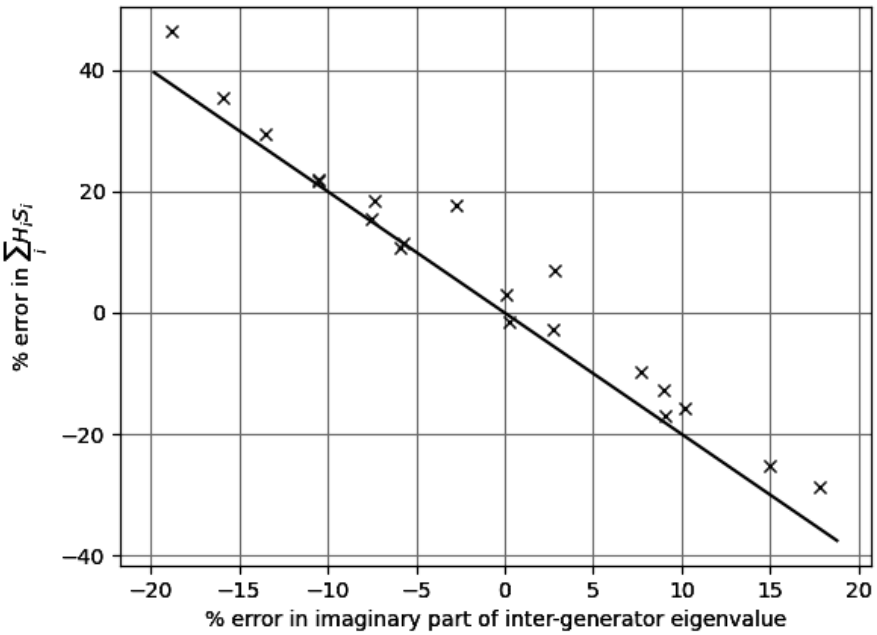


Figure 49: The error in $\sum_i H_i S_i$ as a function of the error in the imaginary part of the measured inter-area eigenvalue in a two-generator system. Only the imaginary part of the inter-area eigenvalue has been used to estimate $H$. The line is given by $y = -2x$.

Initial attempts have not shown the mode shape to improve the results for the two-generator system when the imaginary part is incorrectly estimated. It might help some, but the effect was not clear. It seems likely that the uncertainty in the estimated mode shape will be large compared to that in the imaginary part, nullifying any gain from using it.

When only one mode was used and a direct function between the imaginary part and the inertia was found, as was the case with the two-area system in section 5.5.3, it was possible to estimate the sensitivity to an error in the imaginary part by calculating the derivative of the function. Doing this, it could be concluded that disregarding other sources of errors, a relative error in the imaginary part of the eigenvalue gives rise to an relative error in the estimated total inertia that is slightly less than twice as large. This is the same conclusion as for the two-generator system.

When several modes are used, and there are errors in both the imaginary part and mode shape in all of them, it is harder to determine the sensitivity. An attempt was made running the estimation program when the modes where disturbed. The disturbances were based on the results in chapter 4 on mode estimation. The imaginary parts of the inter-generator modes were multiplied with a normal distributed disturbance factor with mean 1 and standard deviation 0.1. The mode shape was disturbed by adding a normal distributed value with mean 0 and standard deviation 0.03 to the normalised activity of each generator and normalise again such that the sum of the activity was 1. On average, the sum of the total disturbance was then 0.11.

Ten estimations in this scenario were run using 2, 3 and 4 modes. The results are shown

in Figure 50. The standard deviation of the relative error was 11.1%, 9.4% and 6.0% using 2, 3 and 4 modes, respectively. That is worse than when there was no disturbance, but the deterioration was still within reasonable bounds.

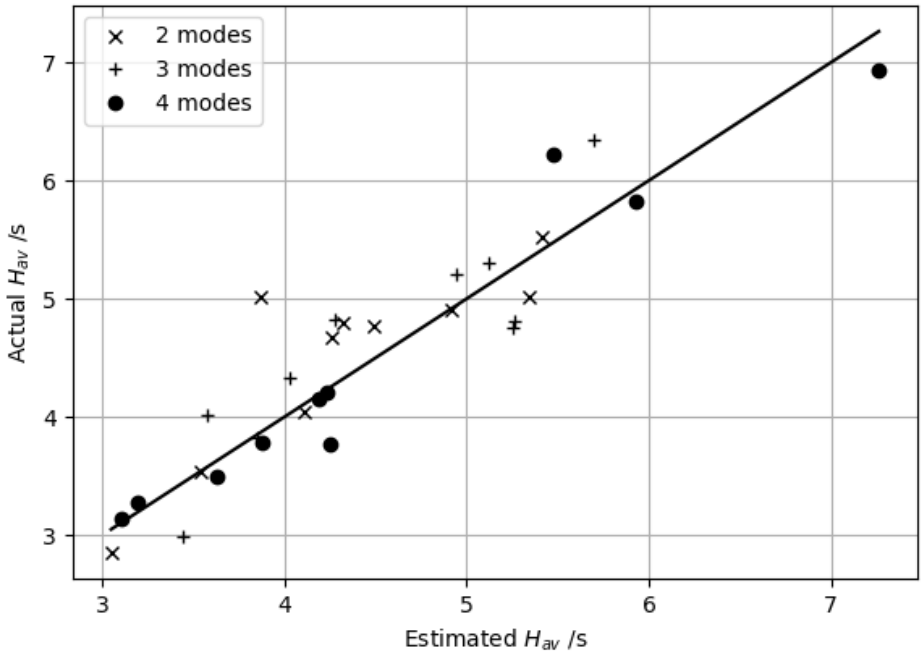


Figure 50: Actual vs. estimated total inertia for the IEEE-14 bus test system, using the imaginary part and the mode shape.

## 5.6 Inertia estimation using both the rigid body mode and the inter-generator modes

To use both the rigid body mode and inter-generator mode, the error must be merged into one objective function that is to be minimised. The task of constructing an objective function is non-trivial. A suggestion is:

$$\begin{aligned} &|\mathrm{Re}\{\lambda_{rb,est} - \lambda_{rb,meas}\}|^2 w_{rb-Re} + |\mathrm{Im}\{\lambda_{rb} - \lambda_{rb,meas}\}|^2 w_{rb-Im} + \\ &+ \frac{w_{IG-Re}}{N-1} \sum_i |\mathrm{Re}\{\lambda_{IG,i,est} - \lambda_{IG,i,meas}\}|^2 + \\ &+ \frac{w_{IG-Im}}{N-1} \sum_i |\mathrm{Im}\{\lambda_{IG,i,est} - \lambda_{IG,i,meas}\}|^2 + \\ &+ w_{activity} \left( \sum_i \frac{\sum_j |NA_{i,j,est} - NA_{i,j,meas}|}{N(N-1)} \right)^2 \end{aligned} \tag{11}$$

where $rb$ stands for rigid body, $IG$ for inter-generator, $est$ for estimated (numerically calculated), and $meas$ for measured, $\lambda_{rb}$ is the rigid body eigenvalue, $\lambda_{IG,i}$ are inter-generator eigenvalues, $NA_{i,j}$ is the normalised activity of generator $i$ in mode $j$, $N$ the number of generators and $w_{damping}$ and $w_{activity}$ are weights. How these weights should be chosen depends on the accuracy of the estimations. Some may be zero.

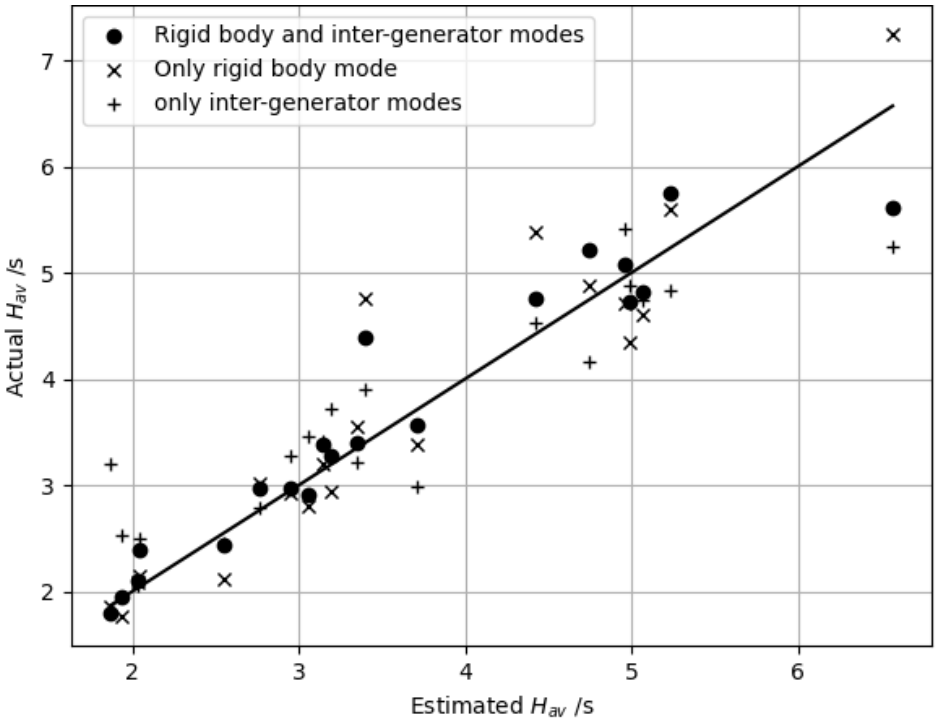


Figure 51: The estimated vs. the actual $\sum_i H_i S_i$ of the IEEE 14-bus system, estimating from only the rigid body mode, only the inter-generator mode and both.

It is suggested that $w_{rb-Re} = w_{IG-RE} = 0$, since the estimates of the real part are less reliable and this is what has previously been done. It is further suggested that $w_{rb-Im} = 200$, $w_{IG-Im} = 50$ and $w_{activity} = 1000$.

The method was applied to the IEEE 14-bus system with different inertias. The inertia was estimated using only the rigid body mode, only two inter-generator eigenvalues and both at the same time. To make it more realistic, and motivate the use of all modes, disturbances in the mode estimation were introduced. The imaginary part of the rigid body mode was multiplied with a normal distributed disturbance factor with mean 1 and standard deviation 0.1, the imaginary parts of the inter-generator modes with a similar factor, but with standard deviation 0.05. The mode shape was disturbed by adding a normal distributed value with mean 0 and standard deviation 0.03 to the normalised activity of each generator.

The results from the estimations are shown in Figure 51. The standard deviation of the relative error was 9.64% when using both, 12.66% using only the rigid body mode, and 20.60% using only the two inter-generator modes (it would have been 13.44% if the worst estimate had been excluded). That is, the error was on average less when both mode types were used than when any single mode type was used. However, the difference is not striking, and in individual cases it is not necessarily better than both other methods, or even any.

## 5.7 Discussion

In this chapter it was shown that it is possible to estimate the inertia from the electromechanical modes, both from the rigid body and from inter-generator modes. The results

from the different systems are collected in Table 5.

Table 5: The results from inertia estimations in this chapter.

| **modes used** | **system** | **standard deviation of error** |
|---|---|---|
| rigid body mode | IEEE 14-bus | 8.8% |
| rigid body mode | IEEE 39-bus | 5% |
| inter-generator modes without mode shapes | 3-generator, equal $S$ | 7.8% |
| inter-generator modes with mode shapes | 3-generator, equal $S$ | 3.7% |
| inter-generator modes without mode shapes | 3-generator, unequal $S$ | 32% |
| inter-generator modes with mode shapes | 3-generator, unequal $S$ | 11% |
| 2 inter-generator modes with mode shape | IEEE 14-bus | 7.3% |
| 3 inter-generator modes with mode shape | IEEE 14-bus | 7.4% |
| 4 inter-generator modes with mode shape | IEEE 14-bus | 2.7% |
| inter-area mode without mode shape | 2-area | 10% |
| inter-area mode without mode shape | IEEE-39 | 8.7% |
| inter-area mode with mode shape | IEEE-39 | 6.8% |

In total, there are five aspects that the calculated and measured modes can be compared in. The real and imaginary part of the rigid body eigenvalue, the real and imaginary part of the inter-generator eigenvalues, and the mode shape. Their advantages and disadvantages are presented in Table 6.

The real parts are not recommended to use mainly due to the difficulty to estimate them, and have not been thoroughly investigated in this thesis. Instead, the imaginary part is the main focus. Both the rigid body mode and the inter-generator eigenvalues provide plausible possibilities to estimate the inertia.

The easiest solution is to only use the rigid body mode. In the case of a step response, this seems like the best course of action. The rigid body mode can be well estimated, while the inter-generator modes not so well, making them not only problematic to use, but also unnecessary. In this case both the real and the imaginary part of the rigid body mode may be used, although a preference could be given to the imaginary part, since it has shown to be more useful for estimating the inertia.

Using a step response is however only a back-up solution if ambient estimations do not work. But even for ambient estimations the rigid body mode alone may suffice. In that case only the imaginary part can be estimated accurately enough to be useful. Although the testing is insufficient and depend on the system, the simulation of the hydro governor model gave a 12% standard deviation for the error in the imaginary part, with a few values increasing it drastically. The propagation of the error to the inertia estimate depend on the inertia, and so does the accuracy of the estimation. The major factor deciding is that

Table 6: Table comparing the different aspects used in the numerical estimation of $H$ from eigenvalues.

| **aspect** | **ambient measurement quality** | **step measurement quality** | **numerical quality for estimating $\sum HS$** | **numerical quality for estimating individual $H$** |
|---|---|---|---|---|
| real part of rigid body eigenvalue | bad | decent | very useful | useless |
| imaginary part of rigid body eigenvalue | decent $\sigma \approx 10$–$20\%$ | decent $\sigma \approx 10$–$20\%$ | very useful $\sigma \approx 5\%$ for low inertia $\sigma \approx 10\%$ for any inertia | useless |
| real part of inter-area eigenvalues | quite bad | not very good | probably not very useful | probably somewhat useful |
| imaginary part of inter-area eigenvalues | good | not very good | useful $\sigma \approx 10\%$ together with mode shape | useful |
| mode shape | decent | not very good | useful | useful |

the rigid body mode is not too well damped. Although there are many uncertainties and factors that must be taken into account, it seems plausible to estimate the inertia with an accuracy of 10-20%. A major flaw is the robustness, but if the extreme values somehow can be sorted out and the test rerun, a better result can be expected.

Using the inter-generator modes for inertia estimation is more challenging. However, since they can be fairly reliably estimated from ambient noise, it may be worth the trouble to include them. Nevertheless, there are many factors that must be taken into account making it a delicate procedure. The amount of modes, the activity of the generators in each, the structure of the system and the accuracy of the estimation, especially of the mode shapes, all affect the result, leaving few general guarantees. Furthermore, it is uncertain if enough knowledge of the system can be gathered to make an estimation possible. The test runs here have left the damping ratio unknown though, and most system properties that risks being unknown, e.g. PSS's, exciters, mostly affect the damping. Still, they do affect the frequency and the shape of the mode too, leaving an uncertainty in the method. A large system also poses problems.

Despite all this, it has been shown that inter-generator modes can be used for inertia estimation. A decisive factor is the size of the model. If the system can be described by a small model, with only a handful generators, the method works, and it might be possible with larger models. If the system is such that there is a clear inter-area mode, it is very useful for estimation, as shown for the two-area system and IEEE 39-bus test system.

It is not obvious that the estimates from the inter-generator modes are accurate enough. The relative error can be expected to have a standard deviation somewhere between 5 and 15%, even with perfect estimations. It depends on the system and the number of modes. The lower value can be considered sufficiently good, the upper not quite. In that case, it would be better to use the rigid body mode, which makes the estimates easier and reduces the error almost to the error of the mode estimation. Nev-

ertheless, it has been shown that it is possible to estimate even with errors in the mode estimation, albeit with worse results.

Still, there are two possible uses for the inter-generator modes, assuming that enough system information is available. One is to use them when the rigid body mode is too well damped for reliable detection under ambient condition. Alternatively, if the rigid body mode cannot be reliably estimated in real data for another reason. The other is to improve the estimate using the rigid body mode by supplying more information. Since there must be assumed to be an error in the estimate of the rigid body mode, the extra, independent estimation can limit the effects of it.

If it is possible to have the mode estimates and system information needed for both mode types, they can both be used, giving better results than with only a single mode type. The improvement is hardly surprising since having two independent measurements should decrease the average error.

# 6 The combined method

In this chapter some results are presented using both steps in the method, i.e. first estimating the modes, and then use these modes estimates for inertia estimation.

Since PowerFactory does not allow for simulating ambient noise, there is some difficulty in performing the entire estimation. A work-around is to export the system from PowerFactory to Matlab, simulate with noise and estimate the modes, that are then used for estimation in PowerFactory. The entire model cannot be exported from PowerFactory, but only the system matrix from the linearisation. Furthermore, the load power does not have a state that can be used as input. A work-around to this is to add the disturbance directly as $P_e$ at the generators. It is not quite the same as having the load power vary, since this may give a different excitation. For the rigid body mode the effect should be negligible, since it does not depend on where the disturbance is located. For the inter-generator modes, however, this ensures that all generators are excited, which could give a small benefit to the mode estimation compared to load variations. Nevertheless, it is assumed to not have any significant impact compared to all other simplifications made. Still, doing all this is somewhat cumbersome, and only a limited number of systems are investigated.

Results for the IEEE 14-bus test system with various values on $H$ are presented in Tables 7 and 8. Results for the 39-bus system are presented in Table 9. The same information is also presented as bar diagrams in Figures 52 and 53. Only the rigid body and the inter-area mode between the large and the other generators are considered since it is the main interest. The presented results are values for running the procedure once, running it again would give a different result. This means that the exact values on the accuracy are questionable. The purpose is rather to show that the estimates are possible and consistent with what has been previously concluded.

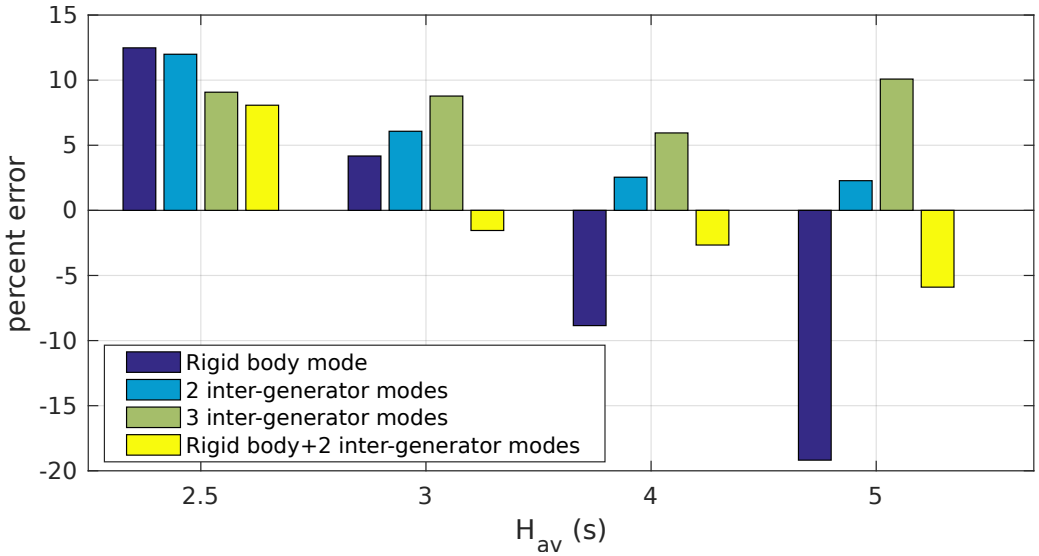


Figure 52: Error for the combined method applied to the IEEE 14-bus system. For more detailed values, see Table 8

.

Table 7: Estimation of modes of the IEEE 14-bus system from ambient noise in Matlab. If a mode was not detected, it is marked with $-$.

| $H$ (s) | true eigenvalues | estimated eigenvalues | true mode shapes | estimated mode shapes |
|---|---|---|---|---|
| $\begin{bmatrix}2.5\\2.5\\2.5\\2.5\\2.5\end{bmatrix}$ | $\begin{bmatrix}-0.61\pm10.98i\\-1.04\pm13.30i\\-1.19\pm14.83i\\-1.77\pm17.39i\\-0.18\pm0.429i\end{bmatrix}$ | $\begin{bmatrix}-0.72\pm10.95i\\-1.14\pm12.98i\\-1.05\pm14.88i\\-2.04\pm17.10i\\-0.17\pm0.388i\end{bmatrix}$ | $\begin{bmatrix}0.43 & 0.042 & -0.013\\ & -0.14 & -0.38\\0.26 & -0.011 & -0.082\\ & -0.42 & 0.23\\0.31 & -0.090 & -0.42\\ & 0.15 & 0.034\\0.28 & -0.49 & 0.19\\ & 0.030 & 0.011\end{bmatrix}$ | $\begin{bmatrix}0.37 & 0.047 & -0.023\\ & -0.15 & -0.41\\0.12 & -0.040 & -0.11\\ & -0.47 & 0.27\\0.17 & -0.11 & -0.51\\ & 0.15 & 0.064\\0.85 & 0.053 & -0.021\\ & 0.031 & 0.044\end{bmatrix}$ |
| $\begin{bmatrix}3\\3\\3\\3\\3\end{bmatrix}$ | $\begin{bmatrix}-0.54\pm9.99i\\-0.95\pm12.07i\\-1.09\pm13.46i\\-1.63\pm15.74i\\-0.17\pm0.321i\end{bmatrix}$ | $\begin{bmatrix}-0.54\pm9.94i\\-1.58\pm12.26i\\-1.82\pm13.81i\\-\\-0.11\pm0.336i\end{bmatrix}$ | $\begin{bmatrix}0.42 & -0.041 & -0.014\\ & -0.14 & -0.38\\0.26 & -0.012 & -0.083\\ & -0.42 & 0.23\\0.31 & -0.090 & -0.42\\ & 0.15 & 0.035\\0.28 & -0.49 & 0.19\\ & 0.030 & 0.011\end{bmatrix}$ | $\begin{bmatrix}0.39 & 0.038 & -0.024\\ & -0.14 & -0.41\\0.20 & -0.059 & -0.13\\ & -0.44 & 0.17\\0.29 & -0.12 & -0.39\\ & 0.11 & 0.086\\- & - & -\end{bmatrix}$ |
| $\begin{bmatrix}4\\4\\4\\4\\4\end{bmatrix}$ | $\begin{bmatrix}-0.44\pm8.60i\\-0.82\pm10.37i\\-0.9\pm11.55i\\-1.41\pm13.47i\\-0.12\pm0.226i\end{bmatrix}$ | $\begin{bmatrix}-0.49\pm8.59i\\-0.67\pm10.06i\\-1.20\pm11.70i\\-2.03\pm13.67i\\-0.11\pm0.244i\end{bmatrix}$ | $\begin{bmatrix}0.42 & 0.041 & -0.013\\ & -0.14 & -0.38\\0.26 & -0.011 & -0.082\\ & -0.42 & 0.23\\0.31 & -0.090 & -0.42\\ & 0.15 & 0.034\\0.28 & -0.49 & 0.19\\ & 0.030 & 0.011\end{bmatrix}$ | $\begin{bmatrix}0.39 & 0.039 & -0.021\\ & -0.15 & -0.40\\0.13 & -0.036 & -0.13\\ & -0.42 & 0.29\\0.13 & -0.14 & -0.46\\ & 0.20 & 0.08\\0.21 & -0.58 & 0.095\\ & 0.044 & -0.069\end{bmatrix}$ |
| $\begin{bmatrix}5\\5\\5\\5\\5\end{bmatrix}$ | $\begin{bmatrix}-0.37\pm7.67i\\-0.73\pm9.23i\\-0.83\pm10.27i\\-1.24\pm11.94i\\-0.089\pm.19i\end{bmatrix}$ | $\begin{bmatrix}-0.48\pm7.61i\\-0.96\pm9.25i\\-0.98\pm10.20i\\-\\-0.006\pm0.212i\end{bmatrix}$ | $\begin{bmatrix}0.43 & 0.040 & -0.017\\ & -0.14 & -0.38\\0.25 & -0.013 & -0.086\\ & -0.42 & 0.23\\0.31 & -0.093 & -0.41\\ & 0.15 & 0.036\\0.27 & -0.49 & 0.19\\ & 0.030 & 0.011\end{bmatrix}$ | $\begin{bmatrix}0.42 & 0.050 & -0.021\\ & -0.12 & -0.39\\0.15 & -0.05 & -0.15\\ & -0.49 & 0.16\\0.032 & -0.16 & -0.52\\ & 0.20 & 0.092\\- & - & -\end{bmatrix}$ |

Table 8: Estimation of $H$ of the IEEE 14-bus system from estimated modes, based on inter-generator (IG) modes and the rigid body mode.

| $H$ (s) | $H_{est}$(s) from 2 IG modes | $H_{est}$ (s) from 3 IG modes | $\sum HS$ (MVAs) | $\sum H_{est}S$ (MVAs) from 2 IG modes | $\sum H_{est}S$ (MVAs) from 3 IG modes | $\sum H_{est}S$ (MVAs) from rigid body mode | $\sum H_{est}S$ (MVAs) from rigid body + 2 IG modes |
|---|---|---|---|---|---|---|---|
| $\begin{bmatrix}2.5\\2.5\\2.5\\2.5\\2.5\end{bmatrix}$ | $\begin{bmatrix}2.74\\4.39\\1.93\\2.77\\2.32\end{bmatrix}$ | $\begin{bmatrix}2.90\\2.73\\2.40\\2.68\\2.41\end{bmatrix}$ | 2000 | 2239.8 (+11.2%) | 2181.5 (+9.1%) | 2249.6 (+12.5%) | 2161.5 (+8.1%) |
| $\begin{bmatrix}3\\3\\3\\3\\3\end{bmatrix}$ | $\begin{bmatrix}3.31\\3.83\\2.57\\2.87\\2.95\end{bmatrix}$ | $\begin{bmatrix}3.81\\2.34\\2.81\\2.90\\2.81\end{bmatrix}$ | 2400 | 2545.8 (+6.1%) | 2610.7 (+8.8%) | 2500.2 (+4.2%) | 2362.9 (-1.5%) |
| $\begin{bmatrix}4\\4\\4\\4\\4\end{bmatrix}$ | $\begin{bmatrix}3.68\\4.84\\4.84\\4.34\\4.07\end{bmatrix}$ | $\begin{bmatrix}4.38\\4.34\\3.83\\4.43\\3.79\end{bmatrix}$ | 3200 | 3281.5 (+2.5%) | 3390.3 (+5.9%) | 2916.8 (-8.8%) | 3114.8 (-2.7%) |
| $\begin{bmatrix}5\\5\\5\\5\\5\end{bmatrix}$ | $\begin{bmatrix}5.62\\4.84\\3.66\\4.96\\4.96\end{bmatrix}$ | $\begin{bmatrix}5.99\\5.33\\5.04\\4.83\\4.88\end{bmatrix}$ | 4000 | 4091.2 (+2.3%) | 4403.3 (+10.1%) | 3232.7 (-19.2%) | 3764.1 (-5.9%) |

Table 9: Estimation of $H$ of the IEEE 39-bus system from estimated modes, based on inter-area (IA) mode and the rigid body mode.

| $H$ (s) | true eigenvalues | estimated eigenvalues | $\sum HS$ (MVAs) | $\sum H_{est}S$ (MVAs) from IA-mode | $\sum H_{est}S$ (MVAs) from rigid body mode | $\sum H_{est}S$ (MVAs) from rigid body + IA mode |
|---|---|---|---|---|---|---|
| $\begin{bmatrix}3\\\vdots\\3\end{bmatrix}$ | $\begin{bmatrix}-0.37\pm0.553i\\-0.39\pm4.90i\end{bmatrix}$ | $\begin{bmatrix}-0.38\pm0.610i\\-0.33\pm4.86i\end{bmatrix}$ | 50400 | 51825.7 (+2.8%) | 53396.3 (+5.9%) | 49596.7 (-1.6%) |
| $\begin{bmatrix}4\\\vdots\\4\end{bmatrix}$ | $\begin{bmatrix}-0.40\pm0.432i\\-0.35\pm4.19i\end{bmatrix}$ | $\begin{bmatrix}-0.67\pm0.396i\\-0.41\pm4.25i\end{bmatrix}$ | 67200 | 70203.6 (+4.5%) | 76833.2 (+14.3%) | 76364.9 (+13.6%) |
| $\begin{bmatrix}2\\3\\\vdots\\3\end{bmatrix}$ | $\begin{bmatrix}-0.37\pm0.738i\\-0.38\pm5.38i\end{bmatrix}$ | $\begin{bmatrix}-0.31\pm0.635i\\-0.31\pm5.51i\end{bmatrix}$ | 40400 | 45817.7 (+13.4%) | 45281.8 (+12.1%) | 45940.5 (+13.7%) |

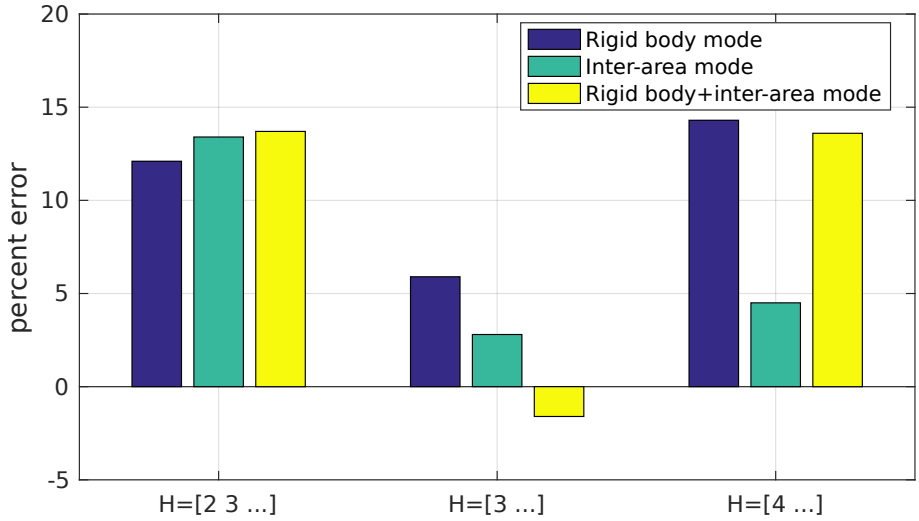


Figure 53: Error for the combined method applied to the IEEE 39-bus system. For more detailed values, see Table 9

.

## 6.1 Discussion

The errors are rather small, typically around 10%, and in line with what has previously been seen. An exception is the estimate using the rigid body mode for the system with highest inertia. Previously it has been noted that high inertia makes the inertia estimation (the curve in Figure 34 flattens out) difficult as well as possibly the mode estimation.

The mode estimates are good in general, and the inter-generator eigenvalues are estimated more accurately than the rigid body eigenvalue, as expected. The mode shapes are quite good for the first two modes, but for the third less so, also as expected. The fourth mode is not reliably estimated, if at all, hence why it was not used in the inertia estimates. Already for the third mode it might be somewhat unreliable. This could explain why the estimate may be more accurate without the third mode. Nevertheless, the shape estimates are sufficiently accurate to match the modes correctly.

The inertia estimation works as well, giving values close to the actual, although with some errors. For the estimations with the inter-generator modes, the errors are within the limits of what could be achieved with true mode values. Therefore, the error can to a large extent be explained by the inherent uncertainty in the method, e.g. due to unknown damping and that modes are not enough to uniquely determine the inertia. For the global mode, on the other hand, the error is most likely almost entirely explained by the error in mode estimation, and the size of the error is in line with the error of the mode estimate. When both the rigid body and the inter-generator modes are used, the result is further improved.

For the 39-bus system the rigid body mode estimates were slightly worse. At least partially it can be explained by the slightly higher damping, although the case with $H$ =[2 3 ... 3] should then be better. It could also be due to the different dynamics that are not captured by this single mode. There is also an element of chance at play given the small sample size. The lower accuracy is reflected in the estimates using the rigid body mode as well as the estimate using both the rigid body mode and the inter-area mode. In this case it could have been beneficial to emphasise the inter-area mode when both are used

for estimation, which shows the difficulty in balancing the two.

The inter-area mode was still possible to estimate accurately, and it was possible to estimate the inertia from it as well with similar accuracy as for the 14-bus system. There is nothing that indicates that the previous analysis in subsection 5.5.5 is not better than what can be achieved from this data. However, the mode shape was estimated with low accuracy, and it was barely possible to distinguish the inter-area properties of this mode and identify it. To use it for estimation was off the map. This is similar to what was seen in section 4.6, how more synchronous machines made the mode estimation more difficult.

# 7 Conclusion

This thesis has shown that it is possible to estimate the electromechanical modes of the system, also from ambient noise, and the modes can then be used for inertia estimation. The errors from the estimations typically had a standard deviation of about 10% and sometimes less.

This accuracy can be reached by using either the rigid body mode or the inter-generator mode. Even better results can be achieved if both are used. Although the types of mode are similar in accuracy, there are many other difference between them. These should be taken into account when selecting which to use.

The rigid body mode is somewhat difficult to estimate. Although it was possible in simulations, it is expected to be more difficult in reality. The mode correlates clearly with the inertia, and once an estimate of it is available, a fairly accurate inertia estimation can be performed. Another advantage is that only a limited amount of system information is needed for estimation from the rigid body mode. The most important information is related to models of the governors in the system. Network topology and voltage dynamics on the other hand have no significant impact on the rigid body mode and are not necessary to model accurately.

The case is more or less the opposite for inter-generator modes. They can be accurately estimated, something also proven in practice by previous research, which is their greatest advantage. Their usefulness for inertia estimation has also been shown, with inter-area modes being especially useful. The drawback of using inter-generator modes is that more aspects of the system must be taken into consideration. Although the governors do not have a large impact on the inter-generator modes, topology does, and voltage dynamics and PSSs may also affect them.

The accuracy of the method in this thesis can be compared to previous results of inertia estimation. Such are presented in Table 10. These studies are all based on different systems, conditions and assumptions, and can therefore not be directly compared. That the errors are reported differently does not make the comparison easier. Still, it seems like the results in this thesis are competitive, even with those that use a disturbance, and may even be considered good. However, definite conclusions cannot be drawn from the limited investigations done here.

The accuracy of the method consisting of adding up the inertia of connected generators is unknown, as mentioned in section 1.2. However, its accuracy is believed to be similar or possibly not quite as good as that achieved in this thesis.

It cannot be definitely determined whether the estimates achieved here are "good enough". That the accuracy compares well with and possibly surpasses other methods indicates that the method is potentially useful. However, to apply this in reality uncertainty in the system parameters must be added to the errors. The fact that everything is performed in a simulated environment and on simple systems also facilitates the estimation, and it is over-optimistic to assume that an equal result can be achieved in reality. Nevertheless, the method provides a new interesting option for inertia estimation, and seems to have potential, although much work remains before any possible real-world application.

Table 10: Some previous results on inertia estimation.

| Study | Description | System | Result |
|---|---|---|---|
| [9] | Uses the RoCoF during a disturbance. | IEEE 39-bus | Median error 1.53% with inter-quartile range of 6.6%. |
| [8] | Uses an adaptive estimation algorithm during a disturbance. | IEEE 1013-bus | A mean error somewhere between 5-10%, although no single is number given. |
| [11] | Uses measured ambient load and frequency. | Icelandic system (real system) | 12% average error in RoCoF. |
| [35] | Uses RoCoF during a disturbance. | Nordic57 | The best method had mean error (from three different load models) 4.9%, 12% and 22% when measurements from 100%, 80% and 50% of the generators were available. |
| [7] | Estimates the inertia from disturbances and compares to the known inertia contribution from generation to find the residual inertia from other sources. | Great Britain system (real system) | Residual inertia between 8% and 25% with average 18%. |

# 8 Future work

Although some results in this thesis seem promising, they are based on simulations. If the method should ever lead to practical value, it must take the step into reality. However, there are many uncertainties.

The mode estimation is not necessarily as easy as for the simulated cases. This is especially true for estimation of the rigid body mode from ambient noise. A reliable method that is applicable to real data is needed. The inter-generator modes have previously shown to be possible to estimate accurately enough, but the accuracy of the mode shape estimation has not been fully researched in this thesis and more definite answers are probably needed before any practical implementation.

Mode estimation is a large field of research that has not been more than superficially covered in this thesis, anything more would be impossible. Therefore, it is possible that there are methods to surpass the accuracy achieved here, or will be in the future. Due to the structure of the method, any mode estimation is possible to connect to the inertia estimation without any major changes and in that way improve the estimation.

In this work, the vast majority of system parameters have been assumed to be known. Although this is to some extent possible, there will be an error in the parameters. How the error affects the inertia estimation based on the rigid body mode has been considered. How the uncertainty in the system parameters affects the estimation based on inter-generator modes has been studied to a lesser extent. Here, more research is needed. Regardless, to get a number on the uncertainty of the inertia estimates, it is necessary to have numbers on the uncertainty in the system parameters, which then must be determined.

As a next step, it is suggested that real frequency data is used for mode estimation in an organised and thorough manner. Although it is not possible to know the true values of the modes, it can be investigated whether the estimates are consistent and plausible. If the estimates are then combined with inertia estimates based on adding the inertia from connected machines, a correspondence (or lack thereof) could be determined. This could also offer the possibility of calibration, i.e. establishing a relation between the inertia and the modes that can then be used to estimate the inertia only from the modes, with or without a system model. If a system model is not used, it is possible to imagine approaches using machine learning to find the relation between modes and the inertia. One may also imagine other approaches than going through the modes and search for a relationship directly between the estimated model (ARMA or something else) and the inertia.

# References


[1] ENTSO-E. (2017-09-20) Nordic System Operation Agreement. [Online]. Available: https://docstore.entsoe.eu/Documents/Publications/SOC/Nordic/System_Operation_Agreement_appendices_(English_2017_update).pdf

[2] M. Kuvaniemi, N. Modig, and R. Eriksson, "FCR-D design of requirements," ENTSO-E, Brussels, Belgium, Tech. Rep., July 2017.

[3] P. Kundur, *Power System Stability and Control*. New York, NY, USA: McGraw-Hill, 1993.

[4] E. Ørum, M. Kuivaniemi, M. Laasonen, A. I. Bruseth, E. A. Jansson, A. Danell, K. Elkington, and N. Modig, "Nordic report Future System Inertia," ENTSO-E, Brussels, Belgium, Tech. Rep., 2015.

[5] IEA, "Nordic Energy Technology Perspectives 2016," IEA, Paris, France, Tech. Rep., 2016.

[6] H. Holttinen, S. Rissanen, X. Larsen, and A. L. Løvholm, "Wind and load variability in the Nordic countries," VTT Technical Research Centre of Finland, Espoo, Finland, Tech. Rep., 2013.

[7] P. M. Ashton, C. S. Saunders, G. A. Taylor, A. M. Carter, and M. E. Bradley, "Inertia Estimation of the GB Power System Using Synchrophasor Measurements," *IEEE Transactions on Power Systems*, vol. 30, no. 2, pp. 701–709, March 2015.

[8] J. Schiffer, P. Aristidou, and R. Ortega, "Online Estimation of Power System Inertia Using Dynamic Regressor Extension and Mixing," *IEEE Transactions on Power Systems*, vol. 34, no. 6, pp. 4993–5001, Nov. 2019.

[9] P. Wall, F. Gonzalez-Longatt, and V. Terzija, "Estimation of Generator Inertia Available During a Disturbance," in *2012 IEEE Power and Energy Society General Meeting, San Diego, CA, USA, July 22-26 2012*, pp. 1–8.

[10] J. Fang, H. Li, Y. Tang, and F. Blaabjerg, "On the Inertia of Future More-Electronics Power Systems," *IEEE Journal of Emerging and Selected Topics in Power Electronics*, vol. 7, no. 4, pp. 2130–2146, Dec. 2019.

[11] K. Tuttelberg, J. Kilter, D. Wilson, and K. Uhlen, "Estimation of Power System Inertia From Ambient Wide Area Measurements," *IEEE Transactions on Power Systems*, vol. 33, no. 6, pp. 7249–7257, Nov. 2018.

[12] J. D. Glover, T. J. Overbye, and M. S. Sarma, *Power System Analysis and Design*, 6th ed. Boston, MA, USA: Cengage Learning, 2016.

[13] V. V. Terzija, "Adaptive underfrequency load shedding based on the magnitude of the disturbance estimation," *IEEE Transactions on Power Systems*, vol. 21, no. 3, pp. 1260–1266, Aug. 2006.

[14] M. Peydayesh and R. Baldick, "Simplified Model of ERCOT Frequency Response Validated and Tuned using PMUs Data," *IEEE Transactions on Smart Grid*, vol. 9, no. 6, pp. 6666–6673, Nov. 2018.

[15] R. Eriksson and N. Modig, "FCR-N Design of Requirements," ENTSO-E, Brussels, Belgium, Tech. Rep., July 2017.

[16] Task Force on Turbine-Governor Modeling, "Dynamic Models for Turbine-Governors in Power System Studies," IEEE Power & Energy Society, Tech. Rep., Jan. 2013.

[17] *39 Bus New England System*, Gomaringen, Germany, 2020, PowerFactory 2020.

[18] P. W. Sauer and M. A. Pai, *Power System Dynamics and Stability*. Upper Saddle River, NJ, USA: Prentice Hall, 1998.

[19] K. Walve and A. Edström, "The Training Simulator ARISTO – Design and Experiences," in *IEEE Power Engineering Society. 1999 Winter Meeting, New York, NY, USA, Jan. 31- Feb. 4 1999*, pp. 545–547.

[20] K. Johansson and B. Martinsson, "Mätning och utvärdering av belastningsvariationer," Diploma thesis, Department of Electrical Power Systems, School of Electrical and Computer Engineering, Chalmers University of Technology, Gothenburg, Sweden, 1986.

[21] RG-CE System Protection & Dynamics Sub Group, "Frequency Measurement Requirements and Usage," ENTSO-E, Tech. Rep., Jan. 2018.

[22] J. W. Pierre, D. J. Trudnowski, and M. K. Donnelly, "Initial Results in Electromechanical Mode Identification from Ambient Data," *IEEE Transactions on Power Systems*, vol. 12, no. 3, pp. 1245–1251, Aug. 1997.

[23] Task Force on Identification of Electromechanical Modes, "Identification of Electromechanical Modes in Power Systems," IEEE, Tech. Rep., June 2012.

[24] *Measuring relays and protection equipment – Part 118-1: Synchrophasor for power systems – Measurements*, IEEE Std. 60 255-118-1, Dec. 2018.

[25] A. J. Conejo and L. Baringo, *Power System Operations*. Cham, Switzerland: Springer, 2018.

[26] N. H. Abel, "Démonstration de l'impossibilité de la résolution algébrique des équations générales qui passent le quatrième degré," in *Oeuvres complètes de N. H. Abel*, B. M. Holmboe, Ed. Christiania: Grøndahl, 1839, ch. II, pp. 5–24.

[27] A. Jakobsson, *An Introduction to Time Series Modeling*, 3rd ed. Lund, Sweden: Studentlitteratur AB, 2019.

[28] S. Føyen, M.-E. Kvammen, and O. B. Fosso, "Prony's method as a tool for power system identification in Smart Grids," in *International Symposium on Power Electronics, Electrical Drives, Automation and Motion, SPEEDAM 2018, Amalfi, Italy, July 20-22 2018*, pp. 562–569.

[29] D. J. Trudnowski, J. M. Johnson, and J. F. Hauer, "Making Prony Analysis More Accurate using Multiple Signals," *IEEE Transactions on Power Systems*, vol. 14, no. 1, pp. 226–231, Feb. 1999.

[30] J. J. Sanchez-Gasca and J. H. Chow, "Performance comparison of three identification methods for the analysis of electromechanical oscillations," *IEEE Transactions on Power Systems*, vol. 14, no. 3, pp. 995–1002, Aug. 1999.

[31] L. L. Grant and M. L. Crow, "Comparison of Matrix Pencil and Prony methods for power system modal analysis of noisy signals," in *North American Power Symposium, 2011, Boston, MA, USA, August 4-6 2011*, pp. 562–569.

[32] G. Liu and V. Venkatasubramanian, "Oscillation monitoring from ambient PMU measurements by Frequency Domain Decomposition," in *IEEE International Symposium on Circuits and Systems, ISCAS 2008, Seattle, WA, USA, May 18-20 2008*, pp. 2821–2824.

[33] L. Dosiek, N. Zhou, J. W. Pierre, Z. Huang, and D. J. Trudnowski, "Mode Shape Estimation Algorithms Under Ambient Conditions: A Comparative Review," *IEEE Transactions on Power Systems*, vol. 28, no. 2, pp. 779–787, May 2013.

[34] H. W. Kuhn, "The Hungarian Method for the Assignment Problem," *Naval Research Logistics Quarterly*, vol. 2, pp. 83–97, 1955.

[35] D. Zografos, "Power system inertia estimation and frequency response assessment," Ph.D. dissertation, Division of Electric Power and Energy Systems, School of Electrical Engineering and Computer Science, KTH Royal Institute of Technology, Stockholm, Sweden, 2019.

# A Simplified pseudocode for optimisation algorithm

```
function findParameters (measuredModes)
    % optimisation parameters
    runs=4
    limit1=12
    limit2=12
    limit3=12
    stepSizeFactor1=0.75
    stepSizeFactor2=0.75

    minError=Inf
    for i=1:runs {
        % initialize
        estParams=random()
        oldError=Inf
        error=getError(estParams,measuredModes)
        %take steps
        k1=0
        while (error<0.98*oldError and k1<limit1) {}
            k1=k1+1
            gradient=getGradient(estParams,measuredModes)
            stepSize=stepSize0
            % decrease step size until error is smaller than
            % at the starting point
            estParams2=estParams-gradient*stepSize
            error2=getError(estParams2,measuredModes)
            k2=0
            while (error2>=error and k2<limit2) {
                k2=k2+1
                stepSize=stepSizeFactor1*stepSize
                estParams2=estParams-gradient*stepSize
                error2=getError(estParams2,measuredModes)
            }
            % decrease step size as long as
            % it decreases the error
            error3=error2
            k2=0
            while (error3<=error2 and k2<limit3) {
                k2=k2+1
                error2=error3
                stepSize=stepSizeFactor2*stepSize
                estParams2=estParams-gradient*stepSize
                error3=getError(estParams2,measuredModes)
            }
            % divide by stepSizeFactor2 since the last step
            % worsened the result
```

```
            stepSize=stepSize/stepSizeFactor2
            estParams=estParams-gradient*stepSize
            oldError=error
            error=error2
        }
        %Check if this is the best parameters yet
        if (error<minError){
            minError=error
            bestParams=estParams
        }
    }
    return bestParams
}

%calculates the gradient
function gradient(estParams, measuredModes){
    error=getError(estParams,measuredModes)
    for i in length(parameters){
        parameters2=parameters
        parameters2(i)=parameters2(i)+dx
        error2=getError(estParams2,measuredModes)
        gradient(i)=(error2-error)/dx
    }
    return gradient
}

%calculates the error
function getError(params,measuredModes) {
    calculatedModes=getModes(params)
    matching=matchModes(calculatedModes, measuredModes)
    error=getDifference(calculatedModes(matching),measuredModes)
    return error
}
```